THE HONG KONG POLYTECHNIC UNIVERSITY
INSTITUTE OF TEXTILES AND CLOTHING

TORSIONAL BEHAVIOR OF SHORT-STAPLE TORQUE-BALANCED SINGLES RING SPUN YARNS AND SPIRALITY OF RESULTANT KNITTED FABRICS

A thesis submitted in partial fulfilment of the requirements for the Degree of Doctor of Philosophy

YANG Kun

Under the Supervision of

Prof. Xiao-ming TAO and Dr. Kowk-cheong LAM, Jimmy

February 2006

CERTIFICATE OF ORIGINALITY

I hereby declare that this thesis is my own work and that, to the best of my knowledge and belief, it reproduces no material previous published or written, nor material that has been accepted for the award of any other degree or diploma, except where due to acknowledgement has been made in the text.

YANG Kun

February 2006

To

my wife *Nancy Chen*

and

my daughter *Becky Yang*

ABSTRACT

Spirality, the distortion in the wale lines, is one of the major quality problems of single jersey knitted fabrics. It influences not only the fabric aesthetics, but also decreases fabric utilization yield during the cutting process. Many factors cause the spirality, some associated with the yarn, and some with the knitting and other processes. Among all these factors, yarn residual torque or twist liveliness is the fundamental one. Spirality occurs when the residual torque is released. A new spinning technique had previously been developed in the laboratory to make a new **Torque Balanced Singles** (**TBS**) ring spun yarn. The TBS technique takes the advantages of the low twist yarn of a low residual torque and a higher productivity, and the high twist yarn of increased fiber migration and higher strength in one step by using a specially designed device which is similar with a pin false twister.

In this study, the spinning mechanism was closely examined and the effect of reduced triangle was investigated. An extremely high twist was introduced for increasing fiber migration and obtaining a compact yarn structure. Then the yarn was de-twisted and a low twist yarn was finally produced. The spinning triangle was also examined by using a transparent top front roller and colored rovings.

The structure of the TBS yarn was examined and compared with corresponding conventional ring spun yarns. Firstly, yarn surface was studied experimentally. Yarn diameter variation was investigated by calculating yarn diameters and observing

Blackboard images; yarn surface features were demonstrated by analyzing SEM photos; and yarn surface hairiness was evaluated by using a Zweigle G566 hairiness tester. The results of these experiments indicate that the TBS yarn exhibits a greater variation of yarn diameter: in some parts of the yarn, fibers are tightly wound on the yarn body, showing a compact structure, and in some parts, the yarn demonstrates a slightly looser structure. Yarn cross-sectional structures were also studied by using the microscopy. The TBS yarn has a radial packing density pattern of a compact core which differs from its corresponding conventional ring spun yarns. This may contribute to the reduction of yarn residual torque and reinforce yarn strength. Fiber path within the TBS yarn was examined by using the tracer fiber technique. The 2-D images of the colored fibers show that the TBS yarn has more frequent fiber migrations which differ from conventional ring spun yarns. 3-D reconstruction of the fiber path demonstrates that the fiber basically follows a helical path with many migrations. Further analysis shows that a certain proportion of fiber segments have a rotational tendency whose direction is opposite to the yarn twist direction. This probably explains the reduction of yarn residual torque in another way.

A mathematical model was established based on the results of the investigation of yarn structure and the assumption that the yarns are elastic and no inter-fiber friction and viscosity. An energy method and the discrete fiber modelling principle were adopted. A series of sinuous functions was used for simulating the fiber migration, and a changeable radial packing density was adopted for representing the fiber distribution in the yarn cross-section. It was demonstrated to be possible to further reduce yarn torque by introducing an appropriate fiber migration pattern.

Several optimization experiments of the yarn modification system were conducted by using the response surface methodology. A two-step scheme was adopted. The yarn twist factor and the speed ratio were identified as the two key factors. Response surface experiments for 16Ne, 20Ne and 30Ne yarns were carried out, and optimal conditions were determined. A comparison was carried out between the optimizations of the yarns with different yarns counts (16Ne, 20Ne and 30Ne). The effect of spinning machines on the properties of the TBS yarns was evaluated by conducting three optimizations of the 20Ne yarn on Spin tester, Zinser 319SL and Toyota RY spinning machines.

Finally, TBS yarns and plain knitted fabrics were produced for evaluating the effect of the modified spinning system on the performance of the yarn and resultant fabrics. The results show that the TBS yarn has a lower residual torque and relatively higher strength simultaneously. Others such as hairiness and evenness are similar with or not worse than their corresponding conventional ring spun yarns. Plain knitted fabrics were produced by using greige yarns and package dyed yarns on two commercial circular knitting machines in a factory. The results of the measurement of the greige, piece dyed and yarn dyed stripe fabrics show that the fabric spirality can be dramatically reduced by using the TBS yarns. Compared to their control fabrics, the TBS fabrics have better or similar properties in dimensional stability, fabric weight, bursting strength and pilling resistance etc. The laboratory results are in agreement with the feedback from a knitting factory who conducted a large scale trial of TBS yarns.

PUBLICATIONS

Conference Publications

1. YANG K., YIP Y.K., TAO X.M., WONG S.K., WONG K.K., MURRELLS C.M., XU B.G., HUA T., and LEUNG C.L. Development of Nu-Torque™ Singles Yarn to Reduce Spirality of Single Jersey Knitted Fabric. Proceedings of The Textiles Institute 83rd World Conference (83rd TIWC). Shanghai, China, pp.515-518, 23-27 May 2004

2. YANG K., TAO X.M., YIP Y.K., WONG K.K. and XU B. G. The Optimization of Working Parameters of Nu-Torque™ Singles Ring Knitting Yarn Using Response Surface Methodology. Proceedings of 4th World Textile Conference (Autex 2004). Roubaíx, France, 22-24 June 2004

3. YANG K., TAO X.M., LAM J. and XU B.G. Effect of the Dimensional Change on Fabric Spirality. Book of abstract of the Fiber Society Spring 2005 Conference. St Gallen, Switzerland, pp.44, 25-27 May 2005

Refereed Publications

1. YANG K., TAO X. M., YIP Y. K., WONG K. K., and XU, B. G. The Investigation and Application of a Novel Ring Knitting Yarn. Journal of Textile Research. Vol.25, No.6, PP.58-60 (2004)

2. YANG K., TAO X. M., XU B. G. and LAM K. C. Structure and Properties of Low Twist Short-Staple Singles Ring Spun Yarns. Submitted to Textile Research Journal.

3. K. Yang, X. M. Tao, J. Lam, B. G. Xu, Torque-Balanced Singles Ring Spun Yarns for knitting, Part I: Spinning Mechanisms, Structure and Properties of Yarns, to be submitted to Textile Research Journal.

4. K. Yang, X. M. Tao, J. Lam, B.G. Xu, Torque-Balanced Singles Ring Spun Yarns for knitting, Part II: Properties and Performance of Resultant Knitted Fabrics, to be submitted to Textile Research Journal.

5. K. Yang, X. M. Tao, J. Lam, A Torsional Model of Yarns with Multi-wavelength Migration Fibers, to be submitted to Textile Research Journal.

ACKNOLODGEMENTS

I would like to express my sincere gratitude to my chief supervisor Prof. Xiao-ming Tao for her patient guidance, continuing encouragement and critical comments. Her enthusiasm in scientific pursuits and indefatigable dedication to research study inspired me.

I would like to express my sincere special thanks to my supervisor Dr. Kowk-cheong Lam for his comments, support and continuing encouragement.

I am very grateful to Mr. Yam-Kuen Yip, Dr. Kowk-po Cheng and Mr. Sing-kee Wong for their support, advice and helpful discussions during the investigation of structure and properties of the developed yarns.

I wish to thank Dr. Ka-fai Choi for his helpful discussions during the investigation on yarn structure and the establishment of yarn model.

Many thanks to Dr. Bing-gang Xu and Mr. Tao Hua for their support and in-depth discussions during the course of this study.

I extend my appreciation to Dr. Debbie Jiang and Dr. Bo-an Ying for their support in the investigation of yarn structure and the computation of the yarn model.

I am indebted to Dr. Ka-kee Wong, Ms. Charlotte Murrells and Mr. Suk-yee Chan for their support and help during the production and test of the developed yarns and fabrics.

Thanks are given to our technicians in the Spinning Workshop, Knitting Workshop and Dyeing and Finishing Working, as well as the Physical Testing Laboratory and Fabric Testing Laboratory for their kind assistance for my experimental work.

The financial support from the Innovation and Technology Commission, The Government of the Hong Kong Special Administrative Region and the Hong Kong Polytechnic University in the form of expenses of international conferences is sincerely acknowledged.

CONTENTS

LIST OF TABLES

LIST OF FIGURES

LIST OF APPENDICES

CHAPTER 1

INTRODUCTION

1.1 Research Background

The origin of this investigation was from an attempt of solving the problem of the spirality of single-jersey plain knitted fabrics by developing a novel yarn.

Spirality, the distortion in the wale lines, is one of the major quality problems of single jersey knitted fabrics. It not only influences the fabric aesthetics shown in Figure 1-1, but also decreases fabric utilization yield during the cutting process shown in Figure 1-2, and leading to the increase of the material cost.

Figure 1-1 Seam displacements on a knitted sweater

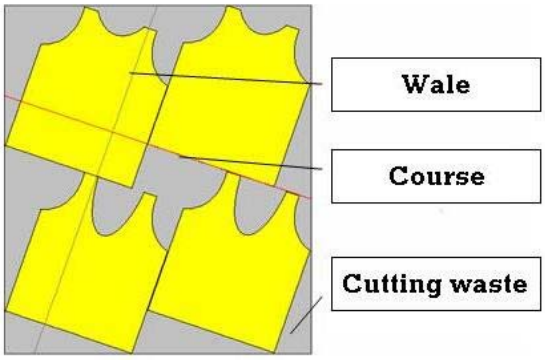

Figure 1-2 Cutting waste

According to previous literatures (Araujo and Smith 1989; Lau et al. 1995; Lau and Tao 1997; Tao et al. 1997; Primentas 2003), spirality is caused by many factors; some are associated with the yarn, and some with the knitting and other processes. Among all these factors, yarn residual torque or twist liveliness is the major one. Spirality occurs when the residual torque is released. Since yarn residual torque is highly related to yarn torque that is inserted during twisting process, thus yarn residual torque is related to the amount of yarn twist introduced during the spinning process.

To eliminate spirality, many methods associated with the yarn used, the knitting and fabric parameters as well as post-knitting treatments are usually used in factories. For example the factory can use plied yarn, steaming treatment, etc., to reduce or eliminate fabric spirality. However, several drawbacks are associated with these techniques, such as high production cost or the limit on the plied yarn count.

1.2 Objectives

The main purpose of the project is to improve the properties of cotton plain knitted fabrics by developing a **Torque Balanced Singles** (TBS) ring spun yarn. The improvements mainly focus on the reduction of spirality angle of the fabric. The investigations of the modification principle, the examinations of the structure of the TBS yarn, as well as and the modeling of the torsional behavior of the TBS yarn are included in the targets. The objectives of the project include:

- To develop technologies for modifying yarn structure and improving yarn properties, and manufacture a TBS yarn for knitting production.
- To investigate the mechanism of the TBS yarn and establish a mathematical model for describing its torsional behavior.
- To optimize the spinning parameters according to practical requirements for producing a TBS yarn with desired performances.
- To investigate the relationship between yarn torque and the spirality of plain knitted fabrics.
- To produce plain knitted fabrics by using the TBS yarn and evaluate their performances.

1.3 Significance

1.3.1 Significance and values

The significance of the project is to develop a novel spinning technology, leading to the resultant products having novel characteristics and improved quality. The novel spinning technology developed can be used to produce the TBS yarns by a single step on a modified ring-spinning machine.

1.3.1.1 Novel spinning technology

A modification device was developed previously and installed between the front rollers and the yarn guide on a conventional ring spinning frame. By using it, the fiber arrangement in produced yarn is modified, leading to the improvement of yarn torsional properties.

1.3.1.2 Novel yarn structure and properties

Yarn properties are mainly determined by its structure and the material used. In this study, therefore, we considered to improve yarn properties by modifying its structure. The novel yarn structure differs from that of the conventional ring spun yarn in its radial fiber distribution and fiber path within the yarn. The TBS yarn also has a unique appearance. These structural features determine the yarn having unique performances, i.e., lower residual torque and acceptable other properties such as yarn strength and hairiness etc.

1.3.1.3 High productivity

Since a lower twist factor would be adopted during the spinning process of the TBS yarn, the reduction of twist results in the increase of the delivery speed of the front rollers, leading to an increase of spinning productivity.

1.3.1.4 Improved fabric properties

The TBS ring spun knitting yarn can meet the requirements of knitting process. By using the TBS yarn, the spirality of the plain knitted fabrics were dramatically reduced, other properties such as fabric bursting strength, pilling resistant etc. were similar with or not worse than those of the fabrics produced by using the corresponding conventional ring spun yarns. It is also estimated that the TBS plain knitted fabric possesses a comfortable and soft handle due to the lower twist of the yarn used. In addition, this technology can save production cost in yarn manufacturing and fabric finishing, as well as save material

cost in the garment manufacturing. In general, it can achieve a balance of the high quality and low cost.

1.3.2 Applications

By using the TBS yarns and fabrics, it is easy to solve the problems related to the shape stability of the knitted garments. For example the TBS yarns can be used for producing stripe or check T-shirts or sweaters. It can reduce the fabric waste during cutting process, and keeps the shape of the garments after washing and other treatments. Its soft handle may lead to other favorable fabric performance. In addition, fabric and garment designers may apply the unique structure and properties of the TBS yarns and fabrics to their products.

1.4 Research Methodology

1.4.1 Literature review

Previous literatures were reviewed with the following focuses:

- Yarn spinning and its modification.
- The relationship between yarn structure, properties and fabric properties.
- The mechanics and models of yarns and fabrics.

1.4.2 Theoretical investigation on torsional behavior of TBS yarns

Previous work shows that it is possible to modify the structure of a conventional ring spun yarn. The mechanism of the modification will be studied for the reduction of the yarn torque.

Yarn structure will be examined firstly. Surface, cross-section, and fiber path within the yarn can be used for revealing some aspects of the yarn structure. Optical and electronic microscopes, blackboard as well as tracer fiber technique were considered as the main tools. After analyzing the results, we can identify the structure of the TBS yarn. Then a model was established by using an energy method and based on a modified cylindrical helix structure as well as other assumptions. The model theoretically verified that if the assumption that it is possible to reduce yarn torque by introducing a migration pattern is true.

1.4.3 Spinning parameter optimization and production of TBS yarns

The spinning and laboratorial trial of the TBS ring spun yarns will be conduced in our lab (spinning workshop). After preliminary spinning trials, the optimization of spinning parameters will be carried out for obtaining the optimal parameters. The Response Surface Methodology will be adopted for this optimization; and the relationships between yarn properties and spinning parameters will be found out. The optimization will also be extended to various finer and coarser yarns and produced by using different machines for verifying the adaptability of the TBS system. Thereafter, a large quantity production of the TBS yarns with the optimal parameters will be conducted for evaluating the reliability and stability of the yarn properties. Others such as the effects of winding, cleaning, and the measurement of yarn faults will be also considered for fully assessing the TBS yarn.

1.4.4 Improvement of fabric properties

Plain knitted fabrics will be produced by using weft circular knitting machines rotating in both directions for evaluating the performance of the resultant fabrics. For comparison, conventional singles and plied ring spun yarns will also be included in this production. The spirality of greige, piece dyed and yarn dyed fabrics will be measured before and after three 5-A washing and tumble cycles. Others such as fabric weight, bursting strength etc will also be evaluated. The results demonstrate the effect of the TBS yarn on the properties of the fabrics. In addition, the relationship between yarn residual torque in terms of wet snarling and the angle of fabric spirality will also be investigated by using the statistical method.

1.5 Scope of the Thesis

This thesis consists of eight chapters. Chapter 1 introduces the background, objectives, the significance and values, as well as the methodology of this investigation. Apart from them, an outline of this thesis is also included.

Chapter 2 briefly reviews previous investigations on spun yarns and knitted fabrics. Many researchers assumed some yarn structural geometries, and studied the yarn properties based on these assumptions. The relationship between the spirality of plain knitted fabrics and the influencing factors was investigated. These literatures are the basis of our development the TBS spinning yarns and the selection of spinning and knitting parameters.

Chapter 3 provides details of a device that modifies yarn structure, and reduces yarn residual torque. Based on the investigations on the fiber arrangement and migration, a mechanism is proposed. The yarn path on a ring frame is divided into two parts: the upper part and the lower part. In the upper part, extremely high twist was introduced to reinforce fiber migration. Setting is conducted with the extremely high twist simultaneously. In the lower part, extra twist is removed from the yarn, and some wild fibers are wound on the body of the yarn by the de-twisting rotation. Preliminary spinning and test are also included in this chapter.

Chapter 4 is mainly concerned with the examination of the structure of the modified yarn. Yarn cross-sectional structure is inspected. Yarn radial packing density shows a non-even distribution of fibers in the yarn cross-section. This distribution partially influences on yarn torque. Fiber path within the yarn is also investigated by using the tracer fiber technique. By a combination of these two aspects of the structure, the structure of the modified yarn can be estimated, and its features then be summarized. Apart from yarn structure, in this chapter, some results of the preliminary study on yarn tensile and torsional properties are presented.

In Chapter 5, a mathematical model is proposed for theoretically describing the torsional behavior of the TBS yarn. A new yarn geometry with fiber migration is introduced from the idealized cylindrical helix. An energy method and discrete-fiber-modeling principle are adopted, and the “shortest-path’ hypothesis and changeable fiber radial density are considered. The verification experiments are reported with some cases.

Chapter 6 of this thesis is the optimization of the spinning parameters. The Response Surface Methodology is adopted and a two-step scheme is presented. The first step is the Fractional Factorial Experiment. Factors that have or may have influences on yarn properties are included. The yarn twist factor and the speed ratio of the rotational speed of the couple rotor and the spindle speed are identified as the two most important factors. Then the second step experiment, Response Surface Experiment, is conducted. The results reveal that it is possible to produce a yarn with desired torsional and tensile properties by using a set of spinning parameters. Further investigations indicate that the modification device can be used for producing the TBS yarns in a wide range of yarn counts, and the spinning process can be conducted by using different materials and on various spinning machines.

The details of the productions of the TBS yarns and resultant fabrics are provided in Chapter 7. Some TBS yarns are evaluated for evaluating their tensile and torsional properties, mass variation, and hairiness. Apart from these, the effects of winding and dyeing processes are also evaluated. Plain knitted fabrics are made from the TBS yarn, conventional singles ring yarn and plied yarn on two types of circular weft knitting machines which rotate in opposite directions in a factory. Greige fabrics, piece dyed fabrics and yarn dyed stripe fabrics are included in this test. Factory trial results show that the TBS yarns can reduce spirality and improve other properties of the TBS fabrics.

Finally, Chapter 8 provides a general summary and conclusions. The discussions of the limitations and problems are also included together with suggestions for future study.

CHAPTER 2

LITERATURE STUDY OF RING SPUN YARNS AND PLAIN KNITTED FABRICS

2.1 Introduction

Fibers are the basic elements to form yarns. A fiber has its own specified geometry and properties. When fibers are spun to form a yarn, the spinning process affects yarn properties by influencing yarn structure. That is to say, the spinning system determines the yarn structure and it works with the fiber to determine the yarn properties.

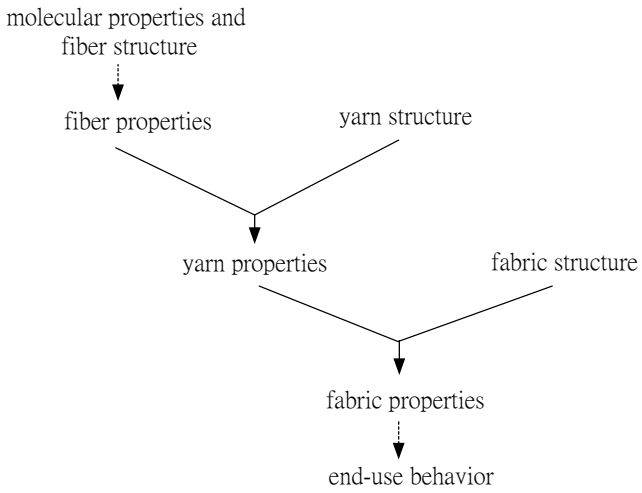

Figure 2-1 Interrelations of the structure and property of fibre, yarn, and fabric (Hearle et al.1969)

Knitted fabric properties are related to the yarn used (Hearle et al. 1969; Wynne 1997). In factories, in order to obtain desired performances, various kinds of yarns are often used. Apart from the yarn, fabric structure, knitting variables and downstream treatments also affect the fabric properties. The interrelations between the structure and properties of fibers, yarns, and fabrics are illustrated in Figure 2-1.

In the past few decades, some unconventional staple spinning processes e.g. rotor and air-jet spinning have been developed for achieving higher production per unit spinning unit. However, ring spun yarn has always been, and still is, the undisputed quality benchmark within the spun yarn sector. Yarns produced by the ring spinning method currently account for a higher percentage of all staple yarns produced (Wynne 1997). It is, by far the most popular method and is likely to retain this position because of the following advantages:

- Ring spinning is a very flexible method of yarn manufacture. It is possible to process most fibers into yarns using ring spinning and the range of linear densities which can be produced is the widest of any spinning system.

- The yarns produced possess the performance, aesthetic and tactile properties to which consumers are accustomed. Ring spun yarns have levels of irregularity which provide interest in flat fabrics, have a pleasant handle due to the orderly fiber arrangement and surface hair, and have predictable strength and elongation characteristics.

- The mechanisms used in ring spinning are relatively uncomplicated and tend to require lower levels of capital and personnel investment than alternative systems.

Therefore, the modification of the structure of the ring spun yarn and the ring spinning system is our main projective.

2.2 Yarn Structures and Properties

2.2.1 Yarn structure

Yarns are defined as long, fine structures capable of being assembled or interlaced into such textile products as woven and knitted fabrics, braids, ropes, and cords (Hearle et al. 1969). The staple yarn is one of the yarns popularly used for making knitted and woven fabrics. In practice, there are two stages usually adopted for manufacturing the staple yarns. The 1st stage consists of processes intended to produce relatively thick strands of more or less parallel fibers, known as slivers or rovings. They have no strength because the fibers slide past one another under tension; in other words, they can be drafted into fine strands. The 2nd stage of manufacture is spinning; it gives coherence and strength to the assembly. Most yarns are held together by frictional forces between the fibers.

Three ways shown in Figure 2-2 can be used to generate the necessary normal forces. They are (a) twisting, (b) interlacing, and (c) wrapping. In varying degrees, these features, or combinations of them, are found in commercial yarns (Hearle et al. 1980).

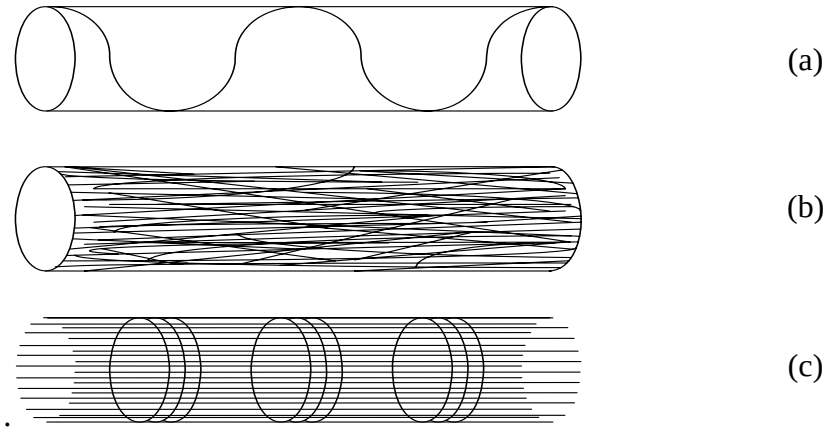

Figure 2-2 Three ways to generate transverse forces to hold staple yarns together (Hearle et al. 1980)

In staple yarns such as cotton yarns, the method of twisting is often adopted. Twist is inserted into yarns to give them coherence. The frictional forces, which alone hold the individual fibers in the yarn, are exclusively due to the transverse pressures, which develop when a fiber wrapped in a particular path round other fibers in the yarn is put under tension.

Every fiber has its distinctive cross section and moduli (tensile, bending, and torsion). For cotton fiber that is a single cell, it has a kidney-shaped cross sectional appearance with a central canal or lumen, and an irregularly twisted, collapsed, flattened tube-like appearance throughout its length. According to previous studies (Wynne 1997), the fiber specifications such as fiber length, micronaire value, fiber strength, uniformity ratio, etc have influences on the properties of the resultant yarn.

2.2.1.1 Idealized cylindrical helix structure

An idealized yarn geometry shown in Figure 2-3 is often adopted for theoretical study. It is assumed that the yarn is circular in cross section, and composed of a series of concentric cylinders of differing radii. Each fiber follows a uniform helical path around one of the concentric cylinders, so that its difference from the yarn axis remains constant. A fiber at the centre will follow the straight line of the yarn axis; but, going out from the centre, the helical angle gradually increases. Since the number of turns of twist per unit length remains constant in all layers, they also assumed that the density of packing of fibers in the yarn remains constant throughout the models; and the structure is made of a very large number of filaments, so that various complicating effects, which are due to the special ways of packing a limited number of fibers together, do not arise.

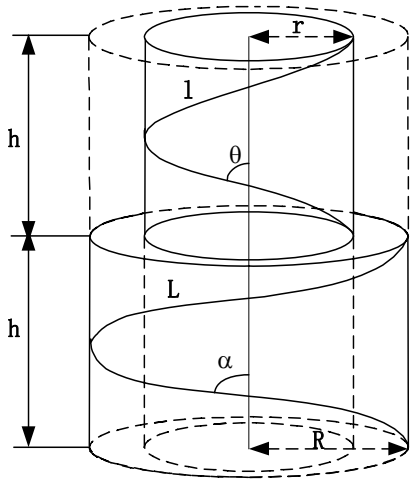

Figure 2-3 Idealized cylindrically helical path of a fiber within the yarn (Hearle et al.1969)

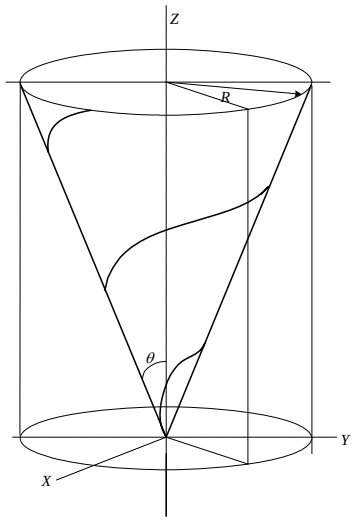

Figure 2-4 Conically helical path of a fiber within a yarn (Önder and Başer1996)

2.2.1.2 Yarn structure modified with fiber migration

Two features are necessary to generate strength and cohesion in spun yarns. One of them is the twist that results in the occurrence of transverse forces gripping the fiber and the other is variation in fiber position with the yarn so that some parts of all fibers are gripped. The former is appreciated by Peirce (1947), and the latter was investigated by Morton with the tracer fiber technique (Morton and Yen 1952; Morton 1956). Morton (1956) also established a mechanism that would result in a more or less regular migration. In this mechanism, fibers lying along the axis of a twisted yarn was assumed following a shorter path, and undergone a lower tension than those lying near the outside. The positions of the fibers under low tension can be replaced by the others, showing a cyclic interchange of position. Then Hearle and Merchant (1962) investigated the nature of migration by using a seven-ply structural model. And Hearle and Bose (1966) established a geometrical mechanism of the fiber migration. Riding (1964) improved the tracer fiber technique by introducing a plane mirror so that the three dimensional path of a fiber can be reconstruction.

Hearle et al (1965) realized that the control of fiber migration is a possible way of controlling yarn properties. Thus they proposed an ideal migration model. The ideal migration pattern was assumed that the fiber migrates regularly and uniformly from the outside to the center of the yarn and then back to the outside. The density of packing of fibers in the yarn is constant throughout the yarn. Treloar (1965) studied the ideal migration of filament in his way by using the same assumptions. He pointed out that the

filament path has both periodic and random features, the degree of regularity being apparently dependent on the type of twisting process and other factors.

Many researchers also studied the fiber migration, and established their own models. For example Önder and Başer developed a yarn model shown in Figure 2-4 based on a conical helix fiber path (1996). They assumed that the yarn is a single fiber yarn uniform along its length, with a circular cross section of uniform specific volume; fibers follow identically conical helix path equally spaced along the fiber axis, and the yarn axis is also the axis of conical helices of all fibers; and the radius of the helix changes regularly between zero and the yarn radius.

2.2.1.3 A staple yarn structure with considering slippage effect

The role of twists in a continuous filament yarn is mainly to produce a coherent structure that does not readily disintegrate under lateral stress. Twist is therefore not essential in offering tensile strength to the structure, but in fact lowers the strength of a yarn because of the induction of filament obliquity. However, the twists in staple fiber yarns have the primary function of binding the fibers together by friction to form a strong yarn. Pan (1992, 1993) developed his constitutive theory shown in Figure 2-5 for staple yarn with considering a slippage effect by assuming that a staple yarn can be considered to a short fiber composite and a fiber can be viewed as embedded in a matrix made of the neighboring fibers, except that this fiber adheres to the matrix by means of frictional force rather than chemical bonding as in a composite.

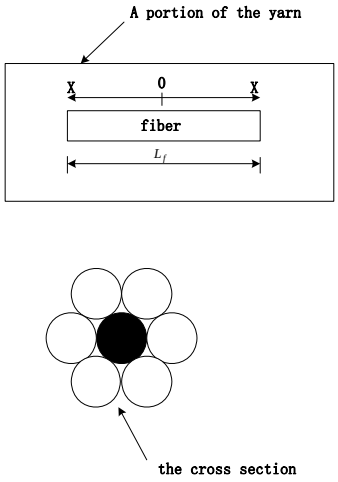

Figure 2-5 A fiber embedded in a matrix made of adjacent fibers in a yarn (Pan 1992)

2.2.2 Some basic mechanisms and theories

Many research studies adopted a model of the idealized cylindrical helical yarn geometry. In practice, however, the lengths of path followed by fibers at different radial positions in the yarn are different. The fiber at the center follows a straight path, whereas the outers follow much longer helical paths. If giving a tension, a migration will occur, the fibers in the out-layer undergo higher tension, leading to a movement towards to yarn core, while the fibers in the center will buckle and be forced out (Hearle et al 1969).

2.2.2.1 Distribution of fiber tensile strain in a yarn cross-section

Previous literatures stated that the torque generated during yarn twisting has three components due to fiber torsion, fiber-bending, and fiber tension. And the torque generated by fiber tension stresses is a major component of the total yarn torque (Postle et al. 1964).

After analyzing the distribution of fiber tensile stresses within a twisted yarn, Bennett and Postle (1979) stated that the basic yarn structure and the mode of twisting are both influential in determining the distribution of fiber tensile and compressive strains through the yarn cross-section and are the key factors in the generation of yarn torque. They analyzed the torque distribution of a yarn in two limiting forms of fiber geometry: no migration, and perfect migration. For the case of no fiber migration, they assumed that all fibers are constrained to form perfect concentric helices. Under such conditions, yarn length retraction happens during twist, and its magnitude directly determines the tensile strain in the fibers. If the fiber tensile strain is zero, from the helix geometry, the corresponding radial position of the fiber r_0 is expressed as

$$r_0 = \frac{1}{2\pi T_y}\left(\frac{1}{\Delta^2} - 1\right)^{1/2} \qquad 2\text{-}1$$

Where T_y is the yarn twist in turns per unit length, and Δ represents a relative length respected to the length of a twisted yarn l_y and its initial untwisted, unstrained length l_0. It is clear that all fibers in the yarn cross-section at radial positions $r > r_0$ are in tension, while all fibers in a central core, i.e., $r \le r_0$ are longitudinally compressed or bulked.

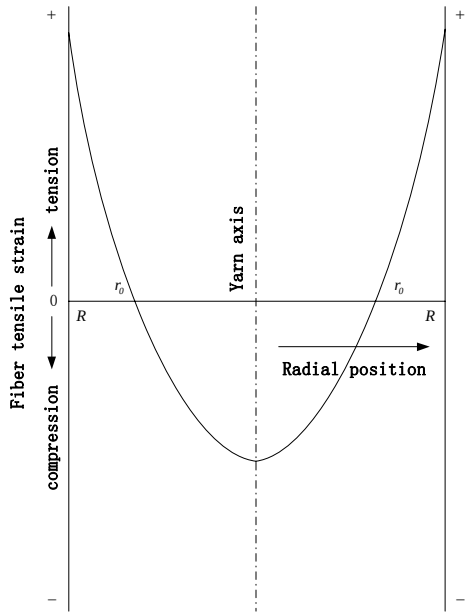

Figure 2-6 The distribution of fiber tensile strain as a function of radial position in a twisted yarn (Bennett and Postle 1979)

Figure 2-6 shows the distribution of fiber tensile strain. When a structure is subjected to high tensile, compressive, and torsional stresses simultaneously, its limits of elastic stability become important factors in the determination of its mechanical behavior. The particular deformations of lateral buckling and torsional buckling may intuitively be necessary considerations on the analysis of the yarn-twisting process.

For the case of a perfect migration, Bennett and Postle (1979) said that the yarn-torque components due to fiber tension in a structure in which fibers freely migrate is much more directly related to the applied yarn tension than is the corresponding component in a non-migration structure.

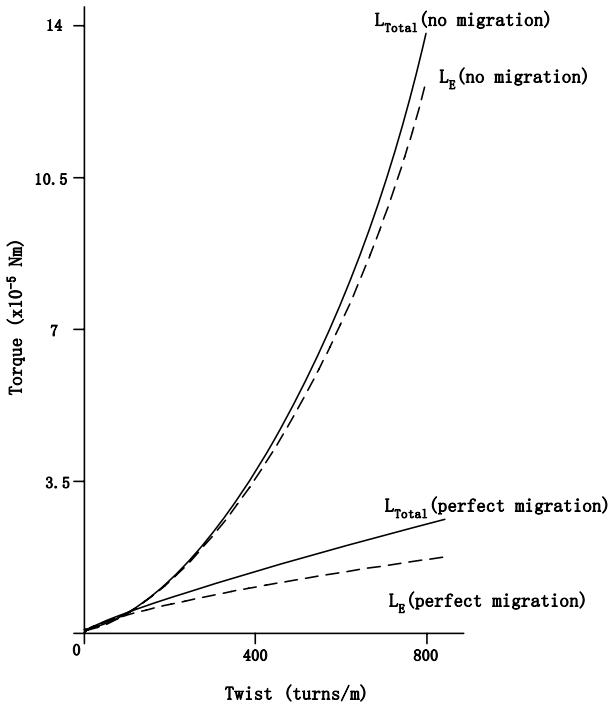

Figure 2-7 A comparison of theoretical torque-twist curves between two extreme forms: no migration and perfect migration (Bennett and Postle 1979)

Figure 2-7 is a diagram showing the torque-twist relationships of two migration assumptions. L_{Total} is the total yarn torque and L_E is the yarn torque due to fiber tension. It indicates that the level of torque generated during yarn twisting is critically dependent on the degree of fiber migration. In a non-migration yarn, its tensile stresses are concentrated in the outermost layers of fibers, where their contribution to the torsional couple about the yarn axis is maximized. No such radial distribution exists in a yarn in which perfect migration takes place, and consequently the yarn torque generated during twist is much lower. It is also noted that the yarn torsional properties are progressively more sensitive to the degree of fiber migration as the yarn twist increase. If fiber

migration is completely inhibited, the total yarn torque at high twist is several times as great as that of the yarn in which perfect migration takes place.

2.2.2.2 Fiber migration

In practice, however, it is difficult to reach this perfect migration state by using the idealized cylindrical helix model. Thus it is necessary to modify the idealized helix model.

Tracer fiber technique is a good manner to identify the fiber path within a yarn. It was developed by Morton and Yen (1952). And then Riding (1964) installed a plane mirror near the yarn in the liquid, with the plane of 45° to the direction of observation. Thus a three dimensional path of a trace fiber can be re-construction. By using the tracer fiber technique, some researchers improved the idealized model. For example Hearle, Gupta, and Merchant (1965) modified the idealized helical geometry. The ideal migration pattern is defined as one in which the fiber migrates regularly and uniformly from the outside to the center of the yarn and then backs to the outside. And the fiber packing density in the yarn is constant throughout the yarn.

2.2.2.3 Mechanisms of fiber migration

As we know that fibers round a long path on the outside of a yarn would develop a high tension while fibers following the shorter straight path in the center would be under lower tension. These differences would cause an interchange of position between high- and low-tension fibers and thus result in a more or less regular migration. In order to push a fiber out from a central position, it is necessary: a) to overcome its own tension,

which is tending to hold it in the central position and prevent it moving to a less favorable position; and b) to overcome the pressure from the neighboring fibers which tend to hold it in position (Hearle et al. 1969). Hearle and Merchant (1962) experimentally investigated the migration in a seven-ply structure. They assumed that migration would take place only when the tension in the central ply has fallen to zero and some slack has accumulated. If the twisting tension is high enough, the central ply will always be under tension and migration will not occur. But, if the twisting tension is less than a certain value, then, when an extended yarn transfers from the outer layer to the core, the gradual supply of excess length of core yarn will reduce the core yarn extension to zero and allow slack to accumulate, resulting in migration.

Fiber migration can also be explained by using geometrical forms (Hearle and Bose 1965). Three possible ways of twisting illustrated in Figure 2-8 were proposed. They are: a) twisted cylindrical form; b) twisted ribbon form; and c) wrapped ribbon form. A major difference between the twisted and wrapped form is obvious. Hearle and Bose (1966) stated that in a solid material, the ribbon forms would be stable; this would not be so for a bundle of fibers. The structures would inevitably collapse to allow the individual fibers to take up more favorable positions with shorter path lengths. In the degenerate forms, the hollow in the center of the wrapped form and the corners of the twisted ribbon form disappeared.

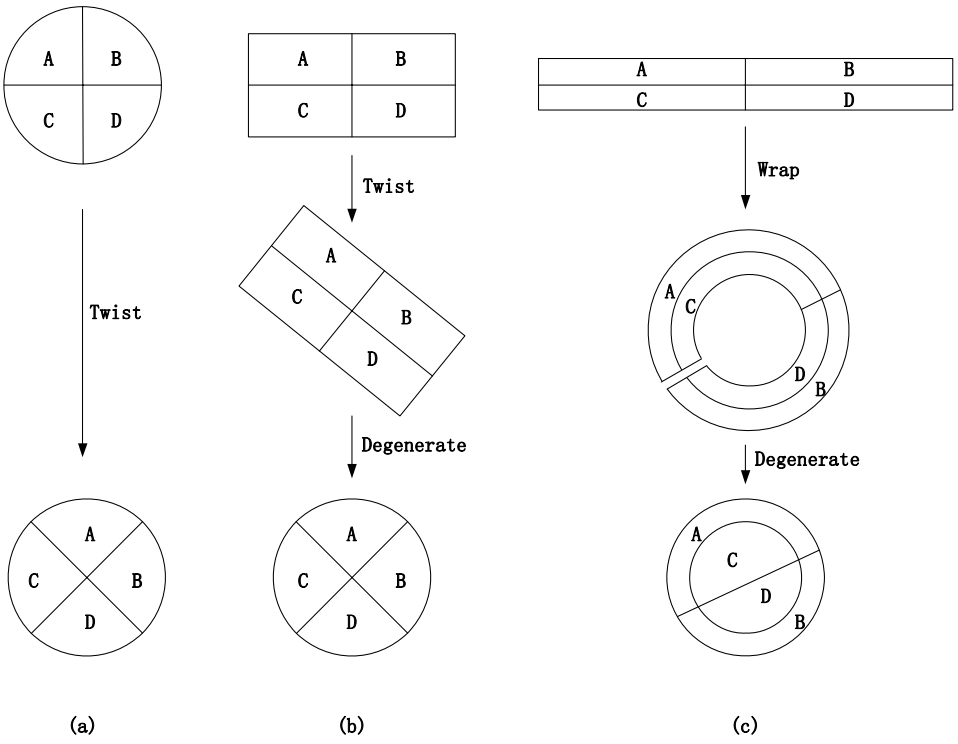

Figure 2-8 Three forms of yarn twisting (Hearle and Bose 1966)

(a) cylindrical twist; (b) twisted ribbon twist; (c) wrapped ribbon twist

Hearle and Bose (1966) also stated that the tendency of the fibers to collapse into the most favorable positions means that all three forms become cylindrical bundles of fibers, although some unevenness of packing may result from a failure to collapse completely. After collapse the twisted forms come to be identical. Thus only two forms to be considered: twisted and wrapped structures. The important distinctions between them are in the relative positions of fibers before and after twisting. Simulation by using filaments showed that at a low level of twist, continuous twisting of two layers fed through a slot gave a twisted ribbon form, finally reaching an irregularly shaped, almost close-packed structure. At a higher level of twist, the buckling was more irregular and a multilayer

structure appeared. Its finial structure was cylindrical close-packed with most of one color of threads on the surface and most of the others in the core.

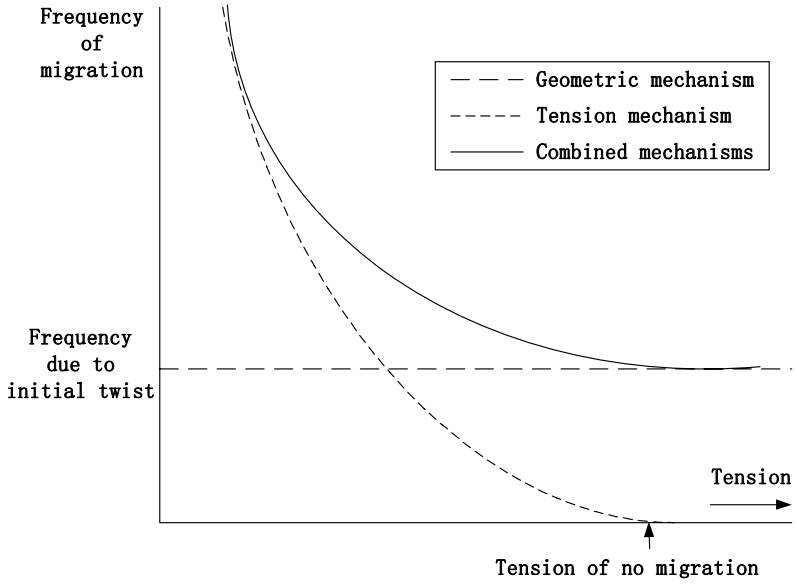

Figure 2-9 Variation of frequency of migration with twisting tension resulting form a combination of mechanisms (Hearle et al. 1965)

Two mechanisms of migration are not mutually exclusive (Hearle et al. 1965) and when both can occur the variation of frequency of migration with twisting tension would be expected to have the general form shown in Figure 2-9. At low tensions, the tension mechanism would demand a rapid migration and would thus be dominant. But in high tension, the migration would not be completely suppressed, but would instead fall to the value given by the geometry mechanism. At intermediate values one can expect both mechanisms to play a part, with the geometric mechanism setting a basic pattern, but deviations from this occurring as necessary to accommodate tension differences.

2.2.3 Previous investigations on mechanics of staple yarns

Yarn mechanical behavior has been investigated by many researchers (Platt 1950; Kilby 1964; Hearle et al. 1969, 1980; Dogu 1972; Postle et al. 1988; Pan 1992, 1993). Most of them focused on the study of the strength and tensile behaviour of staple fiber yarns by using continuous-filament yarns. Sullivan (1942) made a serious attempt to relate the strength of a staple yarn to the properties of the individual fibers and geometry. Platt (1950) conducted the similar investigation for continuous-filament yarns and related yarn strength to the filament strength and yarn parameters. Hearle et al (1969) developed Platt's theory by taking into account the internal pressures acting on the filaments as the result of the applied yarn tension and the curvature of the filament. Since the yarn twist and fiber migration are the only reasons why a bundle of short fibers is held together in a linear assembly. Moreover, in staple fiber yarns, the fiber-volume fraction is low and variable. However most of the success in this research has been in the area of filament yarns, rather than staple yarns.

Recently, many researchers studied the yarn mechanics in their own ways. Miao and Chen (1993) theoretically analyzed the yarn twisting dynamics. Pan (1992, 1993) set up his models (Figure 2-5) for explaining the mechanics of short fiber yarns. Jiang et al (2002) studied the tensile behavior of a rotor spun yarn by introducing the changeable packing density and pitch length into an idealized cylindrical helix model. And Wang et al (2004) studied the tensile behavior of low twist staple fiber assemblies by using the finite element method (FEM). He stated that the deformation of the yarn before peak load is mainly due to the elastic deformation of fibers. At peak load, yarn failure is initiated after which extensive fiber slippage takes place in a local section ("crack

plane"). The deformation in this stage consists of basically two parts: fiber separation at the crack plane and the elastic deformation of the yarn away from the crack plane.

Some researchers also studied yarn torsional behaviour. Platt et al (1958) were the first to calculate the torque due to fiber-bending and fiber torsion in twisted singles yarn by using a force method. Then Postle et al (1964) calculated the torque due to fiber tension and found that the component due to tension is the greatest component contributing to the total yarn torque. Other researchers studied the yarn torsional behaviour by using experimental or theoretical methods (Dhingra and Postle 1974, 1975; Bennett and Postle 1979, 1981; Tandon et al. 1995; Choi et al. 1998, Mitchell et al. 2006). Detail review of the yarn torsional behaviour is reported in Chapter 5.

2.3 Structure and Properties of Plain Knitted Fabrics

Knitting is a fabric forming method that differs from weaving and others. It has many characteristics due to its unique loop structure. The ability to be engineered to exacting requirements and their potential for producing shaped articles as well as fabrics enables knitting technology to rapidly response to requirements of its markets in sweater, hosiery, jersey, etc (Spencer 2001).

2.3.1 Structure of a plain knitted fabric

Knitting is the production of fabric by forming loops with yarn, which are interlaced in a variety of ways to form the fabric. In weft knitting, the loops are formed across the

width of the fabric, and each weft thread is fed, more or less, at right angle to the direction in which the fabric is produced (Spencer 2001).

Plain knitted or single jersey is one of the four primary structures from which all weft knitted fabrics and garments are derived. It is produced by the needles knitting as a single set, drawing the loops away from the technical back and towards the technical face side of the fabric. Its technical face is smooth; with the side limbs of the needles loops having the appearance of columns of V's in the wales (Figure 2-10). On the technical back, the heads of the needle loops and bases of the sinker loops form columns of interlocking semi-circles (Figure 2-11).

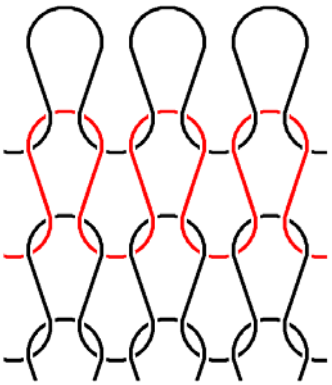

Figure 2-10 Technical face of the single-jersey knitted fabric

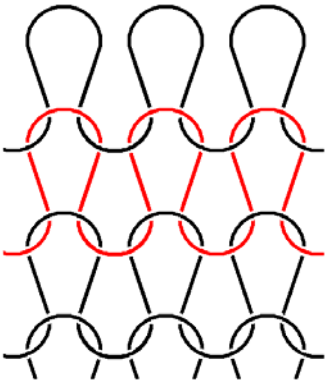

Figure 2-11 Technical back of the single-jersey knitted fabric

Plain structure is the simplest and most economical weft knitted structure to produce and has the maximum covering power. It normally has higher potential recovery in width after stretching. Its products include underwear, outerwear, and hosiery and so on. The fabric and garment have soft hand, comfortable, good elasticity and air permeability, etc

(Punj et al. 2000). However, at the same time, it also has several problems related to dimensional distortion (Ceken et al. 2002).

2.3.2 Loop geometry

For understanding the dimensional behavior of knitted fabrics, Pierce (1947), Doyle (1952, 1953), Shinn (1955), Munden (1959), Leaf (1960, 1961), Postle et al (1967, 1968), as well as Demiroz et al. (2000) and Choi et al. (2003) have contributed to the geometric analysis of plain knitted fabrics. In particular, Leaf (1960) studied the geometry of the plain knitted fabric, and set a model:

$$\text{Stitch density} = \frac{K}{l^2} \qquad 2\text{-}2$$

Where: l is the stitch length, and K is not a constant but a function of several variables, including the ratio of stitch length to yarn diameter.

Since the knitted loop is a three-dimensional unit, the yarn is bent both in the plane of the fabric and in the plain at right angles to the fabric in order to produce a flat knitted structure. After knitting, the yarn, which was originally straight and desires to return to the straight state, is prevented from doing so by equal and opposite reactions from the interlocking yarns. For any one loop or row of loops to straighten, however, greater bending is necessary in neighboring loops or rows of loops in order to accommodate this change, so that the whole structure tends to go into a state of minimum energy or minimum total bending. This is the assumption raised by Munden (1959).

Munden also suggested that this configuration might be expected to be independent of yarn properties or stitch length. With these assumptions, geometrical analysis of the knitted loop indicates that the dimensions of a knitted fabric in its relaxed state are uniquely determined by the length of yarn knitted into the stitch, all other yarn and knitting variables affect only the dimensions of the fabric, either by altering the kitted stitch length or by temporarily distorting the fabric.

Shanahan and Postle (1970, 1974) theoretically analyzed the plain knitted fabrics and their tensile properties. Wada et al (1977) set up a model for controlling the dimension of plain knitted fabric. Marmarali (2003) investigated the dimensional and physical properties of cotton/spandex single jersey fabrics; he summarized the relationship between the amount of spandex and knitting variables. Choi et al (2003) also set up new loop model, and established an energy model of plain knitted fabric. He found that the degree of set of the yarn in the knitted fabric has a great influence on fabric's dimensional stability.

2.3.3 Previous investigations on fabric spirality

Cotton, being a nonthermoplastic fiber, is unstable to be heat set. They will relax naturally after knitting, resulting in changing fabric dimensions. Due to the nature of the knitting process, the fabric is knitted under high stress and extension. Thus greige cotton fabrics off the knitting machine will exhibit large and varied amounts of shrinkage. In addition, the relaxation of the yarn residual torque and other factors may result in the

fabric distortion. The fabric shape distortion has two aspects: spirality (wale skew) and drop (course skew). Here, we mainly focus on the researches of fabric spirality.

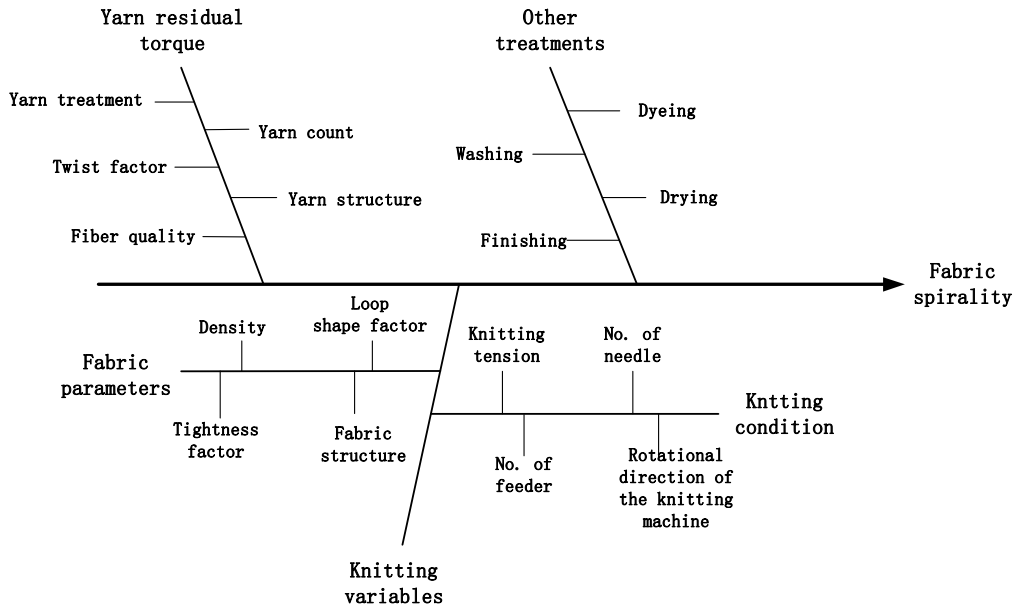

Figure 2-12 Relationships between fabric spirality and main factors which have influences on it

Many factors influence the fabric spirality. Figure 2-12 is a fishbone chart showing many factors. The following discussions will be focused on three major ones.

2.3.3.1 Effect of the yarn used

The twisted yarn is the major factor that has influences on fabric dimensional changes, partially the fabric spirality. Yarn residual torque is the main reason causing fabric spirality (Araujo and Smith 1989; Primentas 2003). The yarn will attempt to rotate inside the fabric, resulting in unsymmetrical or local distortion of the loops causing the

whole wale to be inclined. It usually works with other factors such as knitting parameters, fabric construction etc. to affect the magnitude and direction of the spirality. Normally, the bigger the residual torque, the greater the fabric spirality. In details, some aspects determine the yarn residual torque. The first is the fiber used. The fiber moduli (including tensile, bending, and torsional modules) affect the torque generated when a straight fiber is curved into a spatial path. During the deformation, the energy is stored in the fiber, and it will release in the downstream processes. Yarn linear density also has influences on yarn residual torque. Coarser yarn has more fibers in its cross section; the number of fiber as well as their radial position partially determines the magnitude of the yarn torque. Yarn structure is another factor. Different structures, which are determined by the spinning system adopted, have different fiber path and arrangement, resulting in different yarn torques. For a twisted yarn, its torque direction is determined by the twist direction. A Z-twist yarn has an opposite torque direction to the S-twist yarn. Normally, a Z-twisted yarn will cause the knitted loops to lean to the right, resulting in a fabric with a Z direction of spirality. Alternatively, an S-twisted yarn will cause the knitted loops to lean to the left, resulting in a fabric with an S direction of spirality.

2.3.3.2 Effect of machine and fabric variables

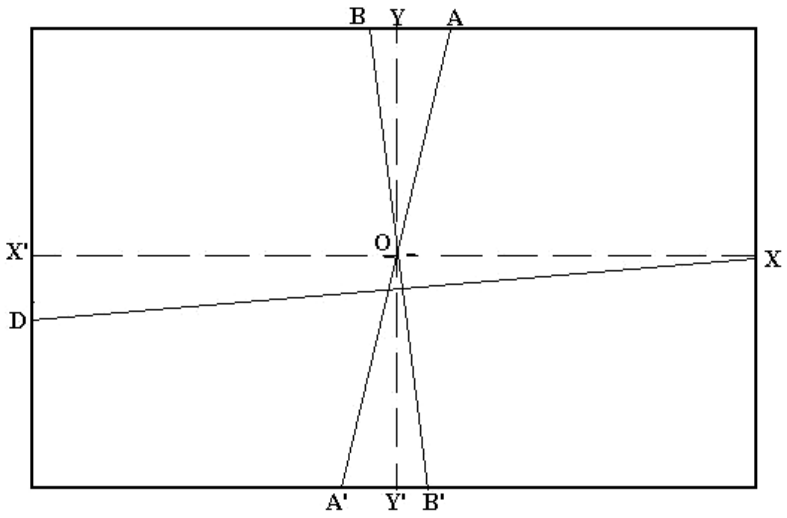

Figure 2-13 Spirality of a single jersey fabric knitted from a Z-twisted yarn on a multi-feeder circular knitting machine and with a clockwise rotational direction (Araujo and Smith 1989)

XX’ = position of a course due to the total spirality;

AA’ = position of a wale due to the total spirality;

BB’ = position of a wale when spirality (drop) due to the number of feeders exists;

XD = position of a course when spirality (drop) due to the number of feeders exists;

X’D = displacement between two consecutive courses knitted by the same feeder;

Some knitting and fabric parameters have influences on fabric spirality. Several researchers (Araujo and Smith 1989; Tao et al. 1997; Chen, Au et al. 2002; Primentas 2003) tried to find out the relationship between spirality and these factors. It was found that the direction of fabric spirality depends on the twist direction and the machine rotational direction. Araujo and Smith (1989) as well as Primentas (2003) explained that in weft circular knitting machines, the yarn are knitted in the circumferential direction and the produced fabrics present a drop that depends on the number of the used feeders.

The degree of fabric spirality is related to the number of needle of the machine, and the number of feeder of the machine. The direction of the inclination of the wales depends on the direction of either the revolving cam box or the rotation cylinder. Figure 2-13 shows the spirality of a plain fabric knitted from a Z-twisted yarn on a multi-feeder circular knitting machine with a clockwise rotational direction.

Araujo and Smith (1989) as well as Primentas (2003) also theoretically calculated the spirality angle of single jersey knitted fabrics. The following equations (2-3 to 2-6) show the relationships between the spirality angle and the factors of knitting variables:

$$\theta = \tan^{-1} \frac{F}{NK_{C/W}} \qquad 2\text{-}3$$

$$K_{C/W} = \frac{K_C}{K_W} \qquad 2\text{-}4$$

$$K_C = lC \qquad 2\text{-}5$$

$$K_W = lW \qquad 2\text{-}6$$

Where:

θ = Spirality angle due to the number of feeders

F = Total number of feeders on the knitting machine

N = Total number of needles in the knitting machine

$K_{C/W}$ = Loop shape factor

C = Courses per unit length

W = Wales per unit length

l = Loop length

From above equations, it is clear that the loop shape factor is a factor influencing on fabric spirality. That means that the changing of loop shape may lead to the change of fabric spirality.

2.3.3.3 Effect of treatments on fabric dimensional properties

The dimensional properties of the plain knitted fabrics can be affected by many factors. The Starfish (Heap et al. 1983, 1985; Stevens 1986), a program was developed to discover the effect of yarn, knitting, dyeing and finishing processes on the fabric shrinkage, it has been used as a database and models for predicting fabric shrinkage before knitting and other processing.

The Starfish states that the dimensional properties of the knitted fabrics are mainly controlled by knitting variables (including yarns), wet processing and finishing variables. The variables of yarns include fiber type and fiber preparation, yarn twist level and direction, yarn type and linear density, etc. The knitting variables are average loop length, loop shape factor and fabric tightness factor, etc. other knitting variables such as machine gauge, knitting tension, friction and so on also have influences on the relaxed dimensions of knitgoods. Wet processing and finishing also have influences on the

dimensional properties of the knitted fabrics. Most often, the fabric can be either wider or narrower after wet processing. In addition, the wet processing affects fabric spirality by helping to achieve the “reference state” of the fabrics.

It is well known that the dimensions of knitted fabrics are not stable, normally after washing and other treatments, the size in two dimensions (horizontal and vertical) will be changed and the shape will be distorted.

Apart from the factors discussed above, there are some other factors that can affect the dimensional properties of the plain knitted fabrics. Since some post-knitting treatments such as washing, drying, dyeing and finishing help to relax the energy stored in the yarn and the resultant fabrics, they can also affect the fabric dimensional properties.

In order to obtain the “full-relaxation” or “reference” state of the fabrics, it is necessary to investigate the relationship between energy relaxation and fabric dimensional properties. The Starfish, as mentioned above, mainly deals with the shrinkage of cotton knitted fabrics. It uses the “reference” state as the reference to study the relationship between fabric spirality and the factors that have influences on it. The analyses of the experimental data indicated that the dimensions of knitted fabrics and their potential dimensional changes and shape retention properties are influenced by the knitting conditions and the state of fabric relaxation. Apart from the Starfish, some other researchers also studied in this field. Postle et al (1968) theoretically and experimentally studied the dimensional properties of wool fabrics. They gave some suggestions for getting the full-relaxation state of the fabrics. Quaynor et al (1999) investigated the

influences of laundering on fabric deformation. The fabrics were subjected to relaxation processes and an extended series of wash and tumble-dry cycles. They measured fabric dimensional changes in every process and cycle and gave some experimental results.

Chen et al (2002) studied the relaxation shrinkage characteristics of steam-ironed plain knitted wool fabrics. Their experimental results show that manual steam ironing generally expands washed and tumble-dried fabrics regardless of whether or not extensions had been given to the fabrics during steam ironing. Steam-ironed fabrics exhibit further relaxation when agitated in water, the effect of the steam ironing on the dimensions of plain knitted wool fabrics is temporary and therefore ineffective in controlling the shape and dimensions of knitwear. The relaxation dimensional change of steam-ironed fabrics after washing depends on yarn linear density, fabric tightness, anti-felting treatment to wool yarn, and the degree of extension imparted to fabrics during steam ironing. They also stated that despite the treatment by steam ironing, all the washed and tumble-dried fabrics with the same yarn parameters and knitting variables approach almost the same dimensions and shapes after being washed in the IWS 1x7A washing cycles. Steam ironing does not affect the final dimensions and shape of the plain knitted fabrics.

2.4 Summary and Conclusions

In this chapter, literatures related to the structure and properties of spun yarns and fabrics were reviewed. Some yarn structural models were investigated. The first is the idealized cylindrical helix model. It has been used by many researchers due to its

simplicity. However, fiber migration was not considered. Models with fiber migration were developed with the “ideal”, conical or other migration patterns.

These models assumed that the yarn is formed by filaments. Some features of the staple fiber yarn such as slippage was not included in the assumptions until Pan (1992, 1993) involved it into his model. Previous literatures also stated that the yarn structure is determined by the spinning system used. Apart from these, some basic theories and mechanisms were also reviewed. They include fiber migration and its mechanisms, fiber tensile stress distribution in the yarn cross section, etc. In addition, the modification is one of our objectives, thus the yarn tensile and torsional properties were briefly reviewed as well.

Since other factors such as fabric and knitting parameters, downstream treatments etc have influences on fabric spirality. These factors were investigated by many researchers. Some reports indicated that loop length is the key parameter that determines fabric dimensional properties. Other investigations found that the fabric has a tendency to reach its minimum energy state. And wet treatments may result in fiber swell and help relax the energies of the yarn due to its residual torque and of the fabric due to knitting process. Based on this state, many researches were conducted, and some relationships between some parameters of yarn, fabric and knitting etc, and the dimensional properties of the final knitted fabric were found out. These findings gave us suggestions for the selection of fabric and knitting parameters, as well as the procedure of the downstream processes.

CHAPTER 3

A METHOD FOR IMPROVING YARN TORSIONAL BEHAVIOR

3.1 Introduction

During yarn forming, fibers undergo tensile, bending and torsional deformation. These deformations contribute to yarn torque in different ways. For a staple yarn, yarn torque is introduced during twisting process. Twisting increases fiber coherence, enhancing yarn strength. However, it deforms fibers into helices, forming yarn torque. The formed yarn torque can be partially released due to the time effect and during further processing, and other will be stored in the yarn as yarn residual torque.

Yarn residual torque causes problems both during the downstream processing of a twist-lively yarn and at the final fabric. During the formation from yarn to fabric, a twist-lively yarn tends to balance its internal torque by forming snarls. These snarls may not be fully opened at the downstream processes and result in faults in the final fabric. In addition, if these snarls get into the neighbouring machine parts, they may cause yarn breaks, resulting in operation stops. When a straight twist-lively yarn is converted into spatial knitted loops, the residual torque leads to fabric deformation in the form of fabric spirality of circular knitting fabrics. Such deformation influences not only the aesthetics of the resultant garment, but also fabric yield during cutting process.

Many methods have been developed and used in industry for reducing or eliminating yarn residual torque. In spinning factories, they often ply two yarns that have the same twist direction with an opposite twist. Steaming and mercerization are another two effective methods, and usually used in factories. However, these processes either increase material and production cost, or cannot eliminate the torque completely.

3.2 Principle of the Modification Process

3.2.1 Basic considerations

Twist is the main cause of the yarn residual torque, thus, before improving yarn torsional properties, it is necessary to investigate the twist distribution in the yarn cross-section (Tao 2003). Figure 3-1 shows the radial twist distributions of the conventional and unconventional spun yarns. They have different distribution patterns, thus various schemes shown in Figure 3-2 can be applied for improving them.

It is obvious that the principle of these modifications is to balance the twist distribution in the yarn cross-section, leading to a “torque free” yarn properties. For the rotor, air-jet and friction yarns, we can achieve it by simply de-twisting the yarn. However, this cannot be applied to the ring spun yarns because of the significant reduction of the yarn strength. Therefore, a structural modification of the ring spun yarn was considered.

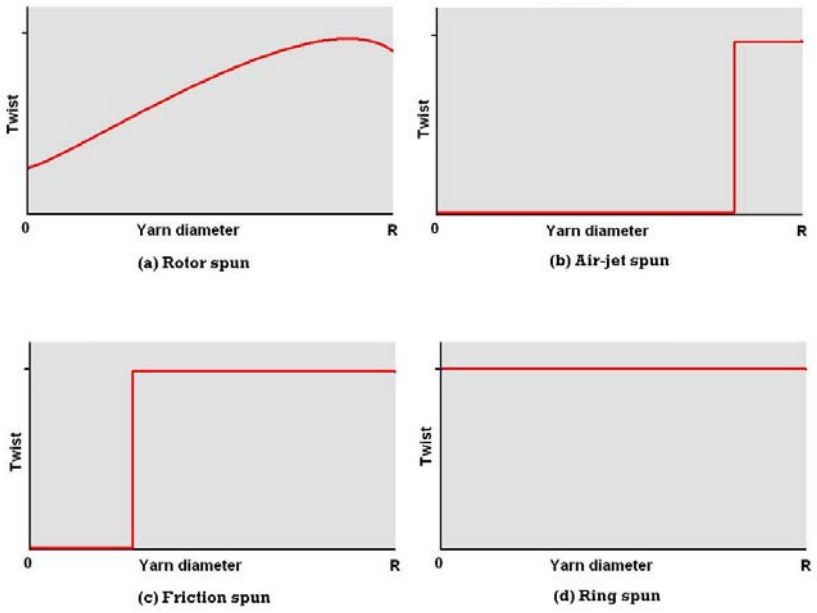

Figure 3-1 Original twist distribution of conventional and unconventional yarns (Tao 2003)

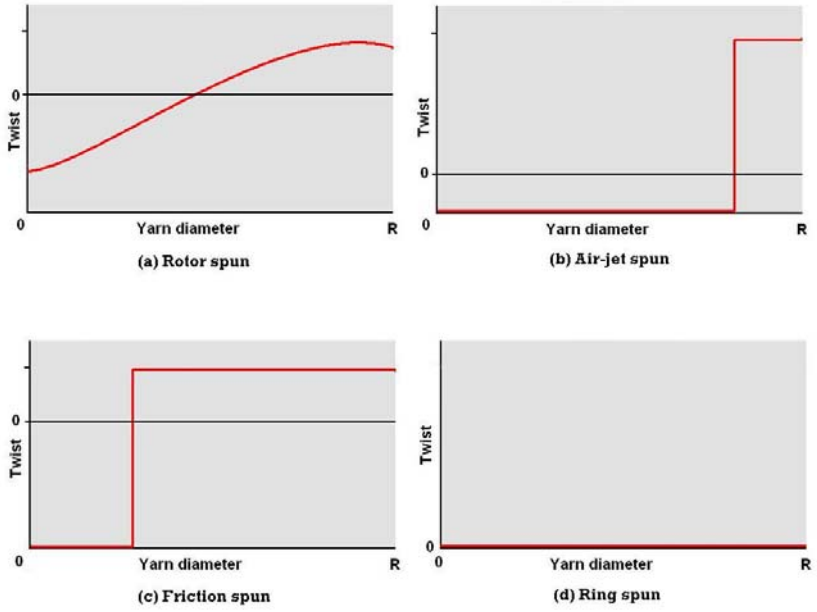

Figure 3-2 Schemes used for improving the twist distribution of conventional and unconventional yarns (Tao 2003)

3.2.2 Structural modifications of ring spun yarns

Sirospun and solospun are two successful examples of the modified ring spinning systems. The sirospun technique is a process that adopted some of the self-twist discoveries to the ring spinning technology of the worsted system. It combines spinning and doubling in the one operation. The technique shown in Figure 3-3 has two separated strands during the spinning process, and this allows a number of fiber binding mechanisms to operate before the strands are twisted about each other.

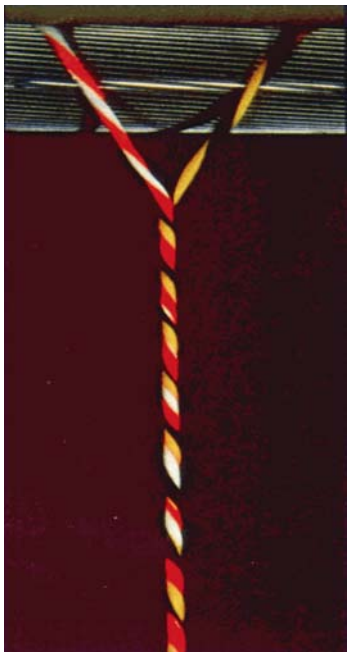

Figure 3-3 The formation of a sirospun yarn (CSIRO textile and fiber technology)

Figure 3-4 A set of device of the solospun system

During spinning process, the twist is introduced like a normal singles yarn by means of ring and traveler. The roving strands are combined after passing the front rollers at the exit from the draft system; and some twists are produced in the individual strands and transferred to the nip point. At the convergence point, the two strands are combined producing a twofold-like yarn. The yarn has uni-direction twist like a singles yarn but the fibers bound sufficiently for reinforcing yarn strength. In-depth analysis indicates that the sirospun is a false-twist system. The twists transferred to the strands can be de-twisted theoretically. In practice, however, the de-twisting is uncompleted. Some twists are remained in the strands, forming a “real unstable twofold yarn”.

During solo spinning, an attachment consisting of a pair of rollers mounted on a bracket shown in Figure 3-4 is installed on the top front roller of the drafting arm. The solo roller interrupts the path of the drafted roving, nipping it against the draft roller and preventing twist from passing to the drafting nip. The slots in the roller divide the strands into a number of sub-strands that, through the intermittent twist-blocking action of the roller, converge at varied angles and rates to achieve a subtly entangled structure of sub-strands with locally differing twist levels. This in turn gives greater fiber security as each fiber is trapped by the neighboring strands and by migration with and between strands.

Although the sirospun and solospun try to simulate a fold-like structure, there are some structural differences between them. The two strands of the sirospun yarn are formed from the two parallel rovings, and the two strands are always formed by using the same fibers respectively. While the sub-strands of the solospun yarns are divided from a

roving by using the separation roller, fibers are grouped randomly, the number of groups and the fibers forming every group vary along the axis of the final yarn.

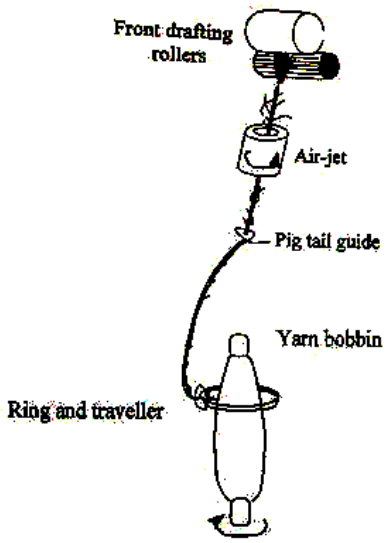

Figure 3-5 A schematic diagram of the JetRing spinning system (Wang et al. 1997)

Wang et al (1997) introduced a method named as Jet Ring spinning shown in Figure 3-5. A single air jet is installed below the yarn-forming zone of a conventional ring spinning system. This technique incorporates features of ring and air-jet spinning system. The air currents in the jet wind the protruding fibers around the yarn body, leading to a reduction of yarn hairiness. These researchers also applied the air-jet attachment on a winder in order to reducing yarn hairiness during winding process Wang et al (1997).

The compact spinning is another example of the modification of yarn structure by modifying yarn-spinning system. It is a technique that attempts to reduce fly liberation during conventional ring spinning by using pneumatic compression. The spinning

triangle shown in Figure 3-6 associated with conventional ring spinning is eliminated by pneumatic compaction (B is the width of fiber spread and b is the width of spinning triangle respectively). This happens by suction and compaction on a perforated revolving apron in front zone of the drafting system.

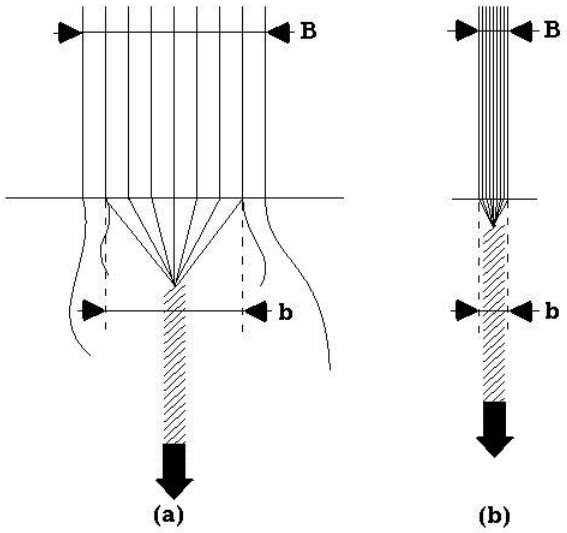

Figure 3-6 Comparison of the spinning triangles between the conventional ring spinning system and compact spinning system (Cheng and Yu 2003)

(a) conventional ring spinning system, B>b; (b) compact spinning system, B>b

While in the conventional ring spinning, a spinning triangle is formed immediately after the drafting mechanism. The triangle is a weak point due to less twist in this region. Under normal working conditions most of the breaks occur near-vicinity of the attainable spinning speed. Hence, if the spinning triangle is avoided or its length reduced, the achievable spinning speed could be increased. It is with this objective in mind that compact spinning is being tried.

These four spinning systems improve yarn properties by modifying fiber arrangement in the yarn path. The former two change the fiber arrangement by permanently or alternately grouping the feed-in fibers; the later two modify the fiber arrangement by winding the wild fibers or changing the shape of the spinning triangle. These seem to say that it is possible to modify yarn structure by changing the fiber arrangement in the yarn path, especially in the spinning triangle.

3.2.3 Fiber distribution during twisting

Hearle and Bose (1966) investigated the yarn formation during twisting by using flat stripe of ribbon. They summarized that at a low twist, the twisted form is preferred, but the wrapped form becomes preferable at higher twist. And they further analyzed it by explaining the filament arrangement during twisting of rubber threads (Hearle et al. 1969).

They pointed out that when continuous twisting of a single layer fed through the front rollers to a moving twist head, Figure 3-7 (a) showing initially the twisted ribbon form; but this then folded into an N-shape form. Finally, an approximation to a close-packed cylindrical form was obtained. Once the initial stage of twisting was over, and end effects eliminated, the form remained unchanged. Whereas for the continuous twisting of a two-layer fed through a slot. They analyzed two states of different twist levels. At a low level of twist (1.9 tpi), the continuous twisting gave a twisted ribbon, followed by an N-shape structure, and finally an irregularly shaped, almost close-packed structure, with all the threads of one color on the surface and as many as possible of the others in the

core. At a higher level of twist (3.5 tpi), as shown in Figure 3-7 (b), the buckling was more irregular and a multilayer structure appeared. However, the final structure was cylindrically close-packed with most of one color of threads on the surface and most of the others in the core.

Therefore, the twist level has influences on the type of yarn formation. In other words, we can, more or less, change the yarn structure by inserting different levels of twist.

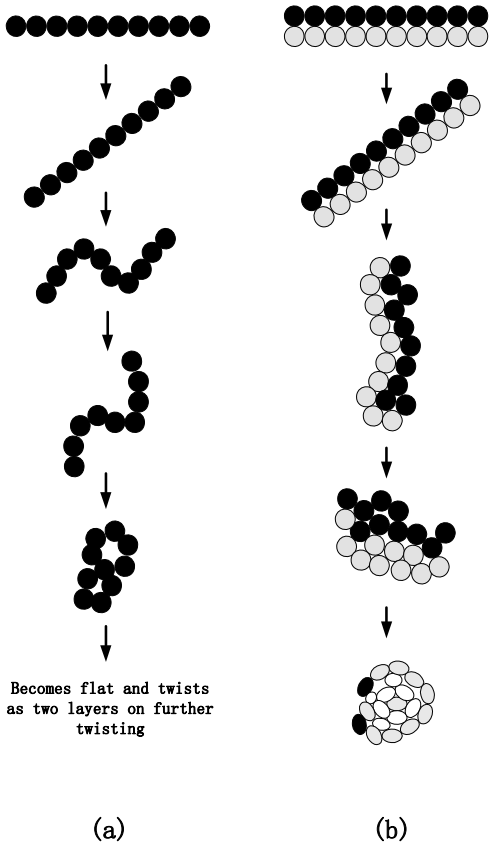

Figure 3-7 Filament arrangement during twisting of rubber threads (Hearle et al. 1969)

(a) Continuous twisting of single layer; (b) Continuous twisting of two layers fed through a slot.

3.3 Design of the Modification System

3.3.1 Yarn modification strategy

Normally, for obtaining a yarn with a low residual torque, it is firstly to consider reducing yarn torque by lowing down its twist factor. The low twist yarns not only have lower residual torque, but also possess better handle and other advantages. However, along with the reduction of the twist factor, the friction and cohesion between fibers are decreased, leading to a reduction of yarn strength. In addition, the low twist yarn either increases the spinning difficulty, or results in some problems related to its appearances such as hairiness etc. On the contrary, the high twist yarns have more compact structure, higher strength and good appearances, but exhibit higher residual torque at the same time. Thus it is necessary to develop a novel yarn which takes most of the advantages of low and high twist yarns. Figure 3-8 shows the strategy used in this study.

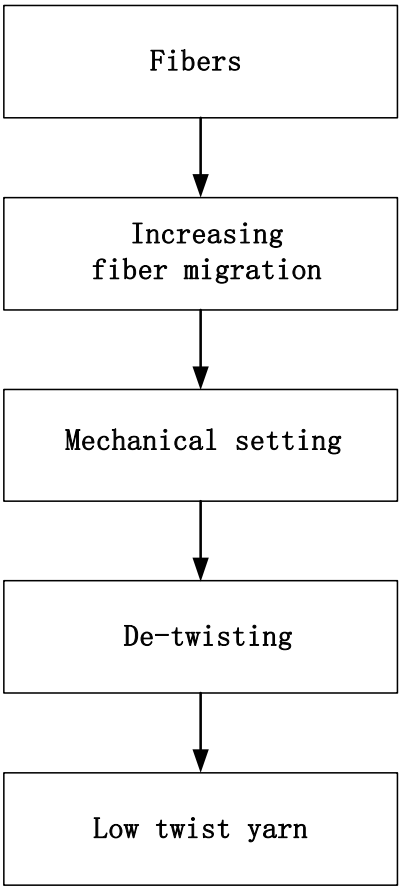

Figure 3-8 A strategy used for reinforcing the strength and further reducing the torque of a low-twist yarn

3.3.2 Modification of the spinning triangle

According to the tension and twisting form mechanisms, we considered to improve yarn structure in the spinning triangle.

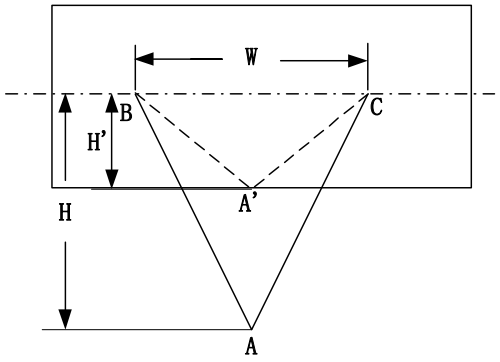

Figure 3-9 The change of spinning triangle

It is supposed that during spinning process, a higher twist is inserted by the rotating traveler. The roving is drafted into parallel fibers during passing through the draft rollers. In spinning triangle, wrapped twist form occurs. At the same time, the higher twist is inserted into the new-formed yarn, leading to a change of spinning triangle from ABC to $A'BC$. And the length of the spinning triangle is shortened from H to H' (see Figure 3-9). Thus the force projection of outer fibers in increased, leading to more fiber migration.

3.3.3 Fiber locking and setting

When migration occurs, fibers move between different concentric layers through opens between fibers. Normally the migrated fibers can change their path when they subject to tension. However, if the adjacent fibers that form the opens endure tension before the migrated fibers, the opens will be closed and parts of the migrated fibers will be locked. Thus the locked migrated fibers will remain their path.

In addition, the cotton fiber is a polymer of viscoelasticity. If a higher tension is applied to it, it is easy to beyond its elastic state. i.e., setting will occur.

3.3.4 De-twisting

For a ring spun yarn, it is well known that the yarn with a high twist possesses high torque. Since we used a high twist in the spinning triangle for reinforcing the fiber migration, de-twisting process is needed for removing the extra twist. In practice, the fiber migration, locking and setting make the fibers in different twists. When a de-twisting process is implemented, under- or/and over-de-twisting may happen. Thus some helices in reverse direction may exist in the final yarn.

3.3.5 One-step process

In this study, we completed the above tasks by simply using a false-twisting process. A false-twister was installed between the front rollers and yarn guide. It applies a higher twist to the part of the yarn above it, and gives a reverse twist to the part of the yarn below it, removing the extra twist.

3.3.6 Selection of the false-twister

The false-twisters were originally used for texturing filaments (Denton 1975; Greenwood 1975, 1977; Backer and Thwaites 1976; Demir 1996). There are several kinds of false-twisters which work by using air flow or mechanical methods. Since the mechanical false-twisters can accurately control the yarn quality by controlling the yarn twist (Greenwood 1975), we decided to use the mechanical ones. However, two types of mechanical false-twisters were available for adopting. They are friction twisters and pin

twisters. The former has a high production speed, but it is difficult to analyze its mechanism due to its complicated geometrical and mechanical system (Denton 1975; Backer and Thwaites 1976; Greenwood 1977). While the latter is simple and reliable, and its theory can be simply expressed by using the Equation 3-1.

$$T = n/v \qquad 3\text{-}1$$

Where T is the twist, n the rotational speed of the twister, and v the surface speed of the front rollers. With the pin twister, the twist can be controlled simply by controlling these two parameters. Therefore, a pin twister was finally chosen as the false-twister.

3.3.7 Torque modification system

A torque modification system was designed and developed (Tao and Xu 2002; Xu et al. 2004). Figure 3-10 demonstrates the whole system. A pin false twister, named as the torque modification device, was adopted. It was installed between the front rollers and the yarn guide on a conventional ring spinning system. The whole modification process can be divided into several zones shown in Figure 3-11. Zone A is the spinning triangle, from the nip point of the front rollers to the point that a new yarn is formed. Zone B is the high-twist zone, from the yarn forming point to the false twister, and zone C is the low twist zone, from the false twister to ring, traveler, and spindle. It is shown that when fibers pass through the nip point of the front rollers, a twist in this zone raises to a maximum value given by the ratio of the pin rotational speed to yarn delivery speed. The extreme tension variation enlarged fiber migration. And the higher tension on the

boundary fibers helps these fibers to overcome their elastic recover tendency, and set these migrated fibers simultaneously. In the downstream zone of the pin, an initial rise of reverse twist is immediately introduced by twist passing through the pin from the upstream zone, until finally the only twist remained is that of the original low twist yarn. Thus the extra twist introduced by the pin is removed and the highly migrated structure is remained. Thus a yarn with low torque and relatively higher strength is produced.

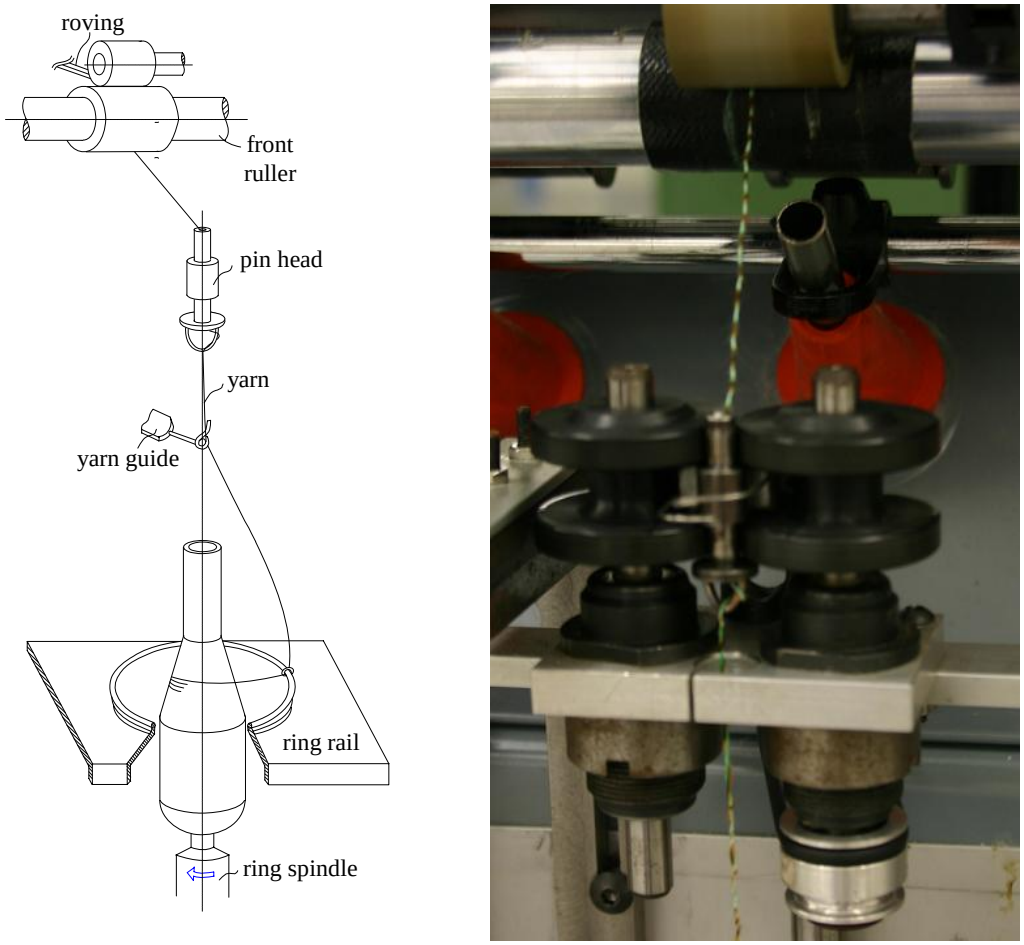

(a) sketch (b) real device

Figure 3-10 A pin false twister for the reduction of yarn torque (Xu et al. 2004)

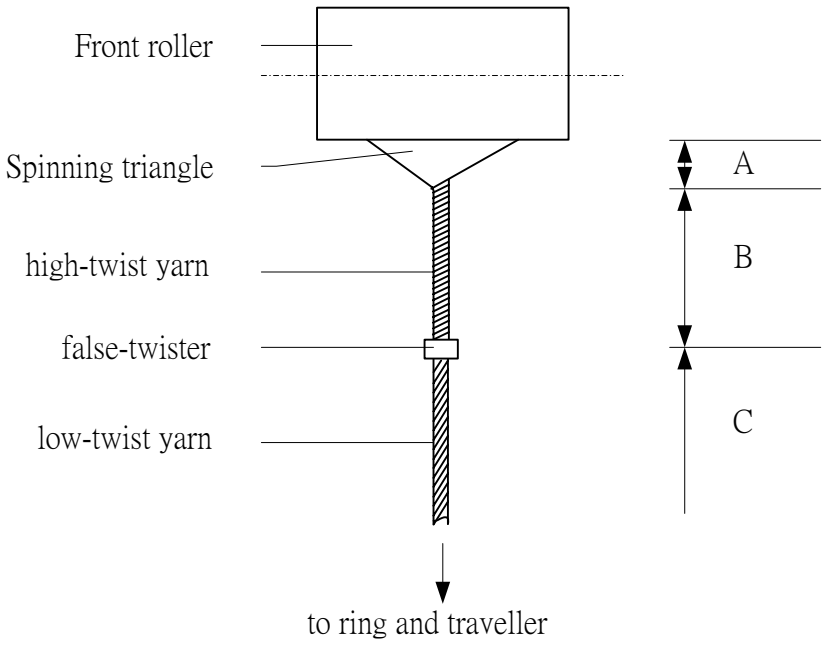

Figure 3-11 The spinning process for TBS yarns

3.4 Preliminary Evaluation

After the design and installation of the torque modification device, it is necessary to conduct a preliminary evaluation of the device and the produced yarn.

3.4.1 Spinning preparation

3.4.1.1 Materials

Rayon fibers whose diameters are 1.5Denier and lengths are 38mm were used for the preliminary trial. 8.0 and 2.5 were selected as the twist factors of the conventional yarns and 2.5 was chosen as the twist factor of the TBS yarn. For better identification, some white fibers were dyed into black, green and orange colors, thus totally the fibers with four colors were used.

In addition, we also used a Spin tester to spin some 20Ne conventional ring spun yarns and the TBS yarns with the same cotton C1 roving (specifications are shown in Table 6-1) and yarn count for the preliminary evaluation of the properties of the TBS yarns.

3.4.1.2 Transparent top front roller

A transparent acrylic roller shown in Figure 3-12 was made for observing the nip point of the spinning triangle. It has the same size as the conventional rubber one. The bottom front roller was covered by using a black tape for preventing from the reflection of the flashlight and the damage of the top roller.

Figure 3-12 A transparent roller

A plate with slots was installed between the middle and break draft for separating the colored rovings. The width of each slot and the interval between every two adjacent slots were determined in such a way that ensures these rovings were completed separated and fibers were fed into the nip point side by side.

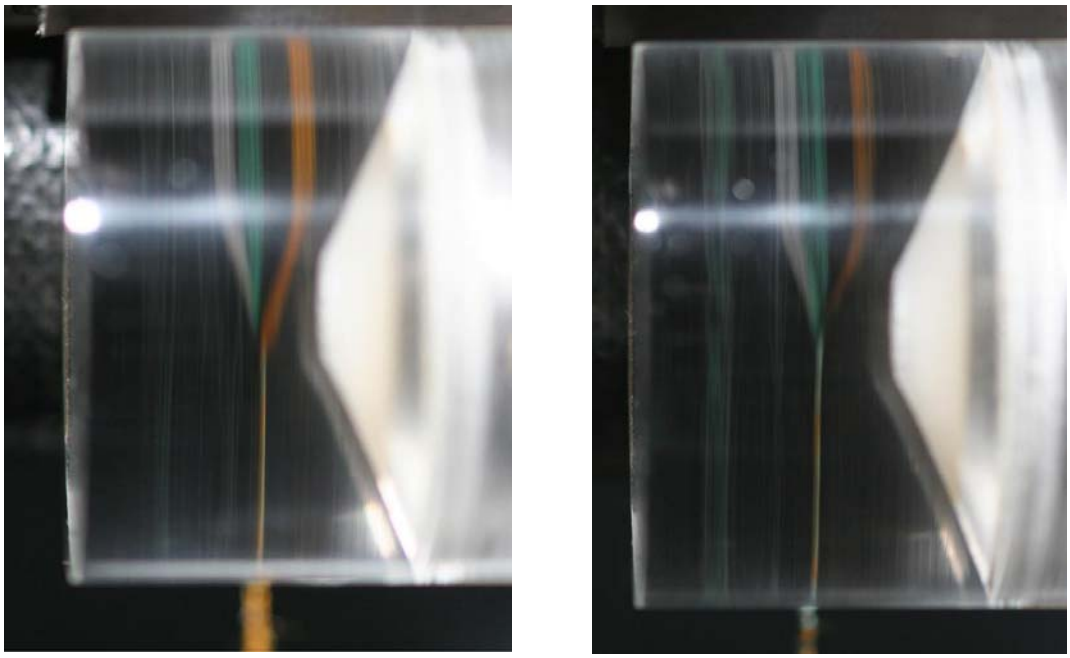

(a). High-twist conventional ring spun yarn, TF = 8.0

(b). TBS yarn, TF* =2.5

Figure 3-13 Images of the spinning triangle

* The twist factor transferred from the ring and traveler.

3.4.2 Observation of the spinning triangle

Yarns were produced and the spinning triangle was observed. Since the length of the spinning triangle of the lower twist conventional yarn is too long to be captured completed, we compared the triangles of the other two yarns. Figure 3-13 is two images of the spinning triangle. Color arrangement (from the left to the right) is white, green, black and orange. The images indicate that the TBS yarn has a similar shape of the spinning triangle with the extremely high twist conventional yarn. In fact, the TBS yarn has a very high twist in the yarn part between the pin and the front rollers despite of a

lower twist used. The very high twist is formed by the high rotational speed of the pin and the yarn delivery speed. This extremely high twist may increase fiber migration and help to set the formed yarn.

3.4.3 De-twisting of the resultant yarn

Figure 3-14 shows a part of the de-twisted TBS yarn. Some wrapping fibers are wound on the body of the yarn. When giving a reverse twist to the TBS yarn, parts of the yarn is de-twisted, showing a bulky structure. However, parts of the yarn can not be de-twisted due to the wrapping fibers. In the bulky parts, several colored fibers are mixed in the fibers of the other colors, showing a migration image.

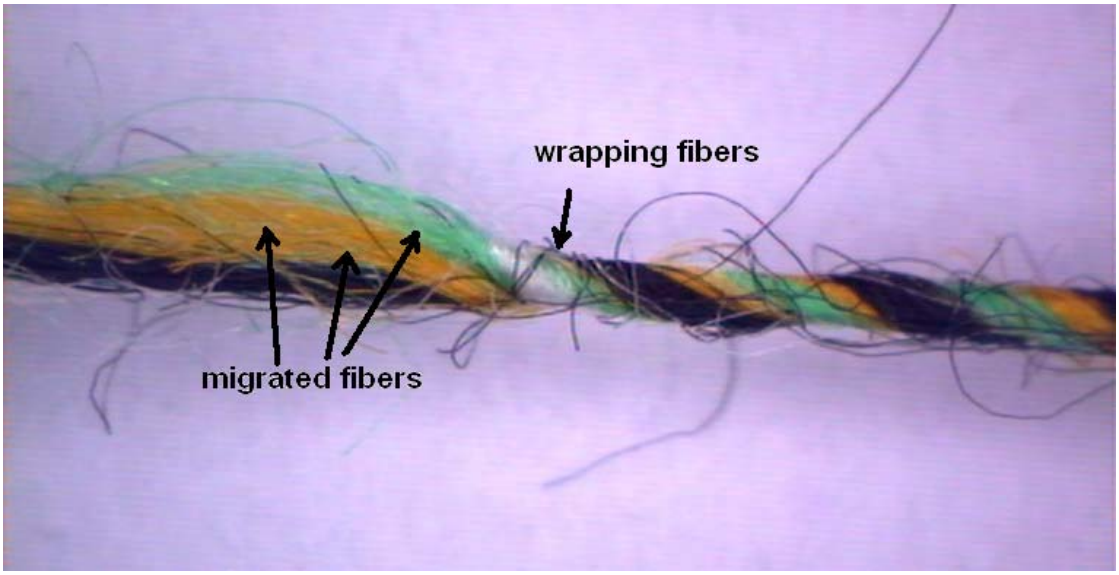

Figure 3-14 A part of the de-twisted TBS yarn

3.4.4 Effect of the torque modification device on the yarn properties

Figure 3-15 shows the results of the conventional yarns and TBS cotton yarns. Apparently, if compared with the conventional ring spun yarns, the TBS yarns have lower residual torque in terms of yarn wet snarling turns, and the reduction is significant. While the tenacity values of the TBS yarns are not very low, especially when the twist factor is less than 3.3, they are greater than those of their corresponding conventional yarns. It seems to tell us that we get the yarn with lower residual torque and relatively higher strength by modifying its structure.

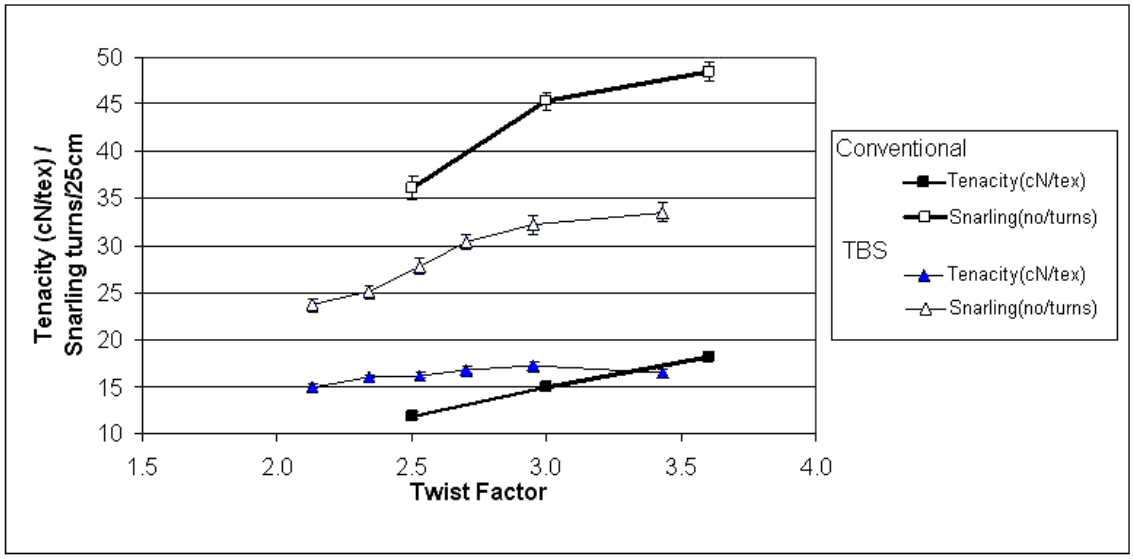

Figure 3-15 Properties of the yarns from the preliminary spinning trial

3.5 Summary and Conclusions

In order to obtain a yarn with lower residual torque and relatively high strength, we firstly attempt to find out a method theoretically. After reviewing previous literatures,

we knew that it is possible to reduce yarn torque by introducing a perfect migration pattern. Fiber migration not only disperses the force distribution in the yarn cross section, but also provides an opportunity for forming yarn segments rotating in reversed direction. Some literatures stated the tension variation and twist-forming geometries are two basic mechanisms for analyzing the yarn formation and fiber migration. Therefore, increasing tension variation becomes a key point of the whole scheme.

High twist can supply higher tension difference between the outer fibers and central fibers in the spinning triangle, as well as set the migrated fibers. However, high twist may result in high torque. For solving this contradiction, a false-twister was adopted. It can achieve a high twist in the part above it and a low twist in the part below it simultaneously. There are several kinds of false-twister. After evaluating, we chose the pin twister, and a torque modification system with a pin false-twister was designed and developed.

For evaluating the performance of the modification device, several experiments were conducted. Firstly, the spinning triangle was observed by using a transparent front roller and colored fibers. The images confirmed that the TBS spinning system can change the shape of the spinning triangle. Then the produced yarn was examined. The results show that some parts of the yarn can not be de-twisted due to the wrapping fibers tightly winding on the body of the yarn. In the de-twisted parts, yarn became bulky, and some fiber migrations were found. Finally, some conventional and TBS yarns were produced by using the same cotton roving. Test results show that the TBS yarns have a lower

torque in terms of yarn wet snarling turns and relatively higher tenacity simultaneously, meeting the requirement mentioned above.

In general, the preliminary evaluation partially validates the mechanism of the modification device. The examination of yarn structure and the numerical analysis of the yarn torque will be stated in the later chapters.

CHAPTER 4

STRUCTURE AND MECHANICAL PROPERTIES OF TORQUE – BALANCED SINGLES RING SPUN YARNS

4.1 Yarn Structure

TBS yarns exhibit a low twist, lower residual torque and relatively higher strength. In practice, it is difficult for a ring spun yarn to possess these properties at the same time. The obvious difference between TBS yarns and conventional ring spun yarns must lie in the unique structure of the TBS yarns.

4.1.1 Investigation approaches

4.1.1.1 Yarn appearance

Yarn appearance is an aspect of the yarn structure and an important parameter indicating the quality of a yarn. This means that there are some relationships between yarn appearance and some properties of the yarn. Yarn appearances are mainly determined by the spinning method and the parameters. For example a ring spun yarn has an appearance with inclined fibers and the angle of fiber inclination varies with the twist factor and other parameters. Several indexes can be used for expressing yarn appearance, and they can be examined by using some methods. In this study, yarn diameter was measured by using a Projectina CH-9435 projecting microscope; the Blackboard method was adopted for evaluating the yarn diameter variation and its projection; and Zweigle

G566 hairiness tester was used for measuring the number of wild hairs whose length is equal to or longer than 3mm; as well as a Leica Stereoscan 440 Scanning Electronic Microscope (SEM) was used for checking up the yarn surface and giving some information about surface arrangement and other features.

4.1.1.2 Yarn packing density distribution

Some researchers systemically studied the yarn packing density (Riding 1959; Hickie and Chaikin 1974; Nectar et al. 1988; Jiang et al. 2004), and proposed some research methods. After the analysis and comparison, the following method was adopted in this study for calculating the packing density.

a) Division of the cross section of the yarn

Generally, three approaches have been used in investigating yarn cross-sectional structure. The first one was proposed by Schwarz (1951); then it was further developed by some researchers (Balakrishna and Phatarfod 1965; Nectar et al. 1988). They assumed that the fibers in the yarn cross-section are arranged into perfectly hexagonal configurations. Thus very high packing density is expected. Then based on it, they examined a small number of fibers (ranging from 1 to 37) in yarn cross section. However, this method is only applicable to filaments, rather than staple fiber yarns.

The second approach is that the yarn cross section is divided into several annular zones based on the assumption that the fibers are arranged in a form of concentric helices (Morton and Yen 1952; Hearle and Gupta 1965). There are two methods i.e., equal

width or equal area methods can be used for the division. The examination of the packing density, which is termed as the numbers of fibers per unit area, is very useful and commonly adopted for evaluating the yarn cross sectional structure. To avoid the large variation in the cross-sectional area of the fibers such as cotton, Nechar et al (1988) used the ratio of the total cross-sectional area of the fibers in a given zone of a yarn cross section to the area of that zone.

The third approach is proposed by Grishanov et al (1997) who introduced a concept of "virtual locations". They assumed that fibers are distributed in the form of a combination of a ring and/or a hexagonal configuration. The advantage of this approach is that it can simulate the air gaps between fibers and gives a good representation of fiber location.

Among these three approaches, the second one is most commonly used because it is relatively easily implemented with satisfactory precision (Jiang et al. 2004). Thus it was adopted in this study. In order to simplify the investigation, we made the following assumptions: (1) fibers had an identical cross section area, and the area variation can be neglected; (2) all fibers had an identical cross section shape; (3) packing density was expressed as the ratio of the total cross-sectional area of the fibers in a given zone of a yarn cross section to the area of that zone; (4) the deformation of fiber cross section due to the compression between fibers was ignored. In the experiments, considerations were given to select Tencel fibers meeting the requirements, as well as the optical homogeneity required by tracer method.

b) Determination of fiber center and equivalent diameter

Tencel fibers have small variation in their cross-sectional shape. In practice, some elliptical fiber cross sections were found due to fiber inclination (Jasper et al. 2005). Thus an equivalent circular cross section was introduced for the ellipse. Before the replacement, it is necessary to identify the location of this elliptical fiber. Since the ellipse has its geometrical center (X_{fe}, Y_{fe}), therefore, this center can be regarded as the center of the equivalent circle (X, Y), and the diameter of the circular cross section was adopted as an equivalent diameter for those ellipses.

c) Determination of yarn gravity center

It is difficult to determine the yarn center because of the non-uniform distribution of the fibers. Therefore, based on the assumption that each fiber cross section is circular and of the same shape and dimension, the center of gravity of a cross section is equivalent to the center of geometry. Thus the coordinates of the center of gravity were obtained by averaging over all the fibers' coordinates.

Assuming a yarn cross section has n fibers, and the coordinate of the center of each fiber is (X_i, Y_i), where $i = 1,2,3,\cdots,n$. Thus the coordinate of the center of the yarn cross section $(\overline{X}, \overline{Y})$ can be calculated by the following equations.

$$\overline{X} = \frac{\sum_{i=1}^{n} X_i}{n}, \quad \text{and } \overline{Y} = \frac{\sum_{i=1}^{n} Y_i}{n} \qquad \text{4-1}$$

d) Determination of yarn radius

The identification of the yarn radius for a particular cross-section is also very important. In this study, yarn radius R_y can be calculated from the sum of fiber radius R_f and the distance between yarn center and the farthest fiber $MAX(R_i)$, as shown in Figure 4-1.

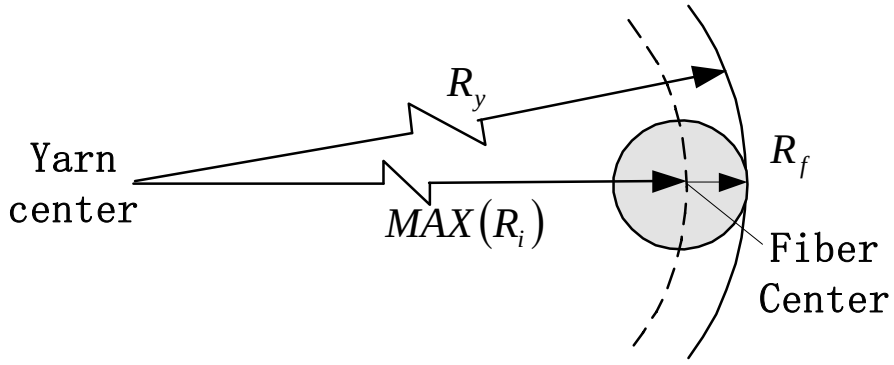

Figure 4-1 Schematic diagram of the calculation of yarn radius

$$R_y = R_f + MAX(R_i) \quad , \quad i = 1,2,3,\cdots,m, \qquad 4\text{-}2$$

Where R_y represents yarn diameter, R_f donates fiber diameter, and

$$R_i = \sqrt{(X_i - \overline{X})^2 + (Y_i - \overline{Y})^2}$$

e) Method of dividing annular zones

After the determination of fiber cross section center, yarn cross section center, and the yarn radius, it is possible to divide a yarn cross section into concentric zones with desired number m. As mentioned above, two zone-dividing approaches can be used for

drawing the concentric circles: one is equal radial spacing method, i.e., all annular zones share one width, the other is to draw the concentric circles in such a way that each successive ring encloses the same area.

Hearle et al. (1965) suggested using the later approach, i.e., the zones of equal area, so that the fibers are equally distributed between all zones. Other researchers such as Zotikov and Trolova (1966) calculated per unit area by using both methods. After analyzing the experiment results, they gave the conclusions that the results should be identical for the same cross section. Therefore, the equal area method was used in this investigation (as shown by Figure 4-2).

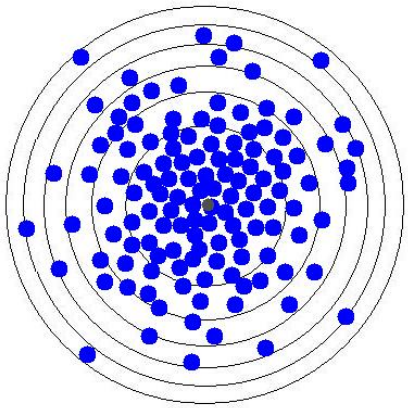

Figure 4-2 Schematic diagram of the zone-dividing method (equal area method)

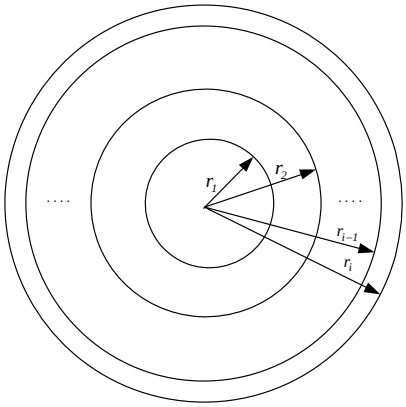

Figure 4-3 Determination of the radius of each concentric circle

It is needed to determine the radius of every concentric circular ring of identical area. Figure 4-3 illustrates the radii of several concentric circles in a yarn cross section. If an annular zone is surrounded by two adjacent circles with the radii of R_i and R_{i-1}, respectively. Thus the area of this zone is the difference between the areas encircled by these two circles. Since every annular zone has the same area, for an arbitrary radius $R_i, (i = 1,2,3,\cdots,m)$, we have:

$$\pi R_i^2 - \pi R_{i-1}^2 = \pi R_1^2 \qquad 4\text{-}3$$

and

$$R_i = R_1\sqrt{i} \qquad 4\text{-}4$$

f) Calculation of zonal fiber total area

Previous researchers (Riding 1959; Hickie and Chaikin 1974; Nectar et al. 1988; Jiang 2003) analyzed all the possible relative locations for a fiber to a given annular zone. A

fiber is either completely or partially enclosed by an annular zone. Therefore the identification of a fiber's relative location for a given zone and calculating the area of fibers in each zone became our tasks. For the former task, when a fiber is surrounded completely by a given zone, its contribution to the total fiber area in this zone is the area of a fiber cross section, A_f. That is,

$$A_f = \pi \cdot R_f^{\,2} \qquad 4\text{-}5$$

For those riding on the boundary between two adjacent zones, the calculation is slightly complicated. Some researchers investigated this situation by analyzing the geometry of the overlaid part between the fiber j and the annular zone i. The part enclosed by an annular zone is either leaflike or of the shape that demonstrates a leaflike shape from a circle or from a bigger leaflike shape (Jiang et al. 2004).

Figure 4-4 illustrates the calculation method of a leaflike shape. The area of a leaflike shape, i.e., the part covered by dashed lines, A_{leaf}, should be given by the sum of the areas surrounded by $ACBD$ and $ADBE$.

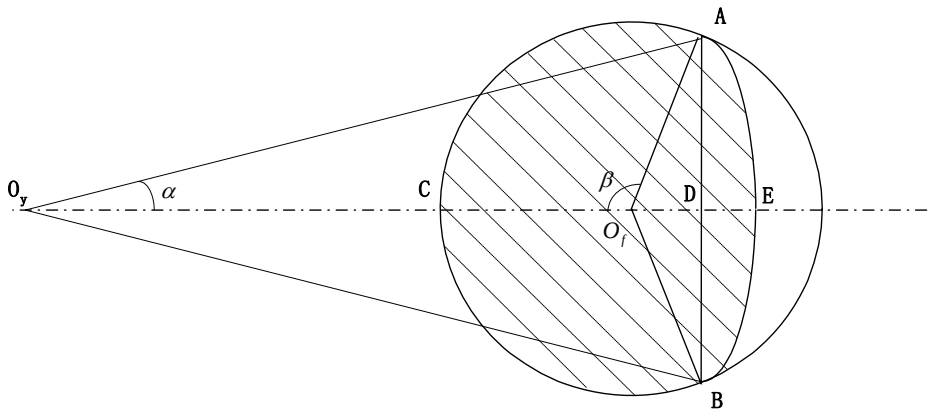

Figure 4-4 Calculation of the area of Leaflike shape

$$A_{leaf} = A_{ACBD} + A_{ADBE} \tag{4-6}$$

The area of $ACBD$ is the sum of the areas of sector $ACBO_f$ and triangle ABO_f .

$$A_{ACBD} = A_{ACBO_f} \pm A_{AO_fB} \tag{4-7}$$

When $\beta < \frac{\pi}{2}$, minus is chosen as the sign of the Equation 4-7.

The area of $ADBE$ can also be determined by the difference between the areas of circular sector AO_yBE and the triangle AO_yB, i.e.

$$A_{ADBE} = A_{AO_yBE} - A_{AO_yB} \tag{4-8}$$

Therefore, the area of a leaf-like shape can be expressed as Equation 4-9.

$$A_{leaf} = R_f{}^2\beta + D_i{}^2\alpha - R_f R_j \sin\beta \qquad 4\text{-}9$$

Where D_i is the radial position of zone i's outer peripheral rim, and R_j is the distance from yarn center to fibre j's center. Equation 4-9 is valid for any value of angle β. With this equation, it is easy to calculate the shadowed area of fiber enclosed by a given annular zone so as to identify the packing ratios zone by zone.

g) Packing density

After completing the above preparation, it is ready to calculate the mean value of packing density. The packing density for a given annular zone i was defined as the ratio of the total area of fibers enclosed by this zone to the area of this zone itself. We assume that the number of fiber in annular zone i is m, thus the packing density of the i th zone

$$\rho_i = \frac{\sum_{j=1}^{m} A_j}{A_{zone_i}} \qquad 4\text{-}10$$

Where ρ_i is the packing density of the i th annular zone, A_j represents the area of fiber j enclosed by the i th annular zone, and A_{zone_i} donates the area of the i th annular zone.

4.1.1.3 Determination of the fiber geometry

A direct approach is to take cross sectional images successively along the yarn axis. Then identify the position of each fiber on each image, and re-construct these pictures. At last, the fiber path is obtained. This approach has many advantages such as getting the yarn radial structures and fiber path at the same time. Recently, it has been reported that yarn and fabric structures can be obtained without cutting the yarn by using x-ray technique (Choi et al. 2003; Shinohara et al. 2003). The technology is under the investigation and has not been used widely.

Another method is the tracer fiber technique, developed by Morton and Yen (1952), which can trace the path that a fiber goes in a spun yarn. Since it is a mature and reliable technique and has been widely used, we adopted it in this study.

a) Tracer fiber technique

The tracer fiber technique was first introduced by Morton and Yen in 1952 for rayon staple-fiber yarns spun on a cotton spinning system. Its principle is to optically dissolve background fibers, and then identify the colored tracers from the background based on their different refractive indexes.

An extremely small proportion of dyed fibers are introduced into an adequate blend with the main body of undyed fibers before drafting and spinning into a yarn. Then the yarns are immersed in a trough of liquid, whose refractive index is very close to that of the undyed fibers. When observed under a microscope, the undyed fibers are “dissolved”,

forming a dim background, and the colored “tracer” fibers reveal their paths clearly. In this way, the paths that a single fiber takes in a yarn body can be identified.

Since the fiber path is actually in three dimensions, thus Morton’s technique has been improved for obtaining the three dimensions of the tracer fiber. A simple method invented by Riding (1964) is to place a plane mirror near the yarn in the liquid, with the plane of the mirror at 45^{o} to the direction of observation, as illustrated in Figure 4-5. The fiber can then be viewed from two directions at right angles simultaneously. By analyzing the fiber positions on these two images, the fiber 3-D path can be easily calculated.

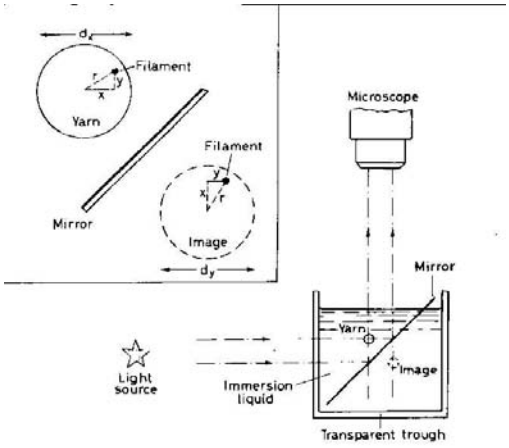

Figure 4-5 Tracer observation apparatus based on Riding’s design (Hearle et al.1969)

This method is simple, and easily to be implemented. However some defects are hided. One of them is the two images are not on the same focus plane. This maybe results in the image out of focus and distorted, leading to the wrong understanding of yarn path. In this study, therefore, an improved method was developed based on Choi’s suggestion

(Choi). Two stainless steel planes were arranged at an angle of 135°, as shown in Figure 4-6. When observed under a microscope, two images would be viewed. Since they are in the same focus plane, the positions of the fiber reveal an actual fiber path within the yarn. In addition, to avoid any disturbance to the magnification that may influence the result, no touch of the microscope is permitted once the magnification is fixed. Therefore, a small lifter is used for the focus adjustment.

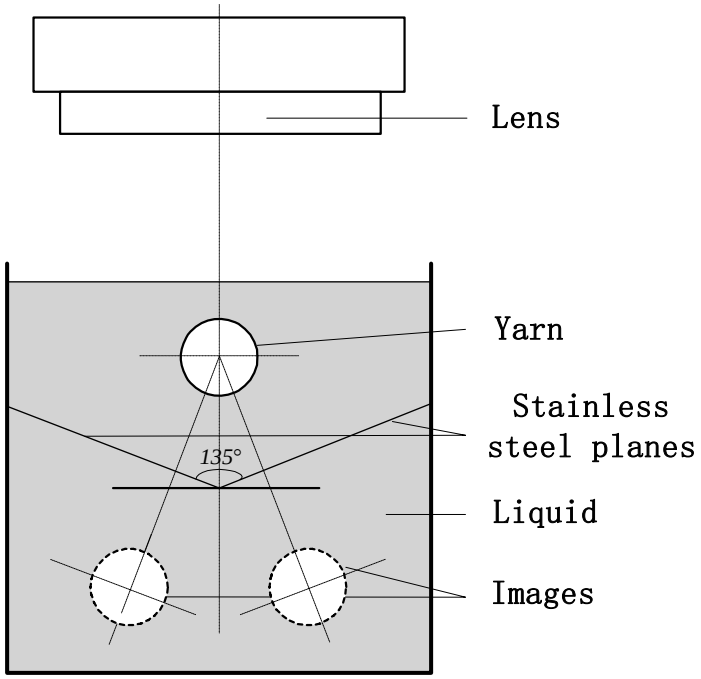

Figure 4-6 An improved apparatus for tracer fiber observation

b) Image Capture

A system including a digital camera with zoom lens was established for observing and capturing of the images, as shown in Figure 4-6. The trough was mounted on an adjustable stage. The yarn, as it was placed in the path of illumination, appeared bright

due to its optical anisotropy with the dark tracer. The image could be brought into view by moving the stage.

c) Data transform and analysis

The image capture was followed by data transfer, i.e., the tracer images were expressed in a set of coordinates. This transfer was accomplished by a small program written in Matlab. With the coordinates of a tracer fiber in a spun yarn, it is possible to calculate the radial positions of the fiber with respect to the center of the yarn along the yarn length.

For image processing, Fast Fourier Transform is one of the most useful techniques for image enhancement and measurement. An image, a two-dimensional function in a spatial domain, consists of some components such as periodic structures, non-periodic element, noise, and background; and it is sometimes difficult to separate and analyse these image components in the spatial domain because they are usually embedded and entangled together. The Fast Fourier Transform can convert the image into a two-dimensional complex function in the frequency domain. Thus their separated spatial frequencies can be expressed by using a power spectrum image. A peak in the power spectrum donates a periodic structure in the image (Hickie and Chaikin 1974; Jiang et al. 2002).

Therefore, the Fast Fourier Transform is capable of dividing the paths of single fibers in a spun yarn into a wide range of periodicities, which are related to spinning parameters and/or fiber characteristics. It is known that, for a typical Fourier spectrum, there was

only one dominant wavelength, on each side of which was long and short wavelengths of varying amplitudes. This dominant wavelength is associated with the nominal twist wavelength (Hearle et al. 1969; Hickie and Chaikin 1974). The equation for converting the coefficient number to wavelength is given below.

$$l_k = l / k \qquad 4\text{-}11$$

Where l_k is the wavelength of the k th coefficient; and l is the extent length of the trace being analyzed.

d) Determination of fiber 3-dimensional Path

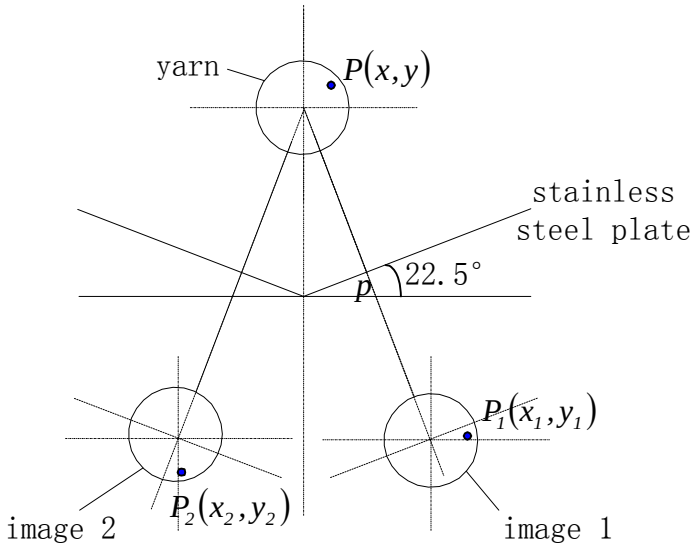

Figure 4-7 Determination of fiber position within a yarn

Figure 4-7 illustrates the relationship between the positions of the yarn and its two images. The position of point $P(x,y)$ can be expressed by the coordinates of its images P_1 and P_2. Since $x_1 = -y_2$ and $y_1 = x_2$, the point $P(x,y)$ can also be represented by using the horizontal coordinates of these two images x_1 and x_2, i.e.,

$$\begin{cases} x = \dfrac{\sqrt{2}}{2}(x_1 + x_2) \\ y = \dfrac{\sqrt{2}}{2}(x_1 - x_2) \end{cases}. \qquad 4\text{-}12$$

4.1.2 Experimental details

4.1.2.1 Yarn cross section

a) Materials

In this investigation, three types of yarns were examined. They were the TBS yarn (TF = 2.5), low-twist conventional ring spun yarn (TF = 2.5) and high-twist conventional ring spun yarn (TF = 3.6). Each yarn had three counts, i.e., 16, 20 as well as 30Ne. Since it was difficult to identify the center of cotton fiber due to its irregular cross-section, Tencel fibers were adopted for making the yarns. Table 4-1 lists the sample specifications used in the present research.

Table 4-1. Specifications of yarn specimens

Fiber Type	Fiber Diameter (cm)	Fiber Length (cm)	Yarn Count (Ne)	Twist Factor
Tencel	1.0×10^{-3}	3.8	16, 20, 30	2.5*, 3.6

Note: * used for the TBS yarns and the low twist conventional yarns

Leica Historesin Embedding Kit was used for making the resin. It has three components: basic resin, activator and hardener. Table 4-2 shows their specifications.

Table 4-2 Specifications of the Leica Historesin Embedding Kit

Basic Resin/Liquid	Activator	Hardener
(2-Hydroxyethyl)-methacrylate	Dibenzolperoxide	Dimethyl Sulfoxide

Table 4-3 Preparation of infiltration solution and embedding kit

1st step	Preparation of Infiltration Solution	50ml Basic resin +1 packet (0.5g) Activator Stir with a magnetic stirrer until dissolved completely
2nd step	Preparation of Embedding Medium	15ml Infiltration solution + 1ml Hardener Mix fully by using the ultrasonic and use immediately

For the preparation of the specimen, Table 4-3 lists the preparation method in two steps. As shown, Tencel fiber was used as the material. The yarn was threaded through a plastic tube on which a hole was cut, and sealed two ends with adhesive tape to guarantee the yarn specimen in the center. A weight was used to ensure that the yarn be straightened without extension. Then the resin was injected into the tube through the small hole. After that, the sample together with the tube was put vertically on a special shelf (see Figure 4-8). Cares were taken to ensure that the yarn was straightened without extension.

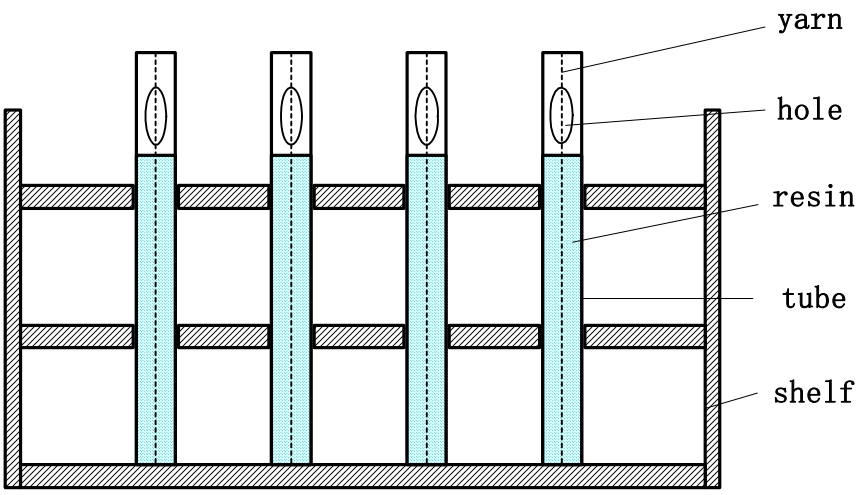

Figure 4-8 Sample preparation

After several hours of solidification, the hardened yarn and resin were ready for cross-sectioning (see Figure 4-9). Yarn cross sectioning was performed manually by using a Leica RM 2135 microtome. The specimen thickness was 10μm and it could give a satisfactory view under an optical microscope.

Figure 4-9 Sample for microtomy

b) Microscopy

The cut specimen was then mounted on a standard slide and wetted by paraffin oil. A Nikon Optiphot-pol microscope with digital head and Leica Qwinlite software was used. The cross section images were successfully observed and captured by a PC. For each yarn type, 30 cross sections were chosen for further analysis. At last, these images were sent to a PC and processed by the aid of a program which provides the means to read the coordinates of each fiber center directly from the yarn cross section images. After the determination of the yarn center and other characteristics, the yarn area and the total area of fibers in each annular zone, as well as the packing density were calculated. Then the discrete data were transferred into a continuous function with the aid of curve-fitting technique provided in Excel.

4.1.2.2 Preparation for the tracer fiber observation

As stated above, an extremely small proportion (around 0.8%) of dyed Tencel fibers was introduced into the main body of sliver before gilling and drafting. Then three yarns (including the TBS and conventional ring spun yarns) were produced with these mixed fibers. After that, the yarn produced was immersed in an apparatus (see Figure 4-10) filled with a special liquid. The liquid was a mixture of 1-Bromonaphthalene and Turpentine at a proportion of 1:1. The refractive index of the mixture was very close to that of the uncolored Tencel fiber so that the white fibers would be optically dissolved. Figure 4-11 illustrates the whole set-up of the tracer fiber observation device.

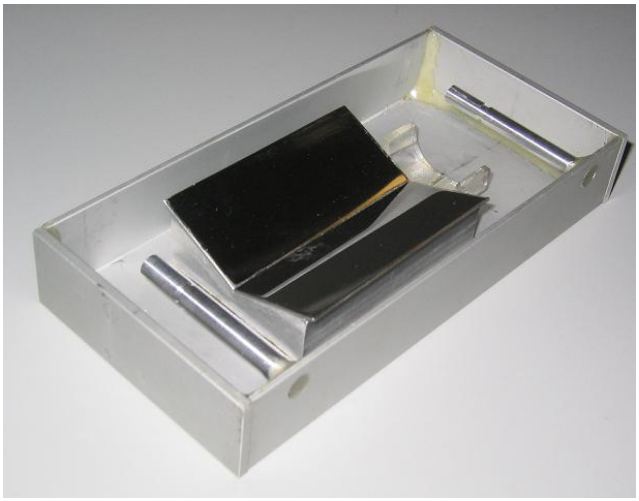

Figure 4-10 A trough for tracer fiber observation

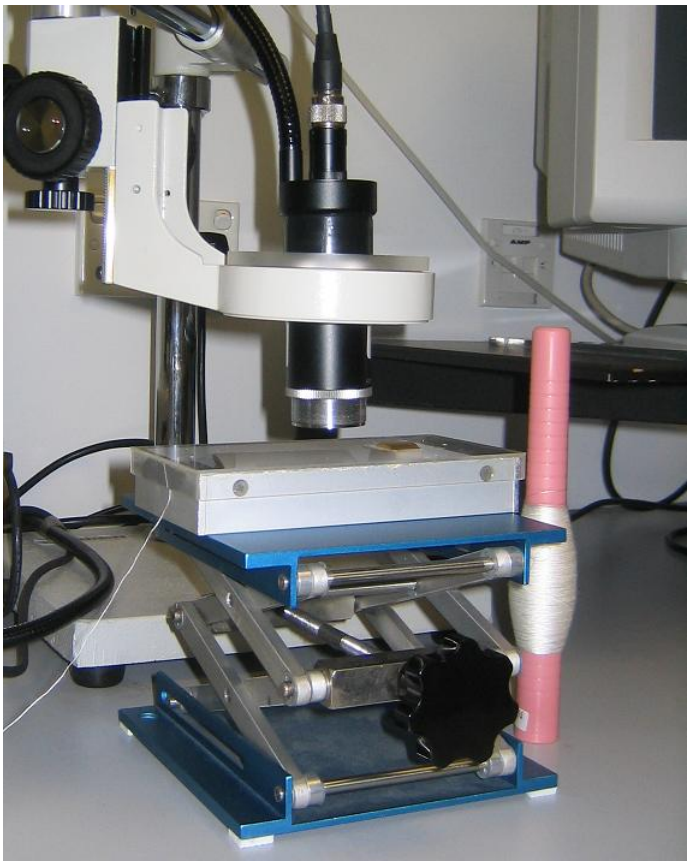

Figure 4-11 Apparatus used for tracer fiber observation

4.1.3 Results and discussion

4.1.3.1 Yarn appearance

The diameters of three 20Ne yarns produced by using the C1 roving were examined by using a Projectina projecting microscope. These three yarns were a TBS yarn with a twist factor of 2.5 and two conventional ring spun yarns with twist factor of 2.5 and 3.6 respectively. The measured results are shown in Figure 4-12. Frankly, they have no significant difference. If compare their mean values, the low twist conventional yarn has a greater diameter, followed by the TBS yarn, and the diameter of the high twist conventional yarn was the least. Apparently, the variation of the TBS yarn was the greatest; followed by two conventional ring spun yarns whose variations are similar. If analyze them with their mean values, we can estimate that some parts of the TBS yarn was looser and some parts maybe tighter.

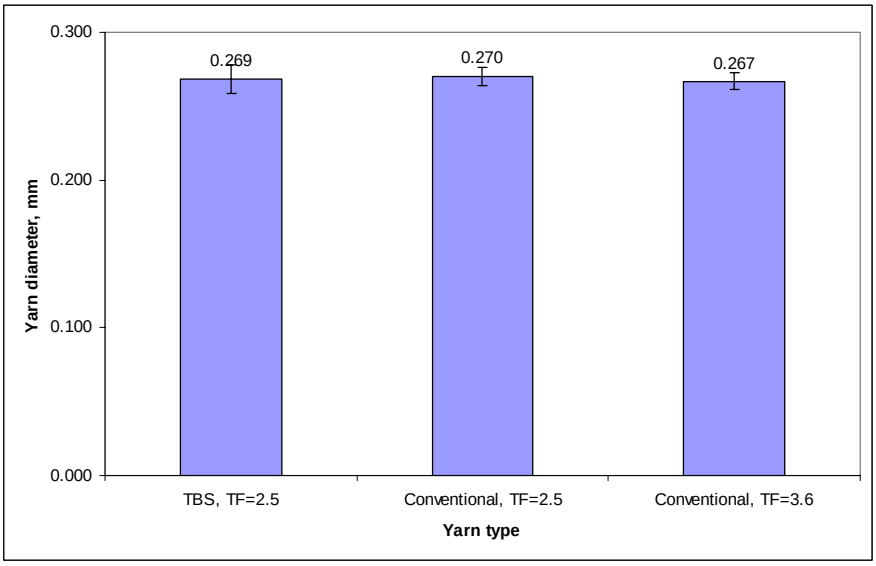

Figure 4-12 Comparison of the diameters of the 20Ne TBS and conventional ring spun yarn (20Ne)

For evaluating the effect of yarn diameter and its variation, these yarns were wound on a black-board. Figure 4-13 shows the images of the TBS and conventional ring spun yarns. They illustrate that the conventional yarn is more even than the TBS yarn. It has an agreement with the result of the diameter examination that the diameter variation of the conventional yarn is smaller than that of the TBS yarn.

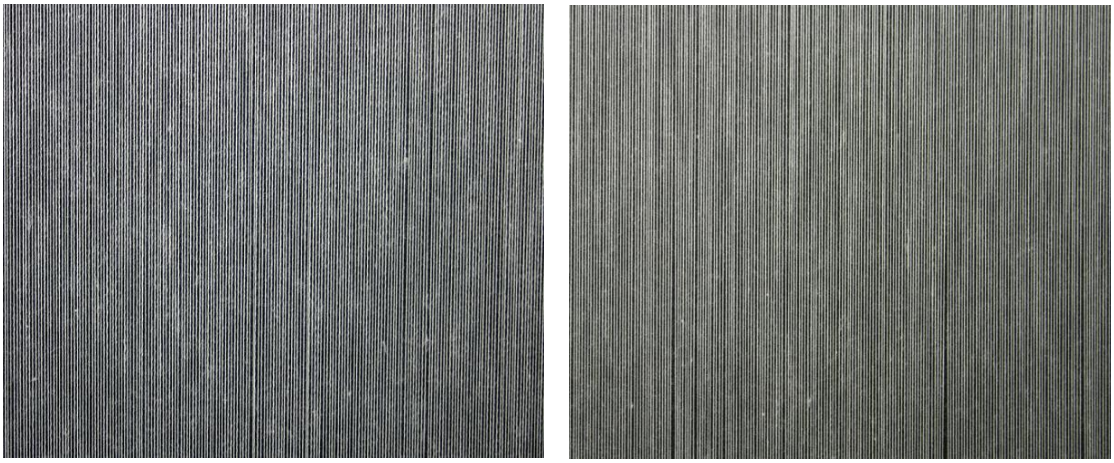

(a) TBS yarn (TF=2.5)

(b) Conventional ring spun yarn (TF=3.6)

Figure 4-13 Black-board images of 20Ne yarns

Yarn hairiness was evaluated by using the Zweigle G566 hairiness tester. Test speed is 50 meter per minute, and the test length was 100 meter. Results shown in Figure 4-14 indicate that the TBS yarn has better hairiness performance than the conventional ring spun yarn. The possible reason is that the de-twisting process wound the wild fibers on the body of the yarn, leading to the reduction of S3 values. However, sometimes the S3 value of the TBS yarn was higher than that of the conventional yarn. This may be

explained that the de-twisting process was unstable, sometimes cannot wrap the wild fibers effectively. In addition, the Zweigle hairiness tester only examines yarn hairiness in one direction; it cannot reflect the real situation completely. This may be another reason.

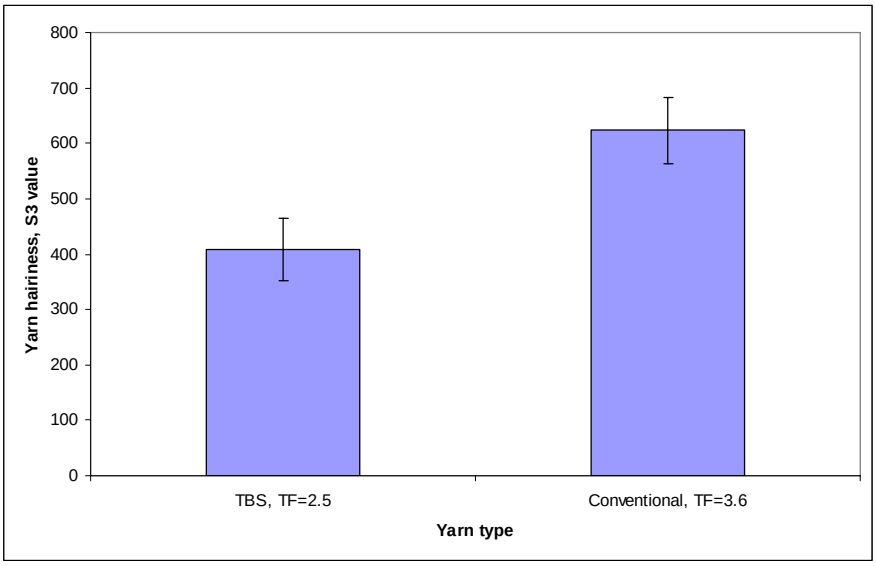

Figure 4-14 Comparison of the hairiness S3 values of the TBS and conventional ring spun yarn (20Ne)

For better understanding yarns' surface structural features, three 20Ne yarns from the same C1 roving were chosen for the examination of their surface features under SEM. They were a TBS yarn with the twist factor of 2.5, a lower twist conventional yarn with the twist factor of 2.5, and a higher twist conventional ring spun yarn with the twist factor of 3.6. Their photos are shown in Figure 4-15. The TBS yarn has two types of appearance characteristics. In type 1, inclined fibers form the yarn body, and some surface fibers tightly wound on the yarn body in the opposite direction to the twisting

rotation, as shown in Figure 4-15 (a). In type 2, the yarn has an appearance, shown in Figure 4-15 (b), similar to the lower twist conventional ring spun yarn. Fibers were loosely arranged each other, showing a bulky yarn diameter; some wild fibers were on the yarn surface, forming hairs. The images of the lower twist and higher twist conventional yarns are shown in Figure 4-15 (c) and (d). They have similar appearances. A major difference is the fiber inclination angle.

These images reveal that the TBS yarn has a unique structure differing from the conventional ring spun yarns. The reversely wrapped fibers contribute not only the reduction of hairiness (Cheng and Li 2002), but also the reduction of yarn torque. In addition, the compact part of the yarn reinforces yarn strength by increasing the lateral pressure between fibers and inter-fiber frictions. Since these two types appearances existed in the TBS yarn simultaneously, these may be one of the causes of the increase of yarn diameter variation, and may result in an increase of strength variation. The proportion of segments of Type 1 and 2 are related to the fiber specifications and the spinning parameters used (Hua).

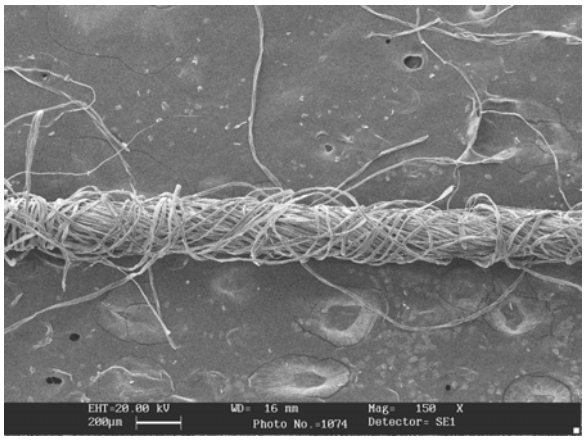

(a) TBS yarn (type 1)

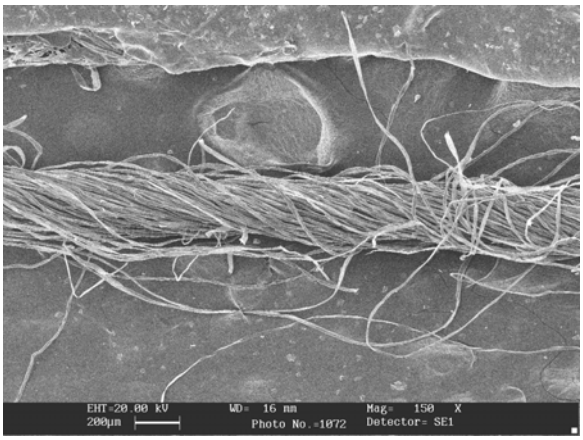

(b) TBS yarn (type 2)

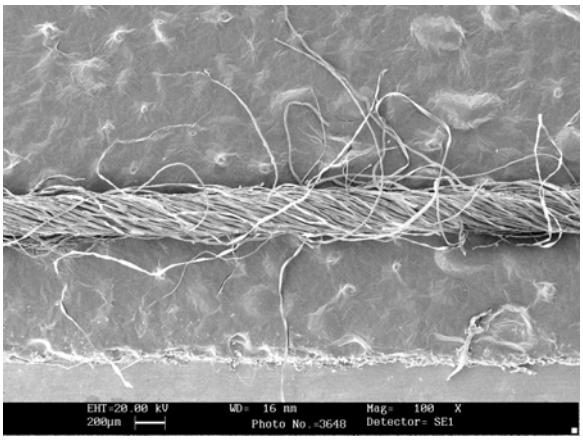

(c) Conventional ring spun yarn (TF=3.6)

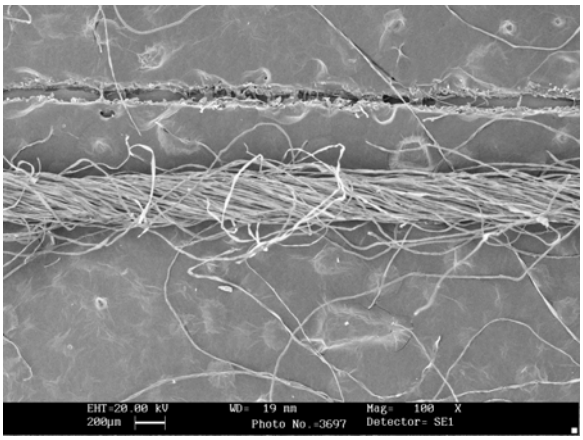

(d) Conventional ring spun yarn (TF=2.5)

Figure 4-15 Typical appearance of 20Ne yarns

4.1.3.2 Packing density

a) Yarn cross-sectional images

Yarn cross-sectional images are shown in Figure 4-16. For all yarn counts investigated, TBS yarns appear to have a packing density bigger than the conventional ring spun yarns of the same twist (TF=2.5).

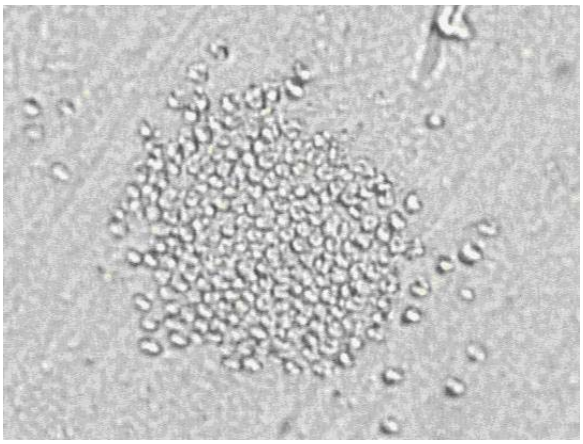

(a) 16Ne TBS yarn, TF=2.5

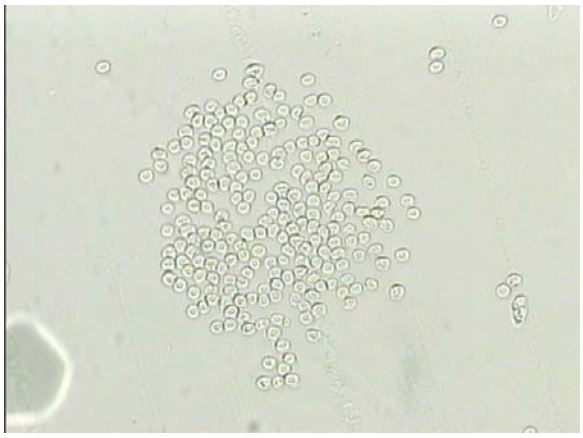

(b) 16Ne Conventional ring spun yarn, TF=2.5

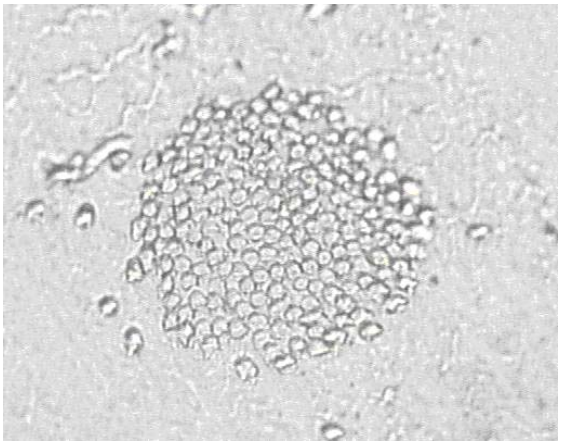

(c) 16Ne Conventional ring spun yarn, TF=3.6

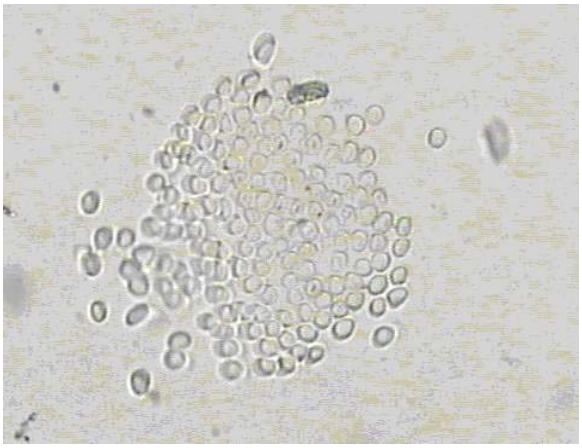

(d) 20Ne TBS yarn, TF=2.5

Figure 4-16 Yarn cross-sectional images

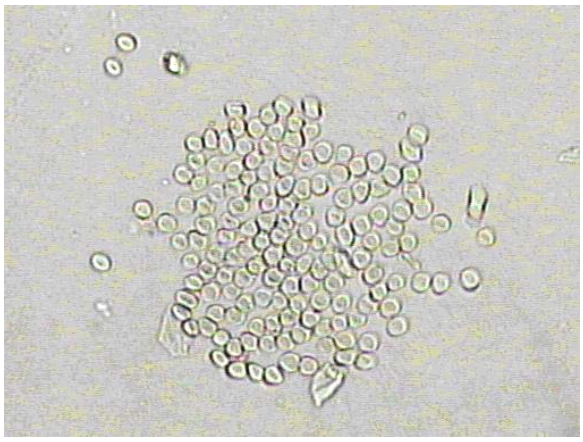

(e) 20Ne Conventional ring spun yarn, TF=2.5

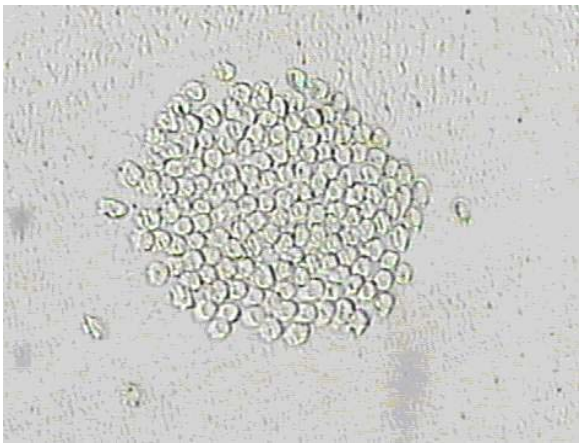

(f) 20Ne Conventional ring spun yarn, TF=3.6

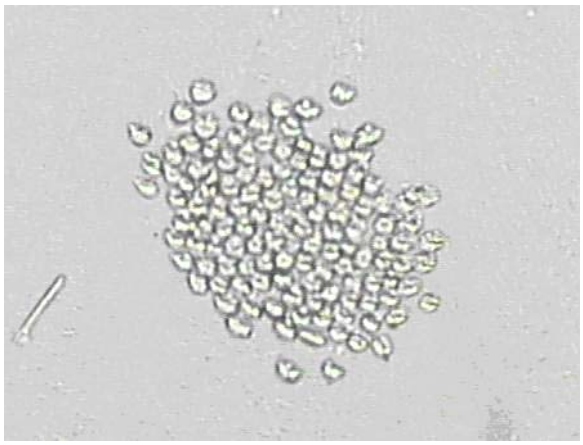

(g) 30Ne TBS yarn, TF=2.5

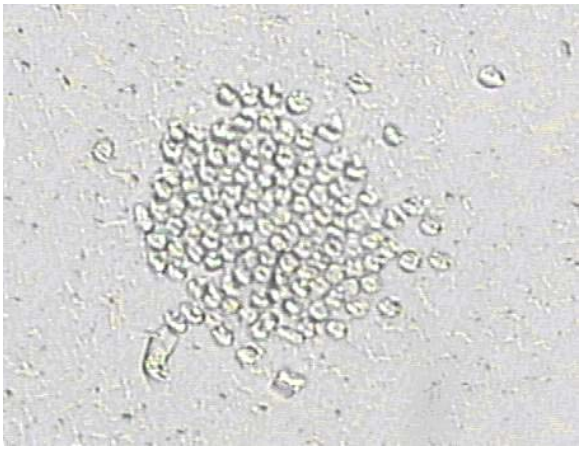

(h) 30Ne Conventional ring spun yarn, TF=2.5

Figure 4-16 Yarn cross-sectional images (continued)

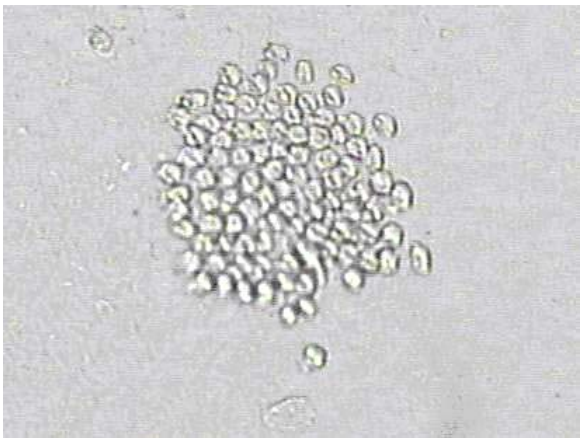

(i) 30Ne Conventional ring spun yarn,
TF=3.6

Figure 4-16 Yarn cross-sectional images (continued)

b) Packing density curves

Figure 4-17 illustrates a series of packing density curves as a function of radial position. The TBS yarn has a different distribution of fiber packing density. The packing density near the yarn axis is the highest among all annular areas i.e., the TBS yarn has a “harder” and “more compact” core, and the density reduces toward yarn surface. These differences of density patterns between the TBS yarn and conventional yarns may be explained by the theory derived by Hearle et al (1965, 1966). These yarns had wrapped-ribbon-form twists. The tension differences between fibers at different radial position in a yarn resulted in the fiber migration. Fibers twisting round the longer path at the outside of a yarn would develop a high tension and force fibers moving towards the center. Thus the centre was filled with the fibers migrated from other layers. These fibers entangled and locked each other, forming a compacter centre. The packing density at the center depended on the level of the fiber migration. Since the TBS yarn endured very high twist

in the part between front rollers and upper point of the torque reduction device. The shortened spinning triangle increased the difference of tension between the central and outer fibers, leading to more fibers migrating to the center, thus the centre became a “jammed” core.

Previous study of the fiber-packing density (Hickie and Chaikin 1974; Huh et al. 2002; Jiang et al. 2004) stated that the packing density of high-twist yarn is greater than that of low-twist yarn. For a higher twist yarn, its maximum packing density occurs at a point around one-quarter of the yarn radius from the yarn axis, and then decreases from this point to the yarn surface. While for a lower twist yarn, there is a linear decrease in packing density from the core to the yarn periphery. However, in this case, all TBS yarns have higher packing density if comparing with the same twist conventional yarns, and in the comparison between 16Ne yarns, the TBS yarn (TF = 2.5) even has a higher density than the higher twist conventional ring spun yarn (TF = 3.6). The maximum packing densities of the TBS yarns occur at the central region, showing a compact core. These imply that the TBS yarn has a structure differing from the conventional ring spun yarns, and the statement derived from the literatures does not always suit for the comparison between different yarns. In addition, the fiber in the outer layer gave more contribution to the yarn torque, thus the less of fibers in the outer layers partially resulted in the reduction of yarn torque.

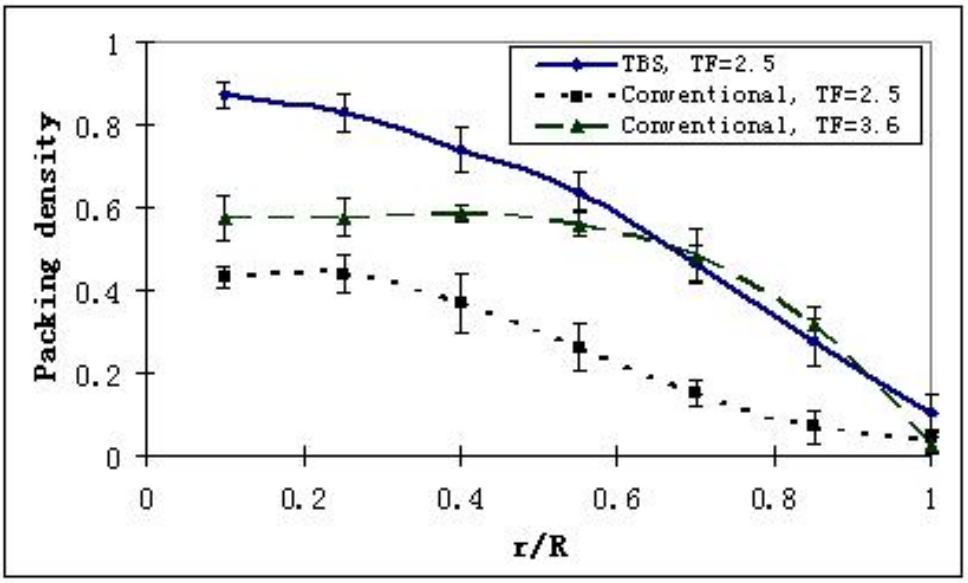

(a) 16Ne yarns

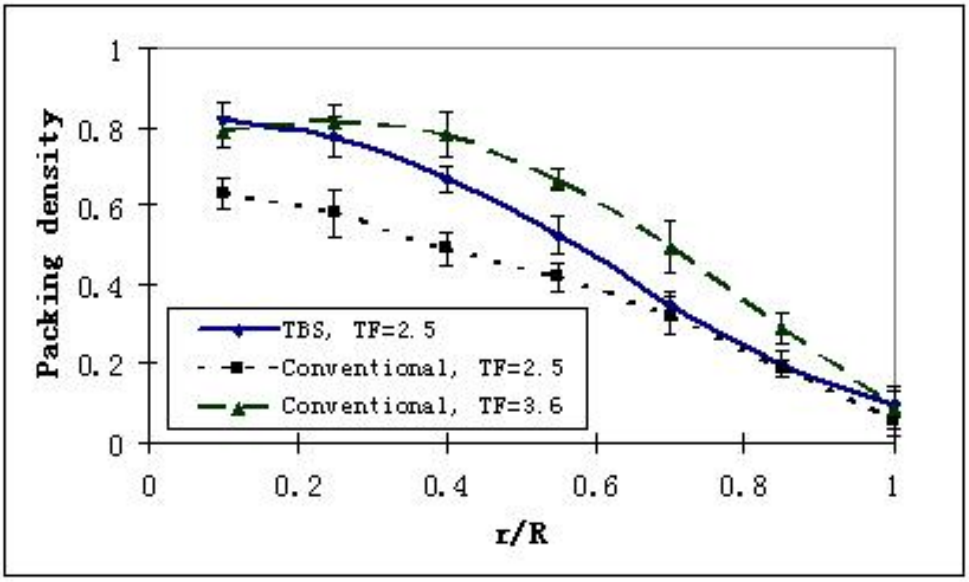

(b) 20Ne yarns

Figure 4-17 Packing density curves

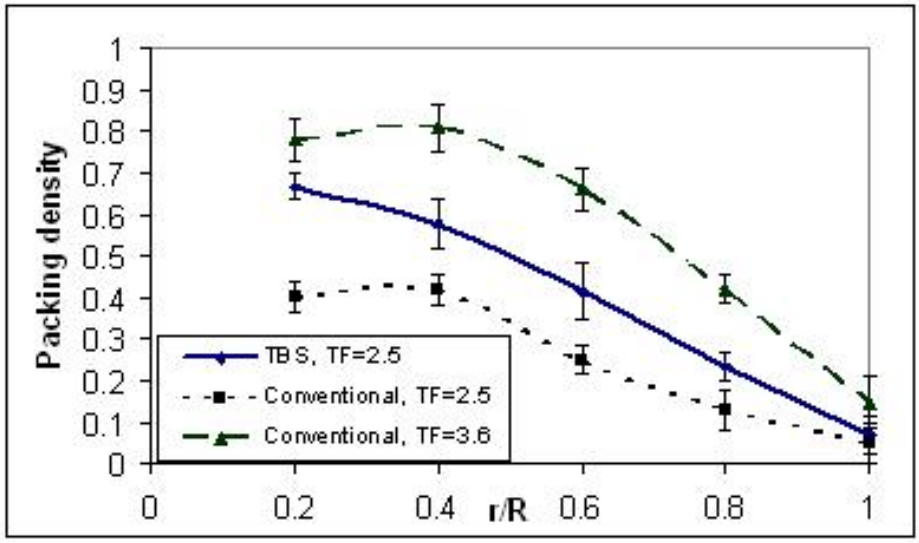

(c) 30Ne yarns

Figure 4-17 Packing density curves (continued)

4.1.3.3 Effect of yarn counts on the packing density

The investigation of the effect of yarn count on packing density is another task of this research. The diagram shown in Figure 4-18 illustrate that a thicker yarn turns out to be more compact. The reason for this phenomenon can be explained that the thicker yarns have more fibers in their cross section. As a result, a rise in the total compressive load acting on the yarn subsequently leads to the increase in its packing density. Moreover, these curves have similar tendencies. The changes in yarn count only affect the magnitude of the packing density on the whole but hardly change the location of the peak packing density. This indicates that the relationship between packing density and yarn count is approximately a linear one.

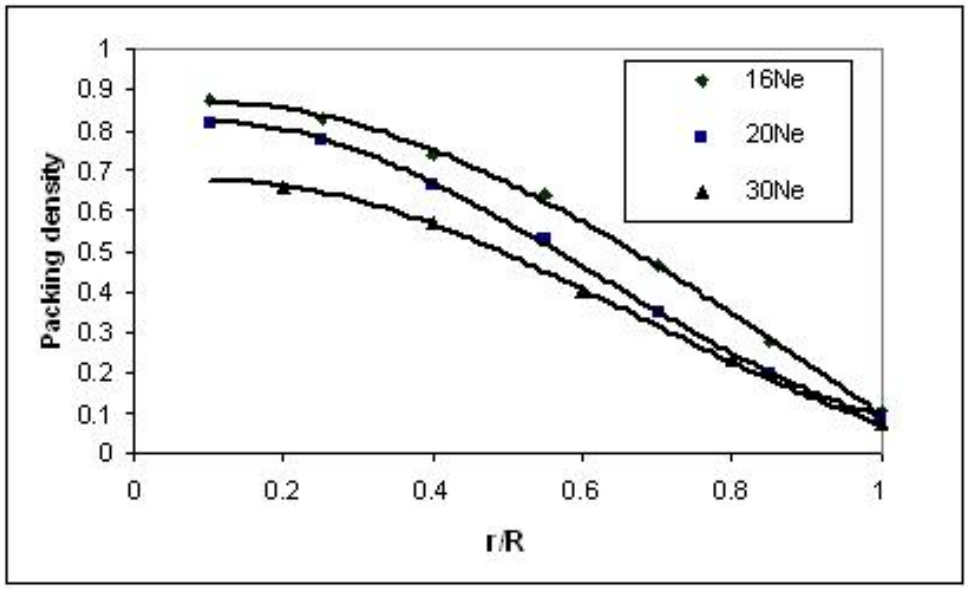

Figure 4-18 Effect of yarn counts on the packing density of the TBS yarns

4.1.3.4 Characteristics of the fiber path within the TBS yarn

a) Tracer fiber images

The fiber images were selected arbitrarily at random intervals based on the consideration that there should be only one fiber image for easy analysis. Fiber ends or entangled fibers are excluded. Portions of typical traces are shown in Figure 4-19. In this case, three kinds of 20Ne yarns were examined. They are two conventional ring spun yarns with different twist multipliers (TF = 2.5 and 3.6), as well as the TBS yarn (TF=2.5). The photos clearly demonstrate that these yarns have different path configurations. Shapes of the conventional ring yarns are similar, like sinusoidal function curves. But their magnitudes and frequencies are different. Obviously they are the results of the differences of the twist inserted. They reveal that the twist level has influences on fiber migration, i.e., fiber path within the yarn. During the formation of the yarn from a flat ribbon wrapping to a cylinder, higher twist leads to the reduction of the height of the

spinning triangle, increasing the variation of tension, and reinforcing fiber migration. Whereas the lower twist yarn has longer spinning triangle, the tension variation is not as greater as the higher twist yarn, and its fiber migration is milder than that of the higher twist one. However, the TBS yarn has a complicated path configuration. Apparently, its path cannot be described by using only one sinusoidal function curve. One explanation of this path is that the device, which is installed between the front rollers and the yarn guide, changes the fiber arrangement, leading to the modification of fiber path. Another explanation is that the de-twisting process might not precisely remove the extra twist inserted by the torque modification device due to fiber migration, entanglement and locking. Thus these parts of the fiber remained their positions, leading to an un-uniform fiber path.

(a) Conventional Ring Yarn, TF=3.6

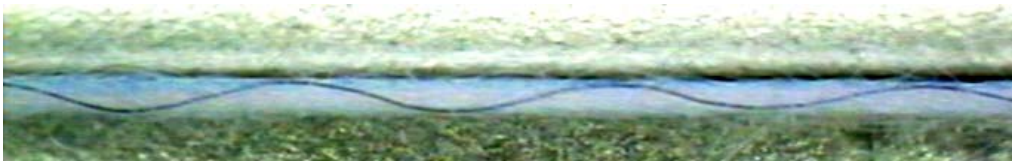

(b) Conventional Ring Yarn, TF=2.5

Figure 4-19 Typical tracer fiber images of 20Ne yarns

(c) TBS Yarn, TF=2.5

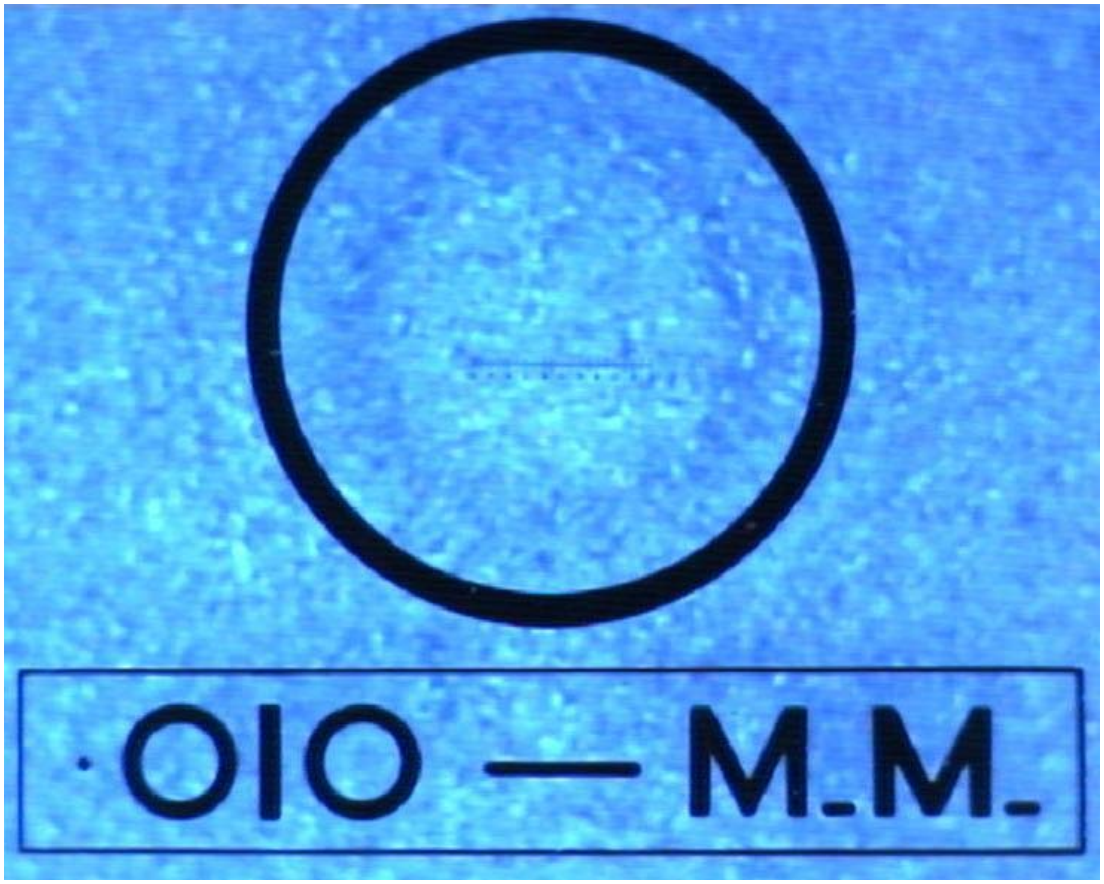

(d) Scale

Figure 4-19 Typical tracer fiber images of 20Ne yarns (continued)

For each yarn type, 30 tracer fibers were observed and analyzed. Since fiber is long and slender, several photos were taken along the length of the fiber in order to get whole images of the tracer fiber.

b) Analysis of the 2-dimensional FFT results

The work of data processing was conducted after the image capture. Its aim is to analyze the frequency of the photos so that we can decide if we use one or several specific functions to describe the yarn 2-D trace. The methodology used in the present investigation is Fast Fourier Transform. And the processing is accomplished by a program written by using the Matlab software.

As we mentioned above, the Fast Fourier Transform is capable of breaking down the paths of single fibers in a spun yarn into a wide range of periodicities. Thus we used it to convert the image into a complex function in the frequency domain. Figures 4-20 to 4-22 are the plots of spatial and frequency domain of the lower twist, higher twist conventional yarns and the TBS yarn, respectively. For the lower twist conventional ring spun yarn, the fiber path likes a periodical curve (see figure 4-20 (a)). Its period and magnitude are relatively even and stable. This is proved by the results of the Fast Fourier Transform as shown in Figure 4-20 (b). The peak means the fiber path can be simulated by using a curve with special frequency and magnitude. The higher twist yarn also has similar pattern. Figure 4-21 (a) illustrates that the path is a periodical curve, its frequency is stable but its magnitude is not as even as that of the low twist yarn. Figure 4-21 (b) shows that there is a peak in its spectrum. But its magnitude is lower than that of the low twist yarn. Moreover, the magnitude of wavelength of these two yarns are different, the periodicity of the lower twist yarn is longer than that of the higher twist yarn. These phenomena are in agreement with Hearle's observation (Hearle et al. 1969). The possible explanation of these phenomena is that the higher twist increases the

tension variation in spinning triangle, enhances fiber migration, leading to the shortening of migration periodicity and unevenness of migration magnitude.

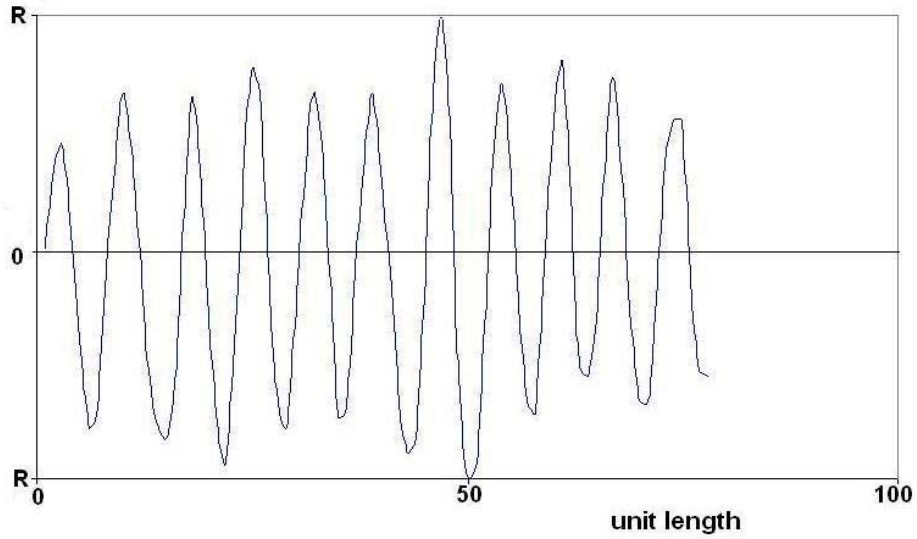

(a) 2-D migration envelope

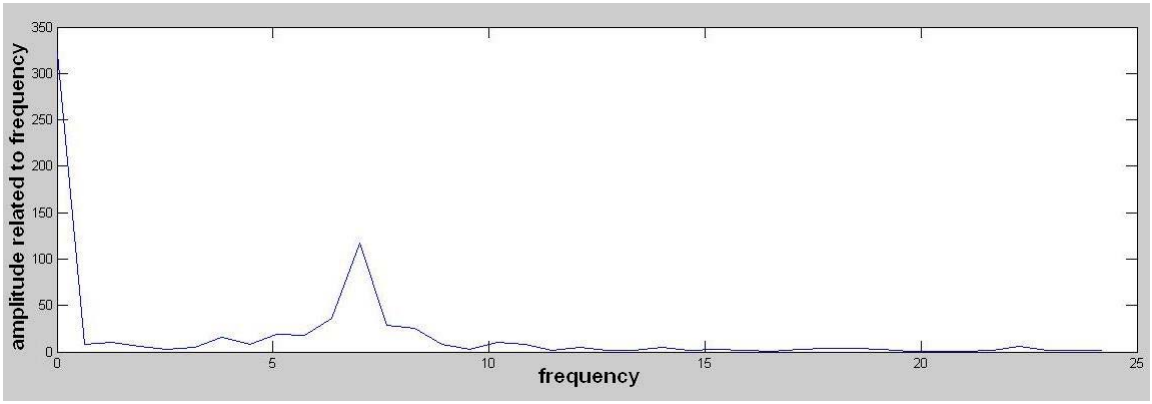

(b) FFT result

Figure 4-20 Data analysis of the 2D image of the 20Ne conventional ring yarn, TF=2.5

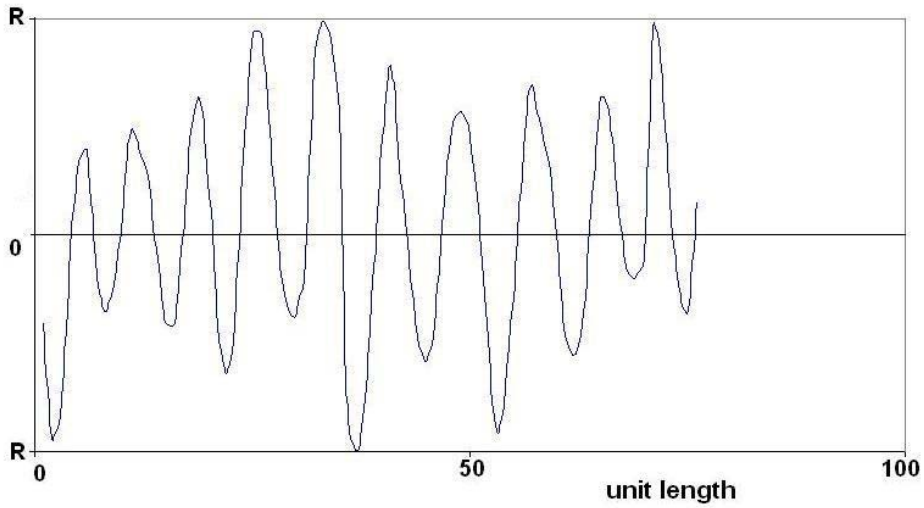

(a) 2-D migration envelope

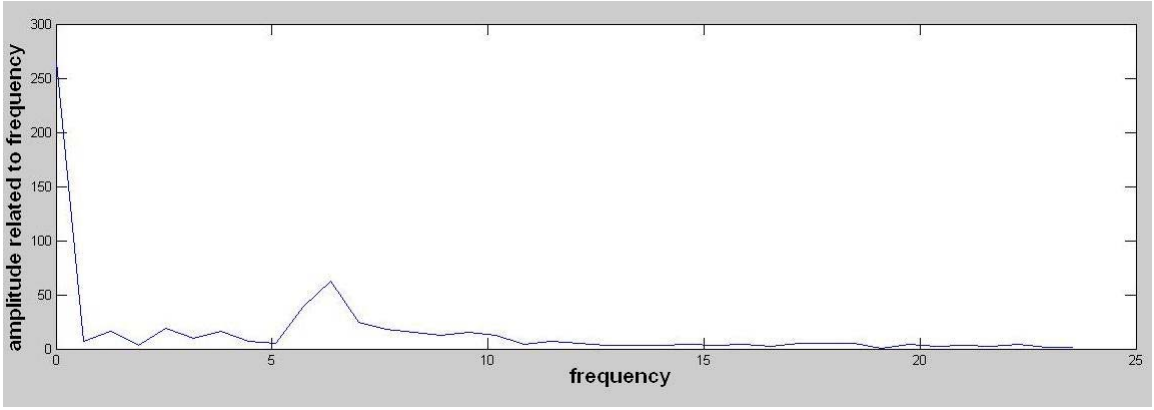

(b) FFT result

Figure 4-21 Data analysis of the 2D image of the 20Ne conventional ring yarn, TF=3.6

For the TBS yarn, its 2-D envelop demonstrated in Figure 4-22 (a) shows that the fiber envelop can be regarded as a combination of many functions which have various wavelength and magnitude. This is verified by its FFT analysis results shown in Figure 4-22 (b). The fiber undergoes dramatic and uneven migration. This may be the result of the combination of the extremely high twist and greater tension variation in the spinning triangle and the de-twisting process. The curve of its FFT spectrum is even and has no

peak, i.e., the curve cannot be represented by using one predominant function. This is different from the two conventional ring yarns.

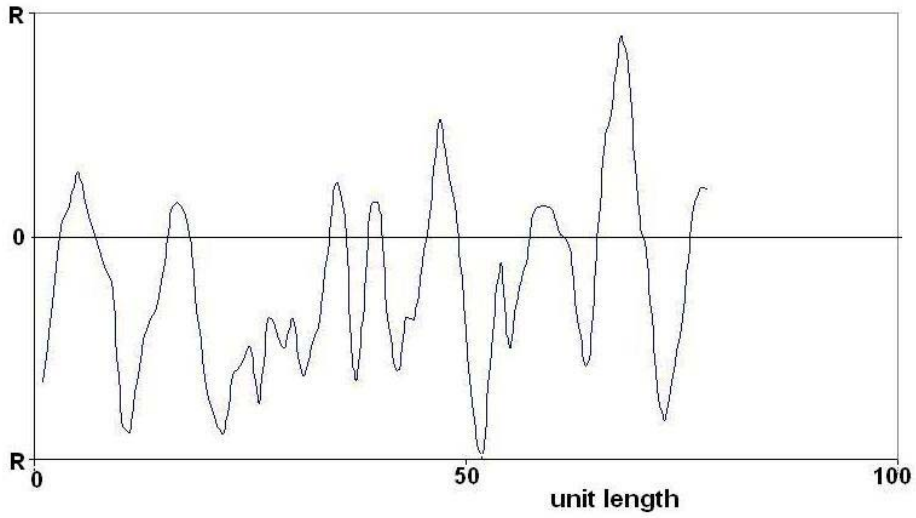

(a) 2-D migration envelope

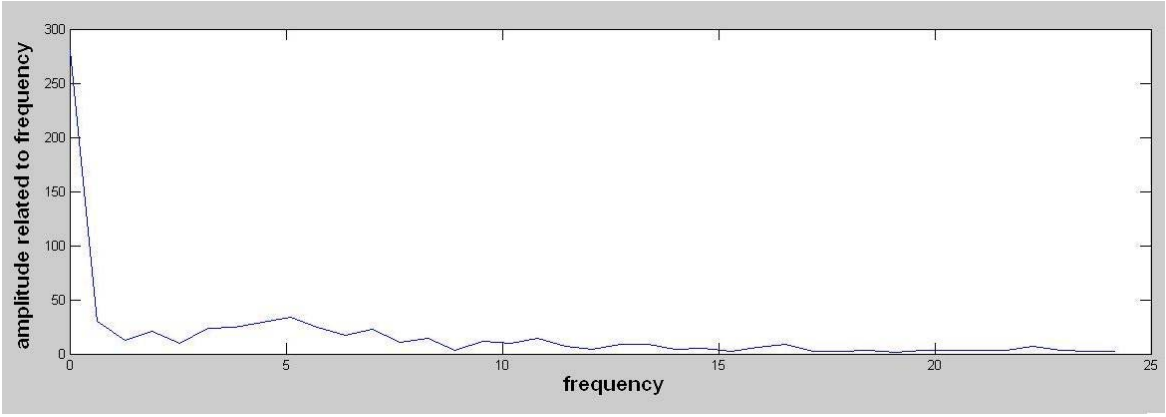

(b) FFT result

Figure 4-22 Data analysis of the 2D image of the 20Ne TBS yarn, TF=2.5

c) Re-construction of the fiber path within the TBS yarn

- *Fiber images*

For the yarns which have one or several dominated peaks and sub-peaks, these peaks or sub-peaks can be used for representing the fiber path. However, we could not simulate the fiber path of the TBS yarn by analyzing one projection of its path. Therefore, in order to fully understand the fiber path within the TBS yarn, it is necessary to identify fiber's 3D position. Using the improved tracer fiber technique (Figure 4-6), we can easily complete this task.

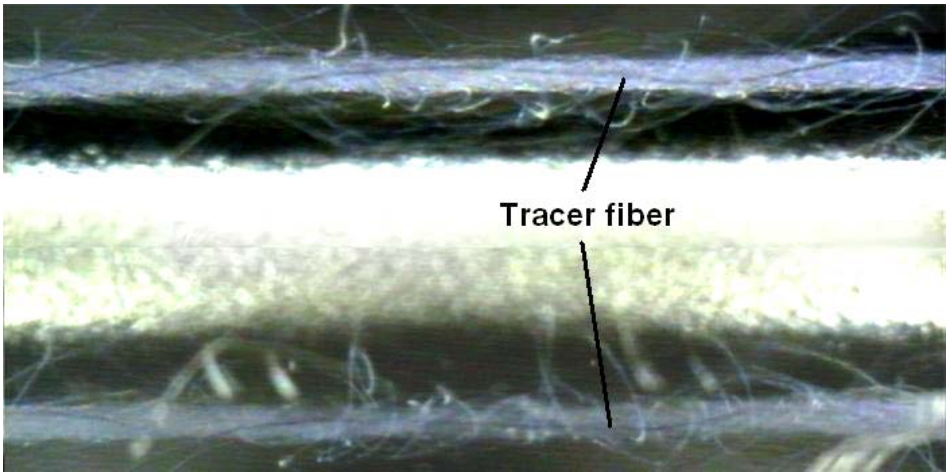

Figure 4-23 Twin images of the tracer fiber of the 20Ne TBS yarn, TF=2.5

Scale: Figure 4-17 (d)

Figure 4-23 is a segment of the twin images of the TBS yarn. Twin images are the images of the tracer fiber projecting on two directions. After the extraction of the coordinates of a tracer fiber, it is possible to calculate the radial positions of the fiber with respect to the center of the yarn along the yarn length.

In the present investigation, the yarn cross sectional shape is assumed as a circle. And the calculation of the 3D position of the dyed tracer fiber was conducted by using Excel software. Each set of data (corresponding to each pairs of photographs) was extracted and were filled into an Excel table. Then the X- and Y- coordinates for each Z position (Z being the length along the yarn) of the fiber at each Z were calculated. X- or Y-coordinates represent the projection of fiber path on X-axis or Y-axis respectively.

- *Data processing*

After the calculations, the 3-D plots were drawn by using the Matlab software. Figure 4-24 (a) is a portion of a 3D fiber path simulated based on the extracted points. It is clear that the fiber path is complicated. Thus for analyzing the details, a plot of the projection of the tracer fiber on its cross section was worked out (Figure 4-24 (b)). The path was divided into many segments. Apparently, these segments can be grouped into two types: the segments rotating in clockwise (CW) and counter-clockwise (ACW) directions, showing different rotational trend. The projections of their torques to the yarn axis may have different signs. For the clockwise segments, they rotate in clockwise direction, giving a Z twist, whereas other segments rotate in the opposite direction, demonstrating an S twist. Therefore, it is possible that the opposite torques counteract each other, leading to the reduction of the total torque.

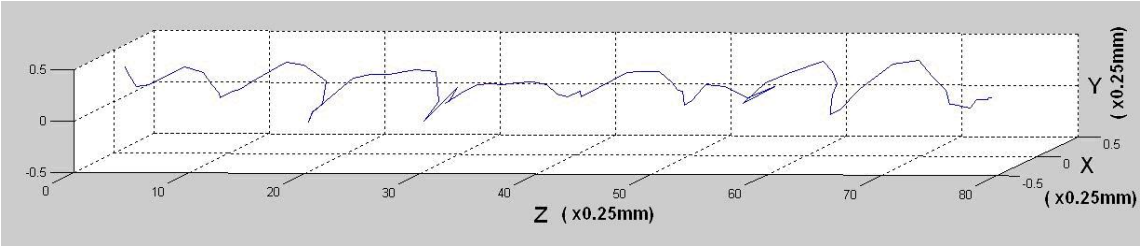

(a) 3-Dimensional plot of the fiber path

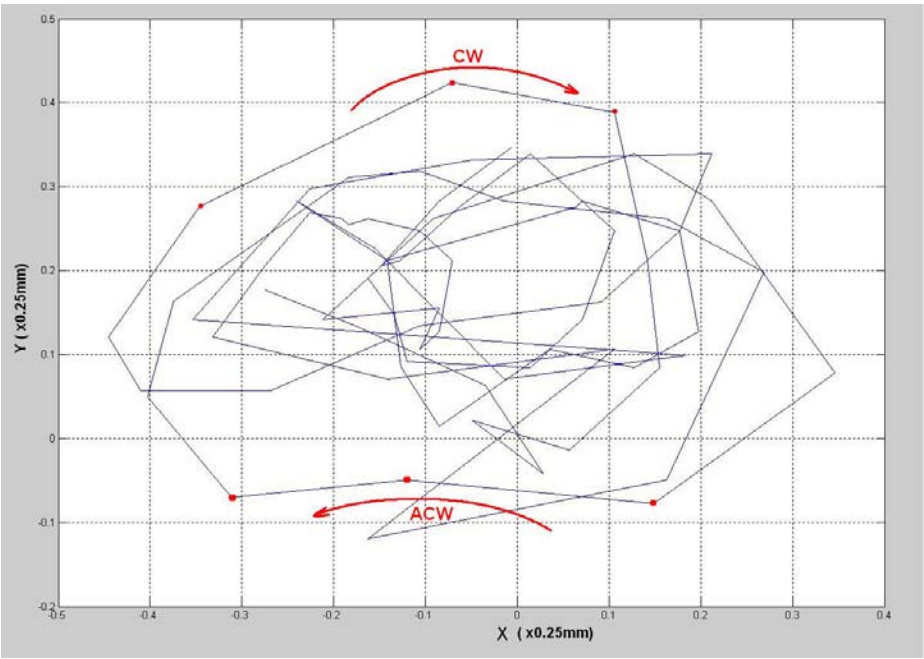

(b) Projection of the fiber path on its cross section

Figure 4-24 A section of fiber path within the 20Ne TBS yarn.

In order to confirm this finding, we did more examinations. After analyzing 30 samples, around 20-25% of segments have a tendency rotating in counter-clockwise direction, others rotated in clockwise direction. It means that the reverse rotations do not accidentally appear; it really exists in the TBS yarn, being a feature of the yarn structure. The reverse rotation partially balances the yarn residual torque, resulting in the reduction of yarn torque liveliness. In addition, the increased fiber migration enhances transverse

movement between layers, reinforces the entanglement between fibers, leading to the improvement of yarn strength. These may help explain why the TBS yarn has such a low torque but can keep relatively high strength.

4.2 Tensile and Torsional Properties of the TBS yarn

Apart from the investigation of yarn structure, we also evaluated the tensile and torsional properties of the TBS yarn.

4.2.1 Experimental details

4.2.1.1 Yarn preparation

Two 20Ne cotton yarns were examined. One is the TBS yarn (TF = 2.5), and the other is a high twist conventional ring spun yarns (TF = 3.6). Both yarns were spun by using the same C1 roving (specifications are shown in Table 6-1) on a Spin tester.

4.2.1.2 Yarn test

Yarns were conditioned under an environment of 65±2%RH and 20±2ºC for at least 24 hours before test. Yarn tensile properties were tested on an Instron 4411 tester by using the recommended procedure. Test speed is 500 mm/min, and the gauge length is 10cm. For evaluating yarn torsional performance, a KES-YN-1 torsion and intersecting torque tester was adopted. Then the results were recorded by using a plotter of Graphtec XY recorder WX3000.

4.2.2Results and discussions

4.2 2.1 Characteristics of the tensile performances of the TBS yarn

Figure 4-25 shows the stress-strain curves of the yarn tensile test. It illustrates that the TBS yarn and the conventional yarn have similar slopes. That is to say, they have similar tensile moduli. It means the modification process has no significant influences on yarn tensile rigidity.

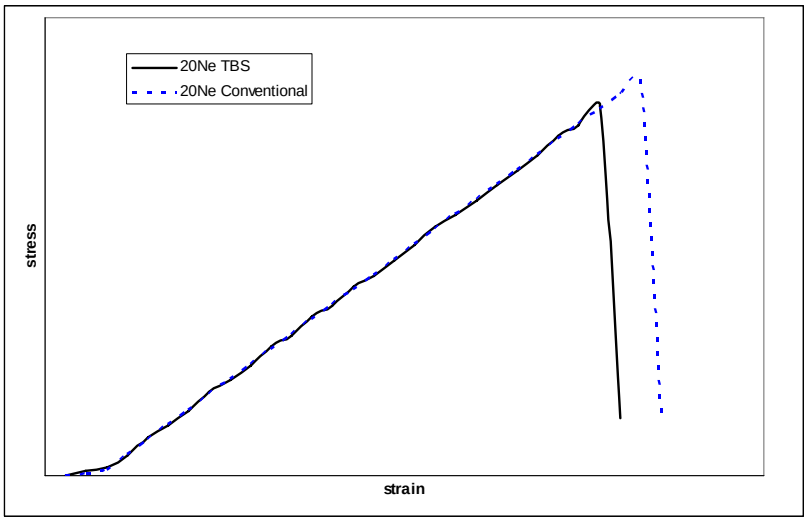

Figure 4-25 Tested tensile stress-strain curves

Table 4-4 Results of tensile test

Yarn	Max load (cN)	Break tenacity (cN/tex)	Break elongation (%)	Modulus (cN/tex)	Break energy (J)
TBS	466.5	16.76	8.43	205.89	0.0264
CV%	10.5	9.4	7.1	4.0	16.6
Conventional	559.4	19.41	9.17	217.17	0.0298
CV%	7.0	5.0	11.6	5.1	12.0

The test results shown in Table 4-4 detailedly demonstrate a comparison of tensile properties between the TBS and conventional ring spun yarns. It is clear that the strength

of the TBS yarn was lesser than that of the conventional. Equation 4-19 is an estimation model derived by Hearle et al (1969). $cos^2\alpha$ represents the effect of twist and $[1-k\,csc\,\alpha]$ expresses tension change due to fiber slippage. Since these two yarns have different twists, and the fiber migration and entanglement played an essential role in the formation of the moduli of the TBS yarn. This, in another way, demonstrated that the TBS yarn has a novel structure that differs from conventional ring spun yarns.

$$E_y = E_f\, cos^2\alpha[1-k\,csc\,\alpha] \qquad 4\text{-}19$$

Where $k=\frac{\sqrt{2}}{3L_f}\left(\frac{aQ}{\mu}\right)^{1/2}$; E_y and E_f are the moduli of yarn and fiber respectively; α is the twist angle; L_f is fiber length; a is fiber radius; Q represents migration wavelength and μ donates friction coefficient.

Table 4-4 also indicates that other items of the TBS yarn are lower than those of the conventional ring spun yarn. This maybe results from the low twist introduced. Another possible reason is that the modified structure reduces the coherence of the fiber arrangement, leading to decrease of yarn strength.

4.2.2.2 Characteristics of the torsion performances of the TBS yarn

The yarn torsional-hysteresis curves shown in Figure 4-26 demonstrate that the slope of the TBS yarn is around two thirds of that of the conventional yarn. That means that the initial shearing modulus of the TBS yarn is much lower than that of the conventional

yarn. And the shearing modulus of the deformed TBS yarn was also smaller than that of the conventional yarn when the direction of the additional twist is reversed. The Figure also reveals that the magnitude of the torque of the TBS yarn was smaller than that of the corresponding conventional yarn when the additional twist was $\pm 3\pi / 6cm$ and when the additional twist was de-twisted to zero. Combining with the low twist used, the modification process can significantly reduce the yarn torque.

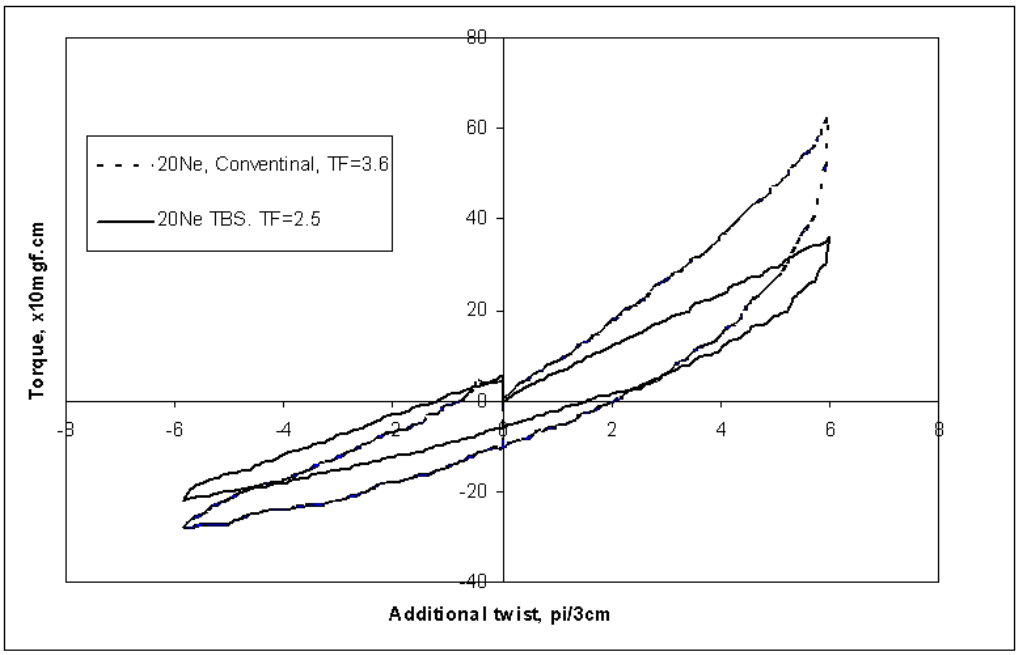

Figure 4- 26 Tested torsional stress-strain curves

Generally, the tensile and torsion performances were evaluated. The results show that the TBS yarn possesses a tensile modulus similar to its conventional ring spun yarn. Other items are slightly lower than those of the conventional yarn. The torsional stress-strain diagram indicates that the TBS yarn has a lower torsional modulus, around two

thirds of that of the conventional yarn. That means the TBS yarn achieves a balance of lower torque and relatively high strength.

4.3 Summary and Conclusions

Yarn structure includes two parts: internal and external structures. The external structure was examined by measuring yarn diameter, evaluating yarn hairiness and observing yarn surface etc. The SEM images imply that the TBS yarn exhibits a unique appearance similar to and/or differing from the conventional ring spun yarns. Some parts of the yarn have an appearance similar to the lower twist conventional ring spun yarn. However, in other parts of yarn, some wrapping fibers were found on the surface of the TBS yarn. These fibers were tightly wound on the yarn body that possesses a ring yarn appearance in an opposite direction to the yarn twist, exhibiting a compact appearance of structure. These wrapping fibers may be the results of the de-twisting process. The two types of yarn appearances may result in a bigger variation of yarn diameter. This agrees with the results of yarn diameter measurement and the analysis of blackboard images. The test results of yarn hairiness S3 value indicate that the TBS yarn has a good hairiness performance if compared to its corresponding conventional yarn.

In the study of yarn internal structure, we examined the radial fiber distribution and fiber path inside the yarn. The investigation of yarn cross-sectional structure reveals that the TBS yarn possesses a radial fiber distribution pattern different from its convention ring yarns. The density diagrams show that the TBS yarn is relatively tighter than the conventional ring yarns with the same or slighter higher twist. Its central packing density

is the highest among all annular areas, which means it has a “harder” or “ more compact” core, whereas the core of the conventional yarn is slightly “softer” or “looser” than its adjacent annular region. This is a major feature of the cross-sectional structure of the TBS yarn, and it can be explained by using the mechanism of the wrapping-ribbon-form twist and the theory of fiber migration due to tension variation.

The fiber path within the yarn was examined by using the tracer fiber technique. The results indicate that the TBS yarn did not migrate uniformly inside the yarn. The FFT analysis implies that the envelop of the TBS yarn can not be expressed simply by using one function; it may be a combination of many functions. The 3-D analysis reveals that the segments of a fiber of the TBS yarn rotate in different directions inside the yarn simultaneously; the projections of their torques to the yarn axis may partly counteract each other, leading to the reduction of yarn residual torque.

Generally, the TBS yarn has a novel ring structure differing from the conventional ring structure. It possesses a “more compact” core maybe due to its fiber migration. The magnitude and frequency of its fiber migration are not as stable and even as those of its conventions yarns. Thus it can not be expressed simply by using one function.

Apart from the yarn structure, the tensile and torsional performances were also evaluated. The results show that the TBS yarn has tensile properties similar to its conventional ring spun yarn. It has similar modulus and other items are slightly lower. For the torsional properties, the TBS yarn has smaller torsional modulus and other properties than its conventional yarn. These directly indicate that the torque reduction device efficiently

modifies the torsional performance of the TBS yarn with the help of low twist used. Therefore, the TBS yarn achieves the balance of lower torque and relatively higher strength.

CHAPTER 5
MODELING THE TORSION BEHAVIOR OF TORQUE-BALANCED SINGLES RING SPUN YARNS

5.1 Introduction

The establishment of a mathematical model not only helps us understand the nature of the TBS yarn, but also enables us to design better experiments and interpret the results. One of the most important features of the TBS yarn is its low residual torque, therefore, we concentrate on modeling the torsional behavior of the TBS yarn.

Platt et al (1958) were the first to calculate the torque generated in a twisted singles yarn by using a force method. They calculated the torque due to fiber-bending and fiber torsion based on the assumptions of elastic fibers, uniform cross-sectional packing density and idealized cylindrical helix yarn geometry. They neglected the component of torque due to fiber tensile stresses imposed during spinning and usage. However, Hickie and Chaikin (1960) found that yarn tensile strains are large enough to contribute an appreciable component to the torque in a freshly spun yarn. Then Postle et al (1964) investigated the influences of the component due to fiber tension on yarn torque. By using the force method and assuming an idealized cylindrical helix yarn geometry with uniform fiber-radial- packing density, they found that the contribution to the total yarn torque of the torque due to fiber tension was far greater than the sum of the contribution due to fiber-bending and fiber torsion, and the component due to fiber-bending being negligible. Mitchell et al. (2006) recently investigated the torque in worsted wool yarns

by using a torquemeter. After analysis, they resolved the torque into two components: the torque due to the applied tension and the intrinsic torque due to fiber bending and twisting.

Bennett and Postle (1979) investigated, by using a force method, the dependence of yarn torque on the nature of fiber internal tensile-stress distribution introduced during yarn formation. They studied two extreme yarn structures: no fiber migration and perfect migration, and gave some expressions for calculating yarn torque due to corresponding fiber-stress distribution.

For the case of variable packing density, a hypothesis called as ‘shortest-path’ was introduced by Carnaby and Grosberg (1976). They used an energy method and assumed that under tensile load, a yarn will be separated into two regions, a jammed region and an unstrained region surrounding it. In the jammed region, the packing density reaches a maximum value. Tensile strain can only be accumulated within fibers in this region because fibers outside can readily move inward or outward to avoid being strained. Based on it, many researchers (Tandon et al. 1995; Choi et al. 1998) conducted the investigation of torsional behavior of singles yarns.

These studies were carried out based on the idealized geometry of cylindrical helices that are concentric and parallel to the yarn axis, with the maximum helical angle on the yarn surface. However, many fibers in singles spun yarns do not follow the idealized concentric helical path. In ring spun yarns, the fibers move from the yarn center to the yarn surface, following the path of migrating helices. This phenomenon was observed

and examined by Morton (1956) and other researchers by using the tracer fiber technique. In order to simulate fiber migration and investigate the mechanical properties of a migrating fiber, Tao (1996) modified the yarn geometry by introducing a sinusoidal function on a conical helix. She theoretically studied the fiber mechanical properties and identified that the axial component of the couple and transverse component of the force may change their direction if reaching critical migration amplitude.

In a relaxed yarn, the amount of fiber tension in the yarn axis direction is minimal. Therefore, contributions due to fiber bending and torsion became vital. The residual yarn torque in a fully relaxed knitted fabric should be governed by the fiber bending and torsion which are determined by the fiber configuration. From this point of view, the modification of ring spun yarn started. Only when the yarn geometry changes from its helical geometry, the torque balance in a singles yarn can be realized.

Since we assumed that dramatic migration occurs inside the TBS yarns, a Fourier-like series that consists of many sinusoidal functions was adopted for describing fiber migration, and a model of the torsional behavior was established in this chapter.

5.2 Methodology

5.2.1 Some considerations

5.2.1.1 General strategy

The general strategy which was used by many researchers for making a theoretical analysis was outlined by Treloar (Hearle et al. 1969). He said that in a typical engineering

problem, it is required to calculate the response of a structure (i.e. the resultant deformation and also the internal stresses and strains) when a given set of stresses is applied to it. For solving this problem, the engineer must have first a complete specification of the disposition of the components, i.e., of the geometry of the structure. Secondly, he must have the knowledge of the mechanical properties of the materials used in these components, and, finally, he must have at his disposal a method of analysis that will enable him to arrive at a mathematical solution to his problem.

Adopting this strategy to the current study, the first is to calculate the strains due to an imposed deformation; and then to calculate either the stress distribution and the equilibrium of forces or the energy due to the deformation. For the transformation from external deformation to external stress, there are two methods, i.e. force or stress analysis method and energy method. The details of which will be discussed below. In addition, the treatment of fiber involved and the basic assumption in terms of yarn geometry will be explained as well.

5.2.1.2 Selection of the modeling method

Normally, force and energy methods can be used for establishing mathematical model. The former is concerned with the quantitative analysis of internal stresses and strains produced in a body as the result of external loads and deformations. It has been widely used in the fields of structural and mechanical engineering in which quantitative evaluation of internal stresses and movements is a predominant requirement. One of the applications of force analysis method to textile field is the study of the mechanics of flexible fiber assemblies. For example Postle et al (1964) successfully calculated the yarn

torque by introducing such an assumption that the fiber remains a cylindrically helical fiber path within the yarn. However, this method possesses some limitations when it is applied to textile structures which appear to be the extremely low stiffness of fiber assemblies and the inevitable fiber slippage near the fiber ends, there is a large discrepancy between their estimation value and experimental results.

Since the force analysis method firstly needs to calculate the strains due to an imposed deformation, and then to calculate either the stress distribution and the equilibrium of forces or the energy due to the deformation. Therefore, it is important to conduct a detailed analysis of the stresses within the yarn. The force analysis method is suitable for the study of simpler cases, rather than the complicated ones that the stress-strain curve of the fibers is nonlinear or where it is necessary to take account of both large extensions and transverse forces.

The energy method was firstly exploited by Treloar and Riding (1963) in their study of the stress-strain analysis of continuous filament yarns by obeying the law of energy conversation. The adoption of energy method has two advantages. The first is that it can simplify the analysis process because energy is a scalar quantity, permitting numerical summation. Another important feature of the energy method is that for the geometric quantities, only their values in unstrained state need to be considered. It is not necessary to deal explicitly with the geometry in the strained state. However, the energy method possesses several drawbacks. It likes a black-box, only outputs the total exploited stress rather than a full picture of the stress-distribution throughout the system, giving less information than the force method. In addition, the energy method is applicable only for

incompressible materials because lateral strains are involved in compressible materials which may complicate the analysis. Finally, it is necessary to properly assume the yarn structure and energy for working out an ideal yarn modeling.

5.2.1.3 Continuum and discrete fiber modeling principle

There are two principles which were mainly adopted in previous studies of yarn mechanics. They are continuum method and discrete principle.

For the continuum principle, it assumes that the object is infinitely divisible, and an infinitesimal volume of material can be referred to a particle within the continuum, but neglecting the discontinuity, variation, and the molecular nature of the object. This method is convenient and simple, and widely used in the field of textile researches for solving various practical mechanics problems.

Two-phase scheme was often adopted when applying the continuum method to yarn mechanics (Carnaby and Postle 1991). The first phase is to establish the geometrical relationships between the yarn deformation and the strain of the continuum in the local co-ordinates of the yarn element, and the second phase is to translate the local strains into stresses. By properly linking these two phases together, it is possible to find the relationship between the stresses and the external load.

The discrete fiber method can also be used in the field of textile research. It takes each fiber as a discrete component of the structure, thus the whole response of the assembly

can be calculated simply by summing the separate contributions of the individual fibers. Compared with the continuum method, the discrete method has its own advantages: firstly it considers fiber migration and other phenomena of mass transfer like fiber slippage; secondly, simple yarn structures can be easily extended to intricate geometries and deformations; and it needs less computation than the continuum method.

One of the problems of implementing this method is that it is difficult to analyze each individual fiber. However, this problem may be easily solved by classifying fibers into different categories according to their similarities. For example, fibers at the same radial position may possess roughly equivalent helix angle, and other related properties. Apparently, the discrete fiber approach is suitable for the investigation of the yarn produced with staple fibers due to the discontinuities in staple fiber length.

5.2.1.4 Yarn geometry

Normally, yarn geometry model is a description of arrangement of fibers inside the yarn. It is often established based on the observation of tracer fibers and proper assumptions.

The famous and classical model is the idealized cylindrical helix model (Figure 2-3). It is assumed that the yarn is circular in cross section, and composed of a series of concentric cylinders of differing radii, and each fiber follows a uniform helical path around one of the concentric cylinders, as well as the density of packing of fibers in the yarn remains constant throughout the model.

However, the observation of fiber path in a ring spun yarn reveals that the fiber, in fact, does not follow a cylindrically helical path, it often transverses between different concentric layers. i.e., fiber migrates within the yarn (Morton 1956). Previous researchers (Morton 1956; Hearle and Bose 1965) investigated the fiber migration and established two migration mechanisms. For describing the fiber migration path, many hypotheses have been made. For example Önder and Başer developed a yarn model based on a conically helical path (Figure 2-4) in 1996. They assumed that the yarn is a single fiber yarn uniformly along its length, with a circular cross section of uniform specific volume, and fibers follow identical conically helix paths equally spaced along the fiber axis, and the yarn axis is also the axis of conical helices of all fibers, as well as the radius of the helix changes regularly between zero and the yarn radius.

In an attempt to establish a model for solospun yarns, with controlled fiber migration in mind, Tao (1996) investigated fiber migration by successfully introducing a changeable radius to a normal conical helix. With this improvement, she calculated fiber migration and yarn torsional properties. One derivation from that work is that it is possible to reduce the total yarn torque by carefully control the migration path of fibers both in the radial and longitudinal directions.

5.2.1.5 Shortest-path hypothesis

The shortest-path is a jammed-region model. Carnaby and Grosberg (1988) stated that, for a bulky staple yarn, the final positions of the fibers are determined by their need to minimize their tensile strain. Thus, their paths will effectively be the shortest routes that

they can possibly take, subject to the packing limitations imposed by the surrounding fibers. Therefore, as a result, a yarn will be separated into two regions: a jammed region and an unstrained region. The difference between them is that the radial movement of the fibers in the former region is restricted and any tensile load would result in strain accumulation within it. Whereas for the fibers in the later region which surround the former, they can move freely, only strain accumulation will occur. In this study, since the TBS yarn has a relatively compact structure (Chapter 4), we assumed that it is closely packed initially.

5.2.1.6 Fiber slippage

For a staple yarn, its slippage is very important. By testing staple-fibre yarns at short gauge lengths, where slippage near the fiber ends is virtually eliminated, Carnaby and Grosberg (1976) has shown that the relative weakness of staple fibre yarns could not be explained solely by correcting successful continuous filament yarn theories to allow for fiber slippage. They drew conclusions that slippage was in fact a minor effect especially at low strains and that consolidation of the yarn structure had a far greater effect than slippage on the strain distribution and the resultant tensile properties.

5.2.2. Methodology adopted in this investigation

The fundamental approaches used in this modeling include

- Modified cylindrical helix
- Energy analysis method
- Discrete fiber modeling principle

- Non-uniform packing density

In addition, an initial tensile load (pretension) is applied to the yarn in order to prevent the yarn from undergoing torsional bucking during further twisting. Then, the extended yarn is given an increment of additional twist while constrained to the same yarn elongation. During deformation, there is no change in yarn volume. The aim of the modeling is try to establish the torque-twist relationship for a yarn under tension which is twisted at a constant yarn length. If an initial fiber-tensile-strain distribution for an unset, freshly spun singles yarn is known, then this case of yarn torsion would, with minor adaptation, allow us to study the torsional behavior of such a yarn, which will invariably snarl or twist up on itself unless it is prevented from doing so.

5.3 Basic Assumptions

To make the yarn model controllable, some assumptions have to be made before the establishment of the model. They are listed as below.

a. The system is assumed to be conservative.
b. All the fibers in the yarn are identical and uniform along their length, sharing identical properties, i.e., to be perfectly elastic, to follow Hooke's law (stress proportional to strain), and to have an axis of symmetry.
c. Viscosity and plasticity are ignored.
d. All fibers are long enough to consider a complete turn of the helix.

e. No lateral compression of the fiber cross-section takes place, which allows the fiber tensile energy to be calculated independently since it is a function only of tensile strain, irrespective of the stresses causing the strain.
f. Individual fiber follows a modified helical path, all such helices being concentric. After deformation, the fiber helices remain in its shape.
g. Under tension, all helices undergo the same amount of extension in the yarn length direction.
h. Fibers are initially packed in such a way that at any given tension and torsion, fibers undergo tensile, torsional and bending deformations.
i. The distribution of fibers is non-uniform, and can be expressed by a function of radial position.
j. The lateral contraction of helices at different radial positions is uniform.
k. All fibers are arranged in the yarn regularly without folds or kinks.
l. The yarn is cylindrical in shape, uniform along its length, and with a circular cross section.
m. The yarn is considered to consist of discrete number of fibers. The number of fibers in any yarn cross section and the number of turns per unit length of the yarn are constant.
n. Fiber migration is considered.
o. Fiber slippage is ignored.
p. The effects of bending and torsional deformations suffered by constituent fibers of the yarn and the forces and the couples that cause these deformations are considered.

q. Changes in bending curvature and torsion due only to changes in the helical configuration of the fibers are considered.

r. Yarn twist is static.

5.4 Notations

Some notations are adopted and valid throughout this chapter. They are listed as followings.

θ	Helix angle of an arbitrary fiber.
$r_0(\theta), r_1(\theta)$	Radial position of the fiber in the initial and deformed yarns.
r_e	Equivalent radial position of a fiber.
R_f , R_y	Fiber and yarn radii
$p(\theta)$	Ratio of fiber radial positions of the fiber in the initial and deformed yarns.
ϕ	An angle per unit of extended length of yarn due to deformation.
U_e, U_b, U_t	Tensile, bending and torsional energy.
l_0, l_1	Fiber length in one turn of twist in the initial and deformed yarns.
ε_f , ε_y	Fiber and yarn tensile strain.
T_0, T_1	No. of twist per unit of length of the initial and deformed yarns.
A_0 , A_1	Cross-sectional areas of the initial and deformed yarns.
$s_0(\theta), s_1(\theta)$	Arc length of a fiber with angle θ in the initial and deformed yarns.
$\kappa_0(\theta), \kappa_1(\theta)$	Curvature of a fiber with angle θ in the initial and deformed yarns.

$\tau_0(\theta), \tau_1(\theta)$	Torsion of a fiber with angle θ in the initial and deformed yarns.
EI_b, GI_o	Bending rigidity and torsional rigidity of the fiber.
q	Yarn radial packing density

Subscripts "0" and "1" denote initial state and deformed state, whereas subscripts "f" and "y" refer to fiber and yarn respectively.

5.5 Theory

5.5.1 Fiber geometry

We assumed that a fiber follows the path of a modified cylindrical helix with the radius $r(\theta)$ shown in Figure 5-1, where $r(\theta)$ is a function which is a combination of basic radius R_{basic} and migration ΔR. We also assumed that $r(\theta)$ can be expressed as a Fourier series, its expression in sinusoidal form is

$$r(\theta) = R_{baisc} + \Delta R = R_{basic} + \sum_{k=1}^{\infty} a_k \sin(b_k \cdot \theta + c_k) \qquad 5\text{-}1$$

Where a_k, b_k and c_k are the coefficients of the Fourier series, and $b_k = 1,2,\cdots,n$.

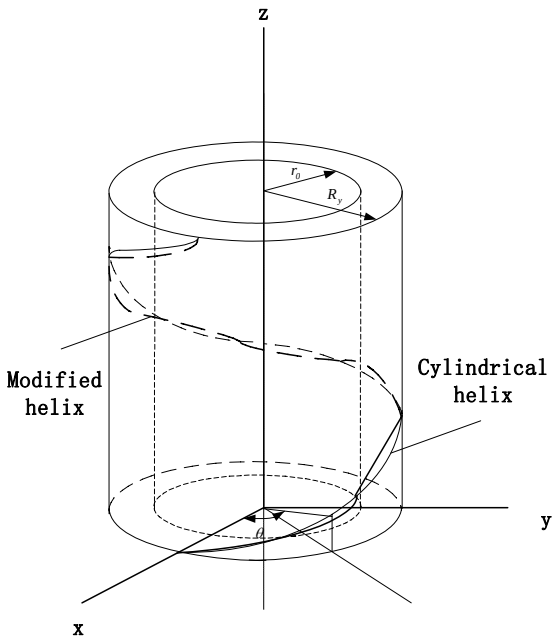

Figure 5-1 A cylindrical helix fiber path

Therefore, the geometry of the fiber can be expressed as:

$$f = \{x,\ y,\ z\} \tag{5-2}$$

Where $x = r(\theta)\cos\theta$, $y = r(\theta)\sin\theta$, and $z = \frac{\theta}{2\pi T}$. Since we assumed that the yarn is extended and rotated during the deformation. Thus we can express as follows:

$$r_0(\theta) = R_0 + \sum_{k=1}^{\infty} a_{0k}\ sin(b_k \cdot \theta + c_k) \tag{5-3}$$

$$r_1(\theta) = R_1 + \sum_{k=1}^{\infty} a_{1k} \sin(b_k \cdot \theta + c_k + \frac{\theta}{2\pi}\frac{\phi}{T_1}) \quad \text{5-4}$$

5.5.2 Equivalent radius

Equivalent radius is a radius which can be used to represent the mean radial position. If the migration period is θ_e, thus the equivalent radius R_e is expressed as

$$R_e = \frac{1}{\theta_e}\int_0^{\theta_e} r(\theta)d\theta \quad \text{5-5}$$

5.5.3 Calculation of tensile energy

5.5.3.1 Radial position of the fiber in the initial and deformed yarns

We assumed that there is a very small tensile strain when the yarn is subjected to tension, and the yarn has the same volume before and after deformation, and the fiber proportionally changed its helical radius along with the change of height.

The radial position of fiber in the initial and deformed yarns are $r_0(\theta), r_1(\theta)$, and the cross section areas before and after deformation are A_0 and A_1. Thus we can establish a relationship of fiber radial positions before and after deformation.

$$A_0 = \int_0^{2\pi} \int_0^{r_0(\theta)} r dr d\theta = \int_0^{2\pi} \frac{1}{2} r_0^2(\theta) d\theta \quad 5\text{-}6$$

$$A_1 = \int_0^{2\pi} \int_0^{r_1(\theta)} r dr d\theta = \int_0^{2\pi} \frac{1}{2} r_1^2(\theta) d\theta \quad 5\text{-}7$$

$$A_1(\theta)\frac{1}{T_1} = A_0(\theta)\frac{1}{T_0} \quad 5\text{-}8$$

The fiber radial position in the deformed yarn can be expressed as a function related to its position in the initial yarn.

$$r_1(\theta) = f(r_0(\theta)) \quad 5\text{-}9$$

And the $P(\theta) = r_1(\theta) / r_0(\theta)$, donates the ratio of fiber radial positions of the fiber in the initial and deformed yarns.

If T_0 and T_1 are the numbers of turns of twist per unit length before and after deformation, and the yarn extensional strain is ε_y, thus $T_1 = T_0 / (1 + \varepsilon_y)$.

5.5.3.2 Fiber length

We assumed that the extended yarn was given an increment of additional twist, ϕ radians per unit extended length of yarn. This means that an axial length $1/T_1$ of the further twisted yarn contains more than one complete revolution, i.e., $(2\pi + \phi/T_1)$revolution of the helical paths.

According to differential geometry, the arc length of a spatial curve can be calculated by using Equation 5-10.

$$s(\theta) = \sqrt{\dot{x}^2(\theta) + \dot{y}^2(\theta) + \dot{z}^2(\theta)} \qquad 5\text{-}10$$

Where "." donates differentiating with respect to θ. Thus the lengths of a fiber in the initial and deformed yarns are expressed as:

$$l_0 = \int_0^{2\pi} |s_0(\theta)| d\theta \qquad 5\text{-}11$$

$$l_1 = \int_0^{2\pi+\phi/T} |s_1(\theta)| d\theta \qquad 5\text{-}12$$

5.5.3.3 Tensile strain

The tensile strain ε_f in the fiber is:

$$\varepsilon_f = \frac{l_1 - l_0}{l_0} \qquad 5\text{-}13$$

5.5.3.4 Tensile energy

The tensile energy U_{ef} per turn of initial twist in a typical fiber is given by

$$U_{ef} = \frac{1}{2} l_0 E A \varepsilon_f^2 \qquad 5\text{-}14$$

And $A = \pi R_f^2$

Since the packing density $q(r)$ expresses the relationship between the no. of fiber and fiber radial position. The total tensile energy per unit turn of twist in a yarn is

$$U_e = \int_0^{R_y} q(r) U_{ef} dr$$

Thus the total tensile energy per unit length of deformed yarn axis is

$$U_e^{'} = T_1 U_e \qquad 5\text{-}15$$

5.5.4 Calculation of bending and torsional energies

Bending energy and torsional energy vary in the deformed yarn due to changes in curvature and torsion of the fiber geometry.

5.5.4.1 Curvature and torsion component

For a spatial curve $f = \left\{ R(\theta)\cos\theta, R(\theta)\sin\theta, \frac{h\theta}{2\pi} \right\}$, its curvature κ and torsion τ can be calculated by using the Equations 5-16 to 5-19.

The curvature and torsion of initial helices are given as:

$$\kappa_0 = \frac{\left| \dot{f}_0 \times \ddot{f}_0 \right|}{\left| \dot{f}_0 \right|^3} \qquad 5\text{-}16$$

$$\tau_0 = \frac{\left(\dot{f}_0, \ddot{f}_0, \dddot{f}_0 \right)}{\left| \dot{f}_0 \times \ddot{f}_0 \right|^2} = \frac{\left(\dot{f}_0 \times \ddot{f}_0 \right) \cdot \dddot{f}_0}{\left| \dot{f}_0 \times \ddot{f}_0 \right|^2} \qquad 5\text{-}17$$

In the deformed yarn, the curvature and torsion of a fiber are:

$$\kappa_1 = \frac{\left| \dot{f}_1 \times \ddot{f}_1 \right|}{\left| \dot{f}_1 \right|^3} \qquad 5\text{-}18$$

$$\tau_1 = \frac{\left(\dot{f}_1 \times \ddot{f}_1\right) \cdot \dddot{f}_1}{\left|\dot{f}_1 \times \ddot{f}_1\right|^2} \qquad \text{5-19}$$

Where $\dot{f} = \{\dot{x}, \dot{y}, \dot{z}\}$, $\ddot{f} = \{\ddot{x}, \ddot{y}, \ddot{z}\}$, and $\dddot{f} = \{\dddot{x}, \dddot{y}, \dddot{z}\}$.

5.5.4.2 Bending and torsional energies

Assuming a circular fiber has elastic longitudinal tensile and shear moduli E and G, which are linked by Poisson's ratio $(v = 0.5): G = \frac{E}{2}(1+v)$, and moments of inertia (I_0, I_b) of the fiber with respect to center and the principal axis of its cross section, $I_b = \frac{1}{2} I_0$.

The bending energy over a definitely small segment of fiber is

$$dU_{bf} = \frac{1}{2} EI_b \left(\kappa_1(\theta) - \kappa_0(\theta)\right)^2 dl = \frac{1}{2} EI_b \left(\kappa_1(\theta) - \kappa_0(\theta)\right)^2 |s_0| d\theta$$

The bending energy U_{bf} per turn of initial twist in a typical fiber is given by

$$U_{bf} = \frac{1}{2} \int_0^{2\pi} EI_b \left(\kappa_1(\theta) - \kappa_0(\theta)\right)^2 |s_0| d\theta \qquad \text{5-20}$$

As stated above, the packing density $q(r)$ expressed as the number of fiber per unit annular area is related to yarn radius. The total bending energy per unit turn of twist in a yarn is

$$U_b = \int_0^{R_y} q(r) U_{bf} dr$$

Therefore, the total bending energy per unit length of deformed yarn axis is.

$$U_b^{'} = T_1 U_b \qquad 5\text{-}21$$

Similarly, the bending energy over a definitely small segment of fiber is

$$dU_{tf} = \frac{1}{2} GI_0 (\tau_1(\theta) - \tau_0(\theta))^2 dl = \frac{1}{2} GI_0 (\tau_1(\theta) - \tau_0(\theta))^2 |s_0| d\theta$$

The torsional energy U_{tf} per turn of initial twist in a typical fiber is given by Equation 5-22.

$$U_{tf} = \frac{1}{2} \int_0^{\theta} GI_0 (\tau_1(\theta) - \tau_0(\theta))^2 (\theta) |s_0| d\theta = \frac{1}{3} \int_0^{\theta} EI_b (\tau_1(\theta) - \tau_0(\theta))^2 |s_0| d\theta \qquad 5\text{-}22$$

The total bending energy per unit turn of twist in a yarn is

$$U_t = \int_0^{R_y} q(r) U_{tf} \, dr$$

And the total torsional energy per unit length of deformed yarn axis is.

$$U_t^{'} = T_1 U_t \qquad \text{5-23}$$

5.5.5 Yarn torque

Based on the "shortest-path hypothesis" and energy conservation, the total elastic energy stored in the deformed yarn is the sum of the tensile energy of the fiber in the jamming regions and the bending and the torsional energy of all the fibers in the yarn. Since, in this case, we assumed that the yarn is initially close packed, thus the total energy is the sum of these three components of all fibers in the yarn.

For a given yarn extension, the applied rotation θ is changed in small step. The torque can be derived from the corresponding increase in stored elastic energy. Let L_b, L_t and L_e be the components of yarn torque due to fiber bending, torsion and tension, respectively. They can be expressed as:

$$L_b = \frac{\partial U_b^{'}}{\partial \theta}, \; L_t = \frac{\partial U_t^{'}}{\partial \theta}, \text{ and } \; L_e = \frac{\partial U_e^{'}}{\partial \theta}.$$

Therefore, the total yarn torque is

$$L_{total} = L_b + L_t + L_e \qquad 5\text{-}24$$

5.6 Computation

5.6.1 Calculation of yarn torque

A computer program was developed in Fortran for calculating the yarn torque. Figure 5-2 is the flow chart. The undeformed yarn cross section was considered to be divided into 10 concentric annular zones, each with the same width (differing from the method used in Chapter 4). There were three cycles. The first is for the calculation and accumulation of the bending and torsional energies of a fiber in a length of a unit of twist of yarn. Then we calculated the fiber's strain and the tensile energy of a fiber in a length of a unit of twist of yarn. The next was to compute the bending, torsional and tensile energy of the fibers at a certain radial position, and finish the computation of the total energy of the bending, torsional, and tensile components of the fibers in the yarn cross section. Following it was the calculation of these energies of the fibers in a unit length of yarn. Finally, we calculated the torque of a yarn in a unit length, then gave an small increment of the additional twist angle and conducted the above computations until finished the total additional twist angle.

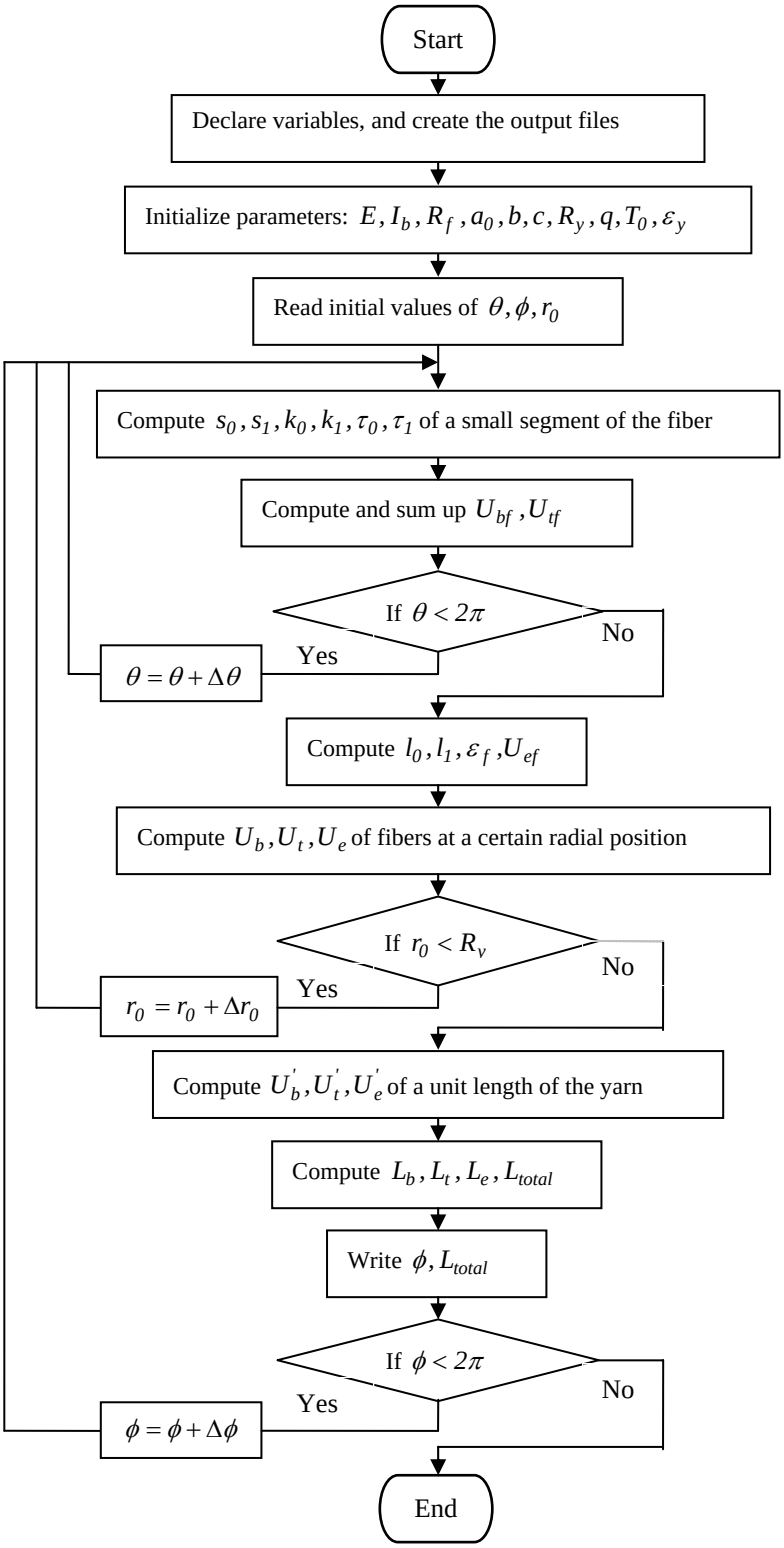

Figure 5-2 A flow chart for computation of yarn torque

5.6.2 Eduction of arc length, curvature and torsion of the fiber

Since the fiber followed a spatial path within the yarn, the equations of the arc length, curvature and torsion of a fiber were educed by using a Matlab program. The function of the symbolic calculation was adopted. Figure 5-3 is the flow chart of these eductions.

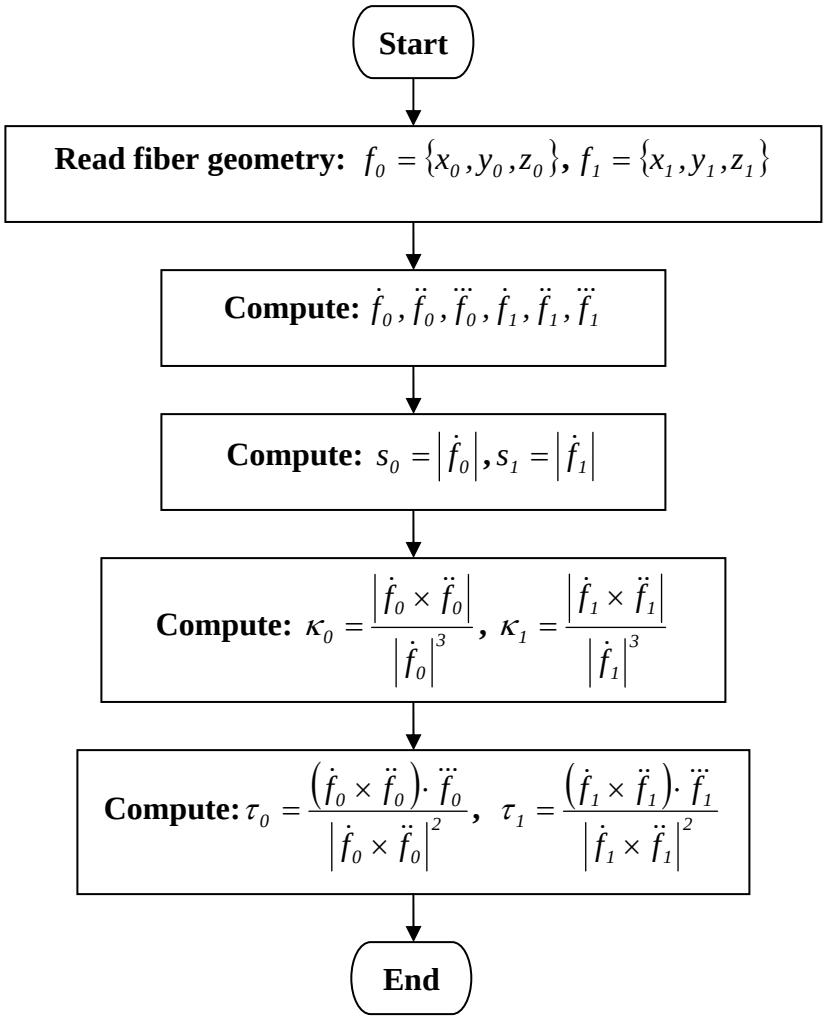

Figure 5-3 A flow chart for the eduction of the arc length, curvature and torsion of a fiber

5.6.3 Determination of $\Delta\phi$

In this study, the yarn torque L was calculated by using a calculation of the derivative of energy U with respect to ϕ. For completing this differential computation, a difference method was adopted. Thus the calculation of the derivative of energy with respect to ϕ at the point of ϕ_i became the key of this computation. The following scheme was used for calculating this derivative.

a) Calculate $U(\phi_i)$,

b) Let $\phi_i^+ = \phi_i + \Delta\phi_i$, and calculate $U(\phi_i^+)$,

c) $L_i = \left.\frac{\partial U}{\partial \phi}\right|_{\phi=\phi_i} \approx \frac{U(\phi_i^+) - U(\phi_i)}{\Delta\phi_i}$,

d) Let $\Delta\phi = \Delta\phi/2$, and re-calculate (b) and (c); if the difference between the new L_i (expressed as L_i^N) and the last L_i (expressed as L_i^0) is smaller than a certain value, we could use the L_i as the final result, otherwise let $\Delta\phi = \Delta\phi/2$ continuously until meets the requirement of the difference smaller than the certain value. The convergence principle is $\frac{\left|L_i^N - L_i^0\right|}{\left|L_i^0\right|} \le \varepsilon$, where ε is the precision of the calculation.

5.7 Verification

After the establishment of the model, it is necessary to conduct a verification experiment. Here we compared the experimental results and their calculated values derived from the

model expressed by using one item of sinusoidal function, i.e., $r(\theta) = R_{basic} + a_0 \sin(b \cdot \theta + c)$. Cotton fiber was used, it has a radius of $5 \times 10^{-4} cm$, Young's modulus of $5 \times 10^{7}\ gf / cm^2$, and its density is $1.54 g / cm^3$. Two cotton yarns were produced by using the C1 roving (specifications are shown in Table 6-1), one yarn is a 20Ne conventional ring spun with a twist factor of 3.6 ($a_0 = 0$), and the other is a 20Ne TBS yarn with a twist factor of 2.5 ($a_0 = r/10$, $b = 1$, $c = -\pi/2$). Their torque-twist curves are shown in the Figure 4-26.

Figure 5-4 shows the comparison between calculated experimental results of the 20Ne conventional ring spun yarn with a twist factor of 3.6. The diagram indicates that the calculated curve has a good agreement with its experimental results for an additional twist less than $0.8\pi / cm$. While for a twist of greater than $0.8\pi / cm$, the theoretical value is higher than its experimental value. The difference is perhaps mainly due to the assumptions that the material is a filament, rather than a staple fiber, as well as an initial close packed yarn structure.

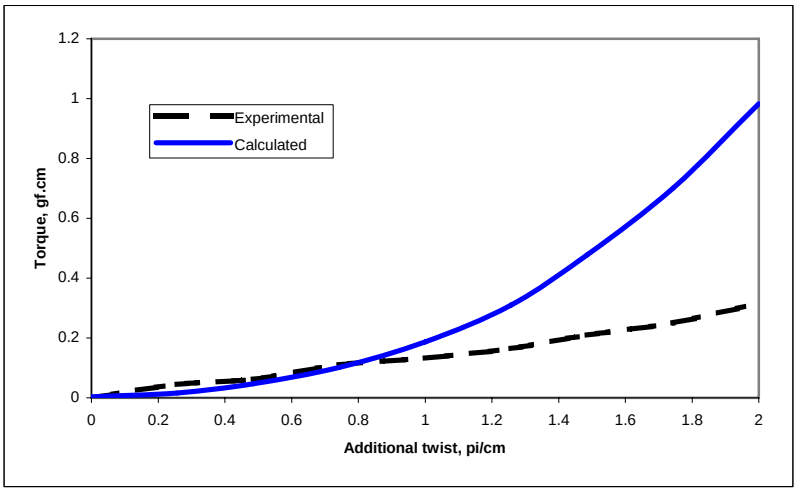

Figure 5-4 Comparison between the theoretical and experimental torque-twist relationship for the 20Ne conventional ring spun yarn (TF=3.6)

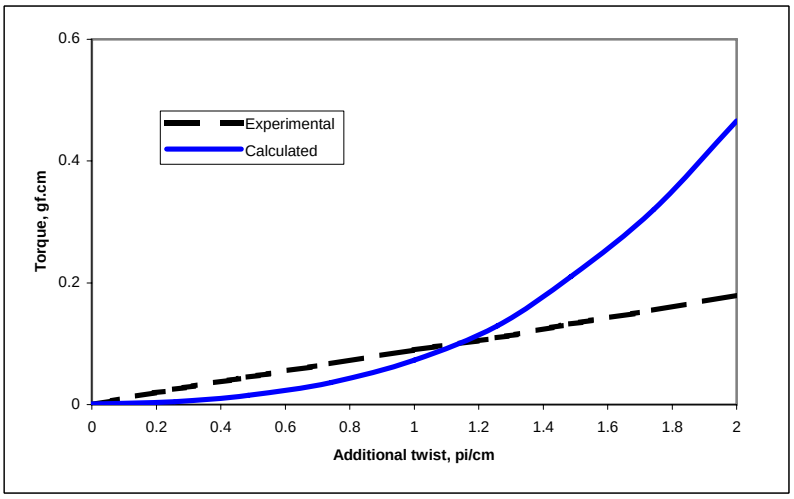

Figure 5-5 Comparison between the theoretical and experimental torque-twist relationship for the 20Ne TBS yarn (TF=2.5)

The comparison of the TBS yarn is demonstrated in Figure 5-5. The diagram shows that the calculated curve has an acceptable agreement with its experimental results for an

additional twist less than $1.1\pi / cm$. While for a twist of greater than $1.1\pi / cm$, the theoretical value is higher than its experimental value. The difference may be explained by using the same reason mentioned above.

5.8 Discussions

5.8.1 Comparison between the TBS and conventional yarns

The torque of some yarns was calculated according to the established model. One item sinusoidal function was chosen, i.e., $r_0(\theta) = r + a_0 \sin(b \cdot \theta + c)$. Here a_0, b, and c donates the coefficients of the magnitude, frequency and phase angle of the one item sinusoidal function. Cotton fibers were considered. And yarn count is 20Ne.

Three curves plotted on Figure 5-6 express the simulated effect of twist on yarn torque. These three yarns were conventional ring spun yarns with the same counts and different twist factors. They were the special cases whose a_0 values were zero. It is clear that yarn torque increases along with the increase of the twist factor, agreeing with previous research results (Postle et al. 1964).

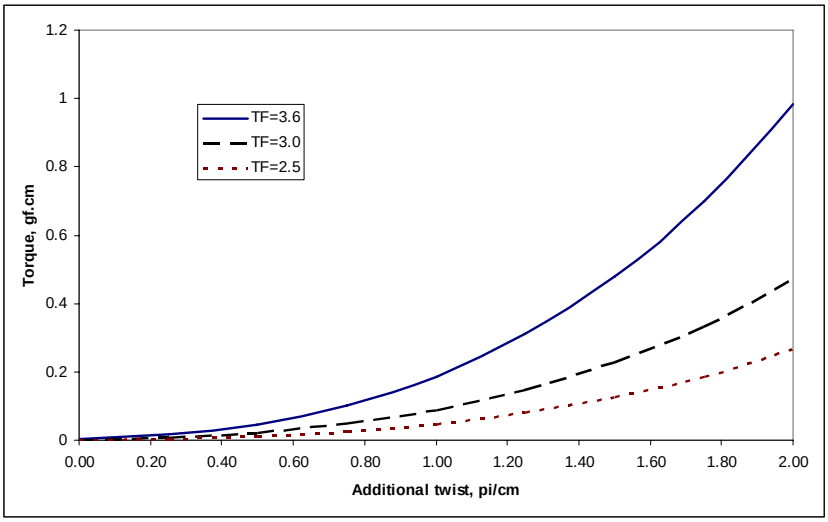

Figure 5-6 Effect of twist on yarn torque (20Ne)

Figure 5-7 is an evaluation of the effect of b value on yarn torque. Three yarns were involved. They had the same twist factors, yarn counts, as well as a_0 and c values. Only difference is that their migration frequency coefficients b values are 1, 2, and 4, respectively. The curves show that the yarn torque increases with the increase of b value. It means that the increase of migration frequency may negatively affect the reduction of yarn torque. This probably results from the increase of migration frequency that increases the fiber length in a unit length of yarn and the change of fiber curvature and torsion, leading to an increase of energy stored in the yarn

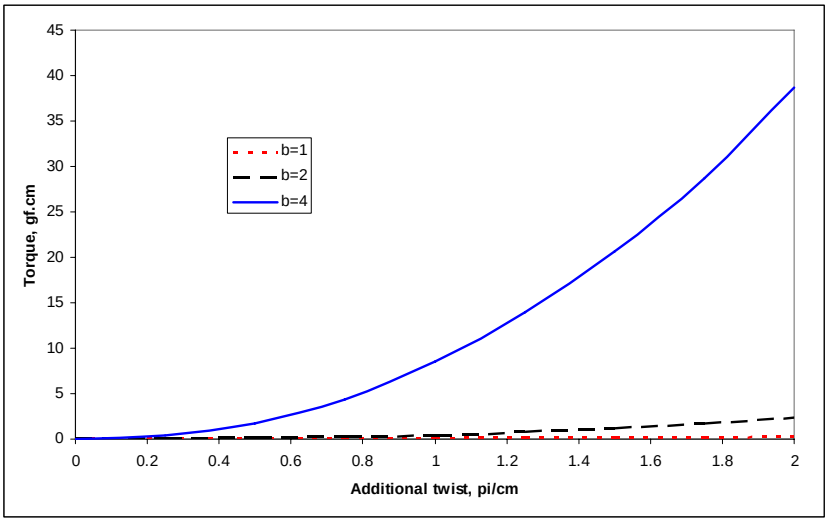

Figure 5-7 Effect of b value on yarn torque

(20Ne, TF=2.5; for the TBS yarns, c =-π/2, a_0 =r/10)

Figure 5-8 shows another comparison of torque between yarns. These yarns have the same twist factors, and yarn counts. For the TBS yarns, they also have the same b and c values. The difference is that their migration magnitude, a_0 values, are r/10, r/8, and r/2. The diagram shows that, for the TBS yarns, there is a torque reduction along with the decrease of migration magnitude. The torques of two low-magnitude-value TBS yarns is lesser than that of the corresponding conventional yarn. While the torque of the high-magnitude-value yarn is greater than its conventional yarn. That is to say lower migration magnitude may help to decrease yarn torque. It may be explained that a low-magnitude-value migration effectively disperse the radial torque distribution in the yarn, leading to a better balance of the fiber torque which is generated due to the uniform cylindrical helix. This comparison reveals that we can further reduce the torque of a low twist yarn by changing its migration pattern.

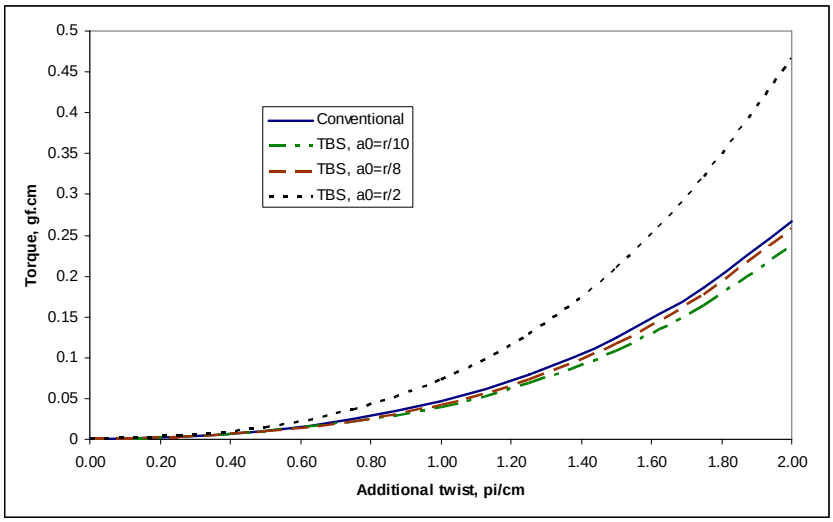

Figure 5-8 Effect of a_0 values on yarn torque

(20Ne, TF =2.5; for the TBS yarns, b =1, c = -π/2)

Figure 5-9 is also an evaluation. Three TBS yarns were included. They have the same twist factors, yarn counts, a_0 and b values. We changed their phase angles c to evaluate its effect. The diagram demonstrates that when $c = -\pi/2$, the yarn has the lowest torque. While the yarn with a phase of $c = \pi/2$ possesses the highest torque. The other two yarns are in between of them. This implies that c is also a very important variable. It has influences on yarn torque by changing the fiber migration phase angle. If we properly change the fiber migration phase, it is possible to balance the fiber torsional moment, leading to a reduction of yarn torque.

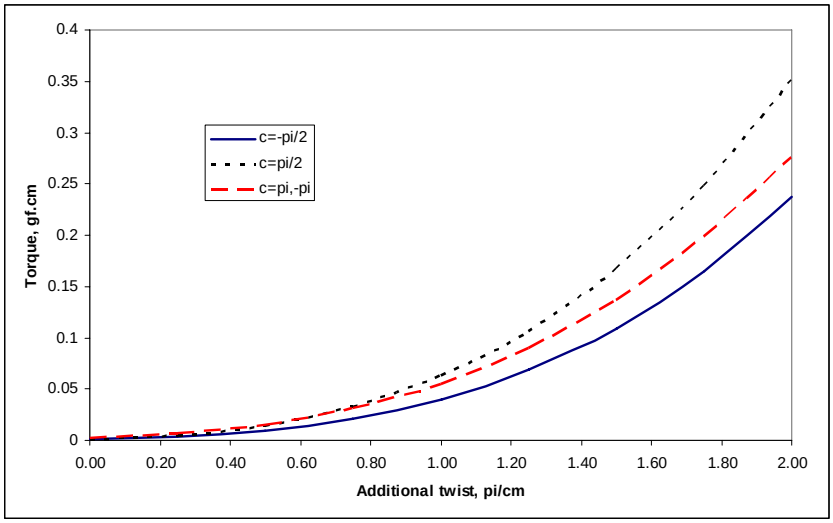

Figure 5-9 Effect of c values on yarn torque

(20Ne,TF =2.5; for the TBS yarns, a_0 =r/10, b =1,)

5.8.2 Effect of the geometrical coefficients on the fiber migration pattern

Table 5-1 Yarn geometrical parameters

Yarn	Coefficients			Marks
	a_0	b	c	
1	0	0	0	Curve a
2	r/10	5	0	Curve b
3	r/10	1	-π/2	Curve c

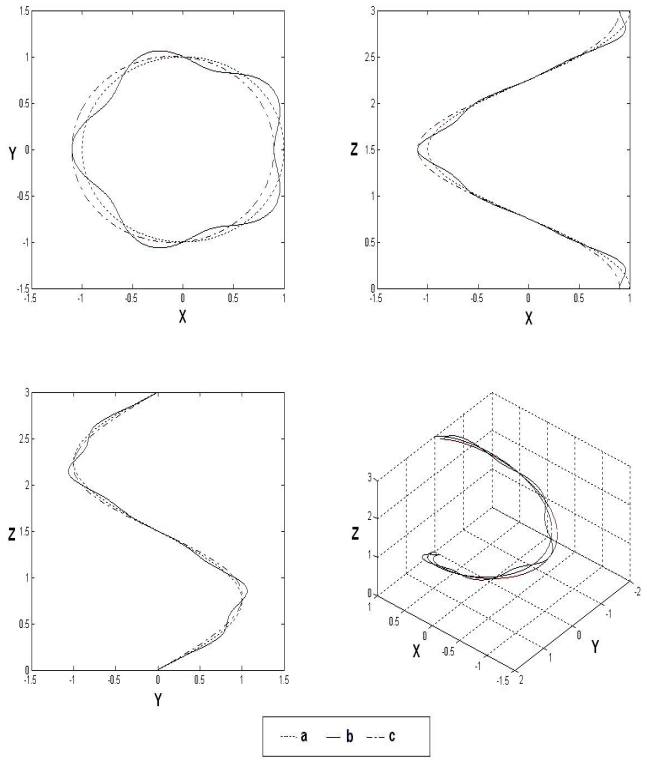

Figure 5-10 Comparison of geometries of the idealized and modified helixes

As stated above, we assumed that the fibers formed the yarn in a modified cylindrical helix, and the helical radius shown in Figure 5-3 is a combination of a basic radius and a Fourier series that was used to express fiber migration.

Figure 5-10 shows the three yarn geometries plotted according to different coefficients, and these coefficients are listed in Table 5-1. Curve a expresses an idealized cylindrical helix, Curve b is a fiber migrating with higher frequency, and Curve c represents a yarn having small migration and a certain phase change angle. It is clear that by increasing the number of b, we easily make this curve complicated. In addition, the introduction of

phase change angle and small migration leads to an eccentric pattern if comparing with Curve a. This eccentric tendency may be one of the reasons of the reduction of yarn torque.

5.8.3 Yarn torque and yarn residual torque

What influences fabric spirality is the residual torque of the twisted yarns. Yarn torque is formed during twisting process. Since the deformed fiber will reach a position which has minimum energy, the formed yarn torque can be partially released due to the time effect and during further processing, and the other will stored in the yarn as yarn residual torque.

For a staple yarn, normally, the higher the torque, the higher the residual torque. Thus in this study, we represented the residual torque by using the total yarn torque. Further investigation on the relationship between yarn parameters and the yarn residual torque will be conducted in the future.

5.9 Summary and Conclusions

In this Chapter, a new theoretical model has been developed for describing the torsional behavior of the TBS yarns. To develop this theory, we firstly defined the geometrical structure of the yarn in the unstrained state, and secondly introduced certain assumptions regarding the geometry of the imposed strain, for instance the relationship between the deformations of the fibers of which the yarn is composed and the overall deformation of

the yarn. Then we calculated the stress-strain properties of the fiber, and finally conducted the mathematical derivation of the resultant torque of the yarn on the basis of the preceding assumptions.

The investigation of yarn structure in the Chapter of yarn structural investigation revealed that the TBS yarns have more migration than those low-twist and high-twist conventional ring spun yarns. Thus a modified cylindrical helix structural model was introduced. Fiber helical radius was expressed as a Fourier series function so as to represent fiber migration. Moreover, an energy method was adopted and initial close-packed structure was assumed.

The torques of some yarns was also calculated according to the torsional model. The calculated results imply that it is possible to further reduce the torque of a low twist (TF=2.5) by introducing some fiber migrations. The frequency and magnitude of fiber migration have different influences on the yarn torque, i.e., a small frequency and magnitude migration with a phase angle may be a good choice for obtaining a significant reduction of yarn torque.

There are some problems remained in current stage. Some are related to the assumptions. For example we supposed that all fibers are in a concentric modified helical shape, and they are filaments rather than staple fibers, however, these fibers are short staple, and not in the same shape in a yarn. Thus slippage and other features of the staple yarns were not included in this model. Some other problems are associated with the method adopted. The energy method neglected some energy components such as the components due to

friction, and compression, etc. These neglects may affect the energy conservation system, leading to an increase of predicting errors. Apart form above reasons, in the verification and discussion sections, we used a simplified one item sinusoidal function to replace the constant radius of an idealized cylindrical helix. This simple function may be one of the reasons resulting in predicting errors. We can try to introduce more sinusoidal functions in the future investigation. In addition, fabric spirality is mainly determined by the direction and magnitude of yarn residual torque, we will investigate the relationship between yarn residual torque and yarn parameters in the future.

Although there are above problems, the model not only describes the torsional configurations of different yarns (conventional ring spun yarns and the TBS yarns), but also reveals that it is possible to further reduce the torque of a low-twist conventional ring spun yarn by increasing a certain fiber migration. It verified the statement that the torque reduction device can change yarn structure, and leading to a reduction of yarn torque in a theoretical manner.

CHAPTER 6

OPTIMIZATION OF SPINNING PARAMETERS

6.1 Introduction

The investigation mainly focuses on the modification of the structure and performance of the conventional ring spun yarn. The target of the modification is to obtain a yarn with reduced residual torque and acceptable strength as well as other performance.

After the installation of the torque reduction device and preliminary spinning trial, it is necessary to optimize spinning parameters and produce some TBS yarns. Many factors determine or have influences on yarn properties. Material, yarn type, yarn count (or linear density), and twist multiplier etc. are often used for describing a yarn, i.e., yarn properties are associated with these parameters. The machine types, spinning geometry and other settings should be included in the optimization experiment, along with yarn structural parameters.

Before conducting the optimization experiment, an appropriate optimization methodology should be selected. Methods included linear programming, dynamic programming and integer programming etc., and some constructional arithmetic like Johnson method, Palmer method and Gupta method etc (Wang 2001). For the estimation of parameters, some techniques such as the Least Squares and Point Estimation etc can give helps (Beck and Arnold 1977; Koch 1999); Since Response Surface Methodology

which uses Least Squares is widely used and probably the most successful optimization technique based on designed experiments (Montgomery 1996), it was chosen and used in the present study.

Response surface methodology, which is introduced as an optimization technique in the field of numerical analysis, was advocated by Box and Wilson (1951). Later, due to the research by Taguchi, as well as Myers and Montgomery (Montgomery 1996; Myer and Montgomery 2002), it has been developed into the current technique, which has been put to practical use in the field of quality engineering for product process optimization and variation reduction.

Response surface methodology has already been adopted in textiles for optimizing process. Ishtiaque et al (2004) adopted it to optimize the ring frame process parameters for better yarn quality and production. They selected spindle speed, top roller pressure, and traveler mass as the variables, EBR, yarn imperfection, irregularity, hairiness and tenacity as yields (responses). Gowda et al (2004) studied the influences of process variables on characteristics of modal sirospun yarns. Box-Behnken design was used and three variables including strand spacing, traveler mass and spindle speed were considered. They studied the relationship between these variables and yarn characteristics such as thin and thick places, hairiness and tenacity etc. Subramaniam et al (1993) investigated the double-rove spun yarn's low stress mechanical properties by using the Box-Behnken design. Response surface methodology has been adopted in other spinning systems. Palta and Kothari (2002) tried to find out the relationships between process variables and the properties of air-jet textured yarns. They chose

overfeed, air pressure and texture speed as the variables, and yarn physical bulk percentage, instability percentage and tenacity as the yields.

a) Theory of response surface

In general, for a system involving response y that depends on the controllable input variables $\xi_1, \xi_2, \ldots, \xi_n$, the relationship is

$$y = f(\xi_1, \xi_2, \ldots, \xi_n) + \varepsilon \qquad 6\text{-}1$$

Where f is the true response function, it is unknown and perhaps very complicated. ε expresses other sources of variability not accounted for in f. Thus it includes effects such as measurement error on the response, other sources of variation that are inherent in the process or system, and the effect of other variables, etc. Normally, ε is considered as a statistical error, assuming it to have a normal distribution with mean zero and variance σ^2. If the mean of ε is zero, then

$$E(y) \equiv \eta = E\left[f(\xi_1, \xi_2, \ldots, \xi_n)\right] + E(\varepsilon) = f(\xi_1, \xi_2, \ldots, \xi_n) \qquad 6\text{-}2$$

Where E represents expectancy. $\xi_1, \xi_2, \ldots, \xi_n$ are natural variables.

b) First-order and second-order models

The variables $\xi_1,\xi_2,\ldots,\xi_n$ which are expressed in the natural units of measurement can be transformed to coded variables $x_1,x_2,\ldots,x_n$, which are usually defined to be dimensionless with mean zero and the same spread of standard deviation. Equation 6-3 is the transform equation. In terms of the dimensionless coded variables, the true response function, Equation 6-2, is written as Equation 6-4.

$$x_i = \frac{\xi_i - [max(\xi_i) + min(\xi_i)]/2}{[max(\xi_i) - min(\xi_i)]/2} \qquad 6\text{-}3$$

$$E(y) \equiv \eta = f(x_1,x_2,\ldots,x_n) \qquad 6\text{-}4$$

The function f can be approximated by using a low-order polynomial in some relatively small region of the independent variables space. In many cases, either a first-order or second-order model is used. Equations 6-5 and 6-6 show the first-order and second-order models of two variables respectively.

$$y = \beta_0 + \beta_1 x_1 + \beta_2 x_2 + \cdots + \beta_k x_k \qquad 6\text{-}5$$

$$y = \beta_0 + \sum_{j=1}^{k} \beta_j x_j + \sum_{j=1}^{k} \beta_{jj} x_{jj}^2 + \sum \sum_{i<j=2}^{k} \beta_{ij} x_i x_j \qquad 6\text{-}6$$

The second-order model is widely used in response surface methodology for the following reasons: (1) the second-order model is very flexible. It takes a wide variety of functional forms, so it often works well as an approximation to the true response surface.

(2) It is easy to estimate the parameters in the second-order model. The method of least squares can be used for this purpose. (3) There is considerable practical experience indicating that second-order models work well in solving real response surface problems.

c) Factorial and response surface designs

Factorial designs are widely used in experiments involving several factors where it is necessary to investigate the joint effects of the factors on a response variable. A very important case of the factorial design is that each of the k factors has two levels. Thus 2^k experimental trials are needed.

Although the 2^k factorial designs are very important in response surface work, but as the number of factors increases, the number of runs required for a complete replicate of the design rapidly outgrows the resources of the most experimenters. For example, a complete replicate of the 2^5 design requires 32 runs. Thus, on the assumptions that certain high-order interactions are neglected, information on the main effect and low-order interactions may be obtained by running only a fraction of the complete factorial experiments.

One-quarter fraction of the 2^5 design has two generators, $D = \pm AB$ and $E = \pm AC$ (Myers and Montgomery 2002). In practice, it is easy to select these two generators in such a way that we can obtain the best possible alias relationships. A reasonable criterion is to select the generators such that the resulting 2^{k-2} design has the highest resolution.

The second-order model described in Equation 6-5 is quite useful and easily accommodates the use of a wide variety of experimental designs. This equation reveals that the model contains $1+2k+k(k-1)/2$ parameters if k factors were selected. As a result, the experimental design used must contain at least $1+2k+k(k-1)/2$ distinct design points. In addition, the design must involve at least three levels of each design variables to estimate the pure quadratic terms.

The nature of the response surface system depends on the signs and magnitude of the coefficients in the model of Equation 6-5. The second-order coefficients play a vital role. It is important that the coefficients used are estimates of the β's of Equation 6-5. As a result the contours represent contours of estimated response. Thus, even the system is part of the estimation process. The stationary point and the general nature of the system arise as a result of a fitted model, not the true structure.

6.2 Experimental Details

6.2.1 Materials

Several cotton fibers with different qualities were obtained from a company and used, as shown in Table 6-1.

Table 6-1 Roving specifications

	C1	C2	C3	P1
Roving count (tex)	760	762.7	671.0	551
Fiber length (inch)	1.34	1.17	1.21	1.44
Uniformity ratio (%)	63.7	62.5	63.5	63.7
Fiber strength (g/tex)	26.1	21.5	23.0	29.8
Elongation (%)	5.6	5.4	5.0	6.0
Micronaire value	4.6	4.6	3.8	4.1

C1 was used for spinning yarns of 16Ne and 20Ne. C2 and C3 were used together with C1 to investigate the effect of fibers. P1 is Pima cotton, it has a finer roving count, and the cotton fiber is longer, finer and stronger. It was used for 30Ne yarns.

6.2.2 Machines

A SDL Spin Tester with 6 spindles was used for the optimization experiment (16Ne and 20Ne TBS yarns). Spinning draft (including total and break drafts) and yarn twist multiplier can be manually adjusted. Spindle speed can be linearly changed. This machine also has a display of spinning parameters such as spindle speed, total and break draft, delivery speed, as well as running time, etc.

For evaluating the adaptability of torque reduction device in different machines, four sets of the device were installed on a Zinser 319 SL and a Toyota RY spinning machines,

respectively. Optimization experiments were also conducted on these two spinning machines respectively.

6.2.3 Yarn counts

Three common knitting yarn counts were selected. They are 16Ne, 20Ne and 30Ne.

6.2.4 Yarn test

Three full bobbins spun by using different spindles were randomly selected for yarn test. Samples were conditioned at 65±2%RH and 20±2ºC for at least 24 hours before further testing. Yarn tensile properties were measured on Uster Tensorapid tester by using the recommended procedure. 50 readings were obtained from each bobbin. Yarn length was 500mm and test speed was 5,000 mm/min. Yarn variation in mass was measured on Uster III tester by using a testing length of 1,000 meters. Numbers of wet snarling turns were measured according to the modified ISO 3343-1984 method and using a test equipment based on ISO 3343-1984 and then modified by our team; and 10 measurements were conducted for one bobbin. Yarn hairiness was tested on Zweigle G566. The standards are listed in Table 6-2.

Table 6-2 Yarn test methods, standards and equipment used

Test / Evaluation	Standard	Equipment Used
Yarn linear density	ASTM D 1907-01	Motor driven reel and balance
Yarn tensile properties	ASTM 2256-02 (Test speed 5,000mm/min, Gauge Length 500mm)	Uster Tensorapid
Yarn irregularity in mass	Uster standard	Uster III
Yarn hairiness	-	Zweigle G566
Yarn residual torque	ISO 3343-1984 (Modified)	Snarling tester and water bath

6.3 Optimization Experimental Design

A commercial software, Minitab, was adopted for the design of the optimization experiment and analyzing results. Response surface is one of its functions. After choosing the factors and levels, the software helps to design a worksheet of the experimental arrangement. After filling in test results, the software can provide the optimization results and regression equations.

A two-stage scheme was adopted in this optimization. They are fractional factorial experiments (1^{st} stage) and response surface experiments (2^{nd} stage). The aim of the fractional factorial experiments is to identify the most important factors based on a one-quarter factorial design. It is also called as a screening experiment. After identifying the most important factors, the response surface experiment was carried out for finding out

the relationship between the yields (responses) and variables, i.e., the relationship between yarn properties and spinning parameters.

6.3.1 Fractional factorial analysis

For reducing the number of variables and runs, only the 20Ne yarns were produced by using a specified roving (C1) on a ring spinning machine (fixed ring diameter and spindle speed). Travellers that have the same shape, and various masses were chosen for providing the same spinning tension. Thus the variables related to traveller were ignored. The spinning production was conducted in a conditioned room in order to minimize the environmental influences. According to previous literature and experience, for a specified cotton and fixed yarn count (20Ne), variables such as yarn twist factor, break draft ratio of the ring spinning system and variables associated with the torque reduction device (the ratio of the rotational speed between the couple rotors and the spindle, and the installation position of the device) were chosen as the factors for this experiment. Yarn tenacity, elongation, wet snarling, and hairiness as well as evenness were the yields.

Each factor had two levels, and preliminary experiments were conducted for determining the boundaries. Table 6-3 shows these factors and levels.

Table 6-3 Factor (F) and level (L)

Level	Speed Ratio V1	Twist Factor V2 (tpi/ count$^{1/2}$)	Position X V3 (cm)	Position Y V4 (cm)	Break Draft V5
-1	0.36	1.9 (334t/m)	0	0	1.2
1	0.52	3.0 (528t/m)	0.5	0.5	1.8

Note: speed ratio = rotational speed of couple rotor/ spindle rotational speed

A five-factor-two-level design has 2^5 runs of experiment (Myers and Montgomery 2002). However, it needs much time. In this case, eight (2^{5-2}) rounds of fractional factorial experiments were designed based on the selected factors and boundaries. This design requires the selection of two independent generators. By carefully choosing the generators, effects of potential interest are not aliased with each other. In this case, we assumed high-order interactions to be negligible, and this greatly simplifies the alias structure. For this experiment arrangement, V1, V2 and V3 were three basic factors; the signs of V4 and V5 were generated based on the interaction arrangement (V4 = ±V1V2, V5=±V1V3). In addition, the selection of these two generators was important; it should be conducted in such a way that we obtain the best possible alias relationships and resolution. Table 6-4 shows the experimental arrangements in coded variables.

Table 6-4 Experiment arrangement expressed in coded variables (1/4 fraction)

Run Order	Speed Ratio V1	Twist Factor V2 (tpi/ count$^{1/2}$)	Position X V3 (cm)	Position Y V4 (cm)	Break Draft V5
1	1	-1	-1	-1	1
2	1	1	1	1	1
3	1	1	-1	1	-1
4	-1	-1	-1	1	1
5	1	-1	1	-1	-1
6	-1	1	1	-1	1
7	-1	-1	1	1	-1
8	-1	1	-1	-1	-1

For the yields, yarn residual torque in terms of wet snarling was considered firstly. Then yarn tenacity, elongation, evenness and hairiness were included. Table 6-5 is the worksheet; actual boundaries are listed in this Table.

Table 6-5 Experimental arrangement expressed in nature variables (1/4 fraction)

Run Order	Speed Ratio V1	Twist Factor V2 (tpi/ count$^{1/2}$)	Position X V3 (cm)	Position Y V4 (cm)	Break Draft V5
1	0.52	1.9	0	0	1.8
2	0.52	3.0	0.5	0.5	1.8
3	0.52	3.0	0	0.5	1.2
4	0.36	1.9	0	0.5	1.8
5	0.52	1.9	0.5	0	1.2
6	0.36	3.0	0.5	0	1.8
7	0.36	1.9	0.5	0.5	1.2
8	0.36	3.0	0	0	1.2

6.3.2 Response surface analysis

6.3.2.1 Central Composite and Box-Behnken designs

In practice, Central Composite design and Box-Behnken design are often adopted. The Central Composite design provides high quality predictions over the entire design space, but requires factor settings outside the range of the factors. And each factor needs 5 levels. The Box-Behnken design requires fewer combinations than the Central Composite design in cases involving 3 or 4 factors. But the design contains regions of poor prediction quality. In addition, each factor of the Box-Behnken designs requires 3 levels. Table 6-6 demonstrates the comparison of the number of runs between the Central Composite design and the Box-Behnken designs (Myers and Montgomery 2002).

Table 6-6 Numbers of runs required by the Central Composite and Box-Behnken designs

Number of factors	Central Composite	Box-Behnken
2	13 (5 center-point runs)	-
3	20 (6 center-point runs)	15
4	30 (6 center-point runs)	27
5	33(fractional factorial) or 52 (full factorial)	46
6	54(fractional factorial) or 91(full factorial)	54

In this study, the Central Composite design was used to get high quality prediction. However, this design needs more runs of trials when more factors (3 or 4) are selected. After the 1st stage of fractional factorial analysis, it was observed that there were only two statistically significant factors. Thus the two-factor-two-level scheme was used. If the number of significant factors were three or more, thus more-factor-two-level scheme

then had to be designed. Table 6-7 shows the experimental arrangement of 2-factor-2-level design generated randomly by using the Minitab.

Thirteen experiments were arranged. The selection of the number of runs on the center and the distance of two axial points on the axis of each design variables from the design center were very important. The center point (0, 0) was verified five times in order to ensure the existence of curvature in the system. If curvature was found, the addition of axial points allows for efficient estimation of the pure quadratic terms. Other eight points are equally spaced on a circle, thus the distance of each axial point from the design center is $\sqrt{2}$. If we assumed that a square was surrounded by four points (1, 1), (-1, 1), (1,-1), and (-1,-1), then other four points outside the square were located on the two axes, and their coordinates were (1.414, 0), (-1.414, 0), (0, 1.414) and (0, -1.414). Cares were taken that, unlike the fractional factorial design, the range of every factor should cover the outer points (-1.414 and 1.414). For example, the range of twist factor in fractional factorial design is from 1.9 (-1) to 3.0 (1), whereas in the response surface design, 1.9 and 3.0 were defined as outer points -1.414 and 1.414. Thus the two levels are 2.06 (-1) and 2.84(1), and the center point is 2.45 (0).

The yields of the response surface experiment were the same as those of the fractional factorial experiment. Yarn wet snarling was considered firstly, followed by yarn tenacity, elongation and hairiness. Since yarn evenness was mainly affected by the quality of sliver and roving as well as the drafting system, thus, it was excluded in this experiment.

Table 6-7 Arrangement for response surface experiment in coded variables

Run Order	Factor 1	Factor 2
1	0	0
2	0	0
3	-1.414	0
4	1	-1
5	0	-1.414
6	-1	1
7	1	1
8	0	1.414
9	0	0
10	-1	-1
11	1.414	0
12	0	0
13	0	0

6.3.2.2 Fitting a second-order model

It is easy to convert the effect estimates in a 2^k factorial design into a regression model that can be used to predict the response at any point in the space spanned by the factors in the design (Myers and Montgomery 2002).

Equation (6-5) can be expressed in Equation (6-7) and converted into the following matrix form using the coded variables:

$$\boldsymbol{y} = \beta_0 + \beta_1 \boldsymbol{x}_1 + \beta_2 \boldsymbol{x}_2 + \beta_{11} \boldsymbol{x}_1^2 + \beta_{22} \boldsymbol{x}_2^2 + \beta_{12} \boldsymbol{x}_1 \boldsymbol{x}_2 + \varepsilon \qquad 6\text{-}7$$

$$\hat{y} = Xb \Rightarrow b = X(X'X)^{-1}X'y = Hy \qquad 6\text{-}8$$

Where $\boldsymbol{H} = \boldsymbol{X}(\boldsymbol{X}'\boldsymbol{X})^{-1}\boldsymbol{X}'$

Where $\hat{y}$ is the response matrix. It is usually called the hat matrix because it maps the vector of observed values into a vector of fitted values. Thus the matrix X and vector y for this model are

$$\boldsymbol{y} = \begin{bmatrix} y_1 \\ y_2 \\ y_3 \\ y_4 \\ y_5 \\ y_6 \\ y_7 \\ y_8 \\ y_9 \\ y_{10} \\ y_{11} \\ y_{12} \\ y_{13} \end{bmatrix} \quad \boldsymbol{X} = \begin{bmatrix} 1 & -1 & -1 & 1 & 1 & 1 \\ 1 & 1 & -1 & 1 & 1 & -1 \\ 1 & -1 & 1 & 1 & 1 & -1 \\ 1 & 1 & 1 & 1 & 1 & 1 \\ 1 & -1.414 & 0 & 2 & 0 & 0 \\ 1 & 1.414 & 0 & 2 & 0 & 0 \\ 1 & 0 & -1.414 & 0 & 2 & 0 \\ 1 & 0 & 1.414 & 0 & 2 & 0 \\ 1 & 0 & 0 & 0 & 0 & 0 \\ 1 & 0 & 0 & 0 & 0 & 0 \\ 1 & 0 & 0 & 0 & 0 & 0 \\ 1 & 0 & 0 & 0 & 0 & 0 \\ 1 & 0 & 0 & 0 & 0 & 0 \end{bmatrix} \quad \boldsymbol{b} = \begin{bmatrix} \beta_0 \\ \beta_1 \\ \beta_2 \\ \beta_{11} \\ \beta_{22} \\ \beta_{12} \end{bmatrix}$$

$$\boldsymbol{b} = (\boldsymbol{X}'\boldsymbol{X})^{-1}\boldsymbol{X}'\boldsymbol{y} \qquad 6\text{-}9$$

Then these coded variables can be converted into natural variables by using Equation 6-3 if necessary.

6.3.2.3 Test for significance of regression

The test for significance of regression is a test to determine if there is a linear relationship between the response variable y and a subset of the regression variables $x_1, x_2, \ldots, x_k$. In this case, the second-order response surface model has two variables: $y = \beta_0 + \beta_1 x_1 + \beta_2 x_2 + \beta_{11} x_1^2 + \beta_{22} x_2^2 + \beta_{12} x_1 x_2$. If we let $x_3 = x_1^2$, $x_4 = x_2^2$, $x_5 = x_1 x_2$, $\beta_3 = \beta_{11}$, $\beta_4 = \beta_{22}$, and $\beta_5 = \beta_{12}$, thus the above equation can be converted into a linear regression model, $y = \beta_0 + \beta_1 x_1 + \beta_2 x_2 + \beta_3 x_3 + \beta_4 x_4 + \beta_5 x_5$. The test procedure includes partitioning the total sum of squares $SS_T = \sum_{i=1}^{n} (y_i - \bar{y})^2$ into a sum of squares due to the model (or to regression) SS_R and a sum of squares due to residual (or error) SS_E.

$$SS_T = SS_R + SS_E \qquad 6\text{-}10$$

Where $SS_E = \boldsymbol{y}'\boldsymbol{y} - \boldsymbol{b}'\boldsymbol{X}'\boldsymbol{y} = \boldsymbol{y}'\boldsymbol{y} - \frac{(\sum_{i=1}^{n} y_i)^2}{n}$ and $SS_R = \boldsymbol{b}'\boldsymbol{X}'\boldsymbol{y} - \frac{(\sum_{i=1}^{n} y_i)^2}{n}$.

Thus the coefficient of multiple determination R^2 is

$$R^2 = \frac{SS_R}{SS_T} = 1 - \frac{SS_E}{SS_T} \qquad 6\text{-}11$$

6.4 Results and Discussion

6.4.1 Determination of key factors

Table 6-8 shows the test results of the fractional factorial experiments.

Table 6-8 Results of the fractional factorial experiments (1/4 fraction)

Run Order	V1	V2	V3	V4	V5	Wet Snarling (no. of turns/25 cm)	Tenacity (cN/tex)	Elongation (%)	Evenness (CVm %)	Hairiness (S3 Value)
1	0.52	1.9	0	0	1.8	19	12.97	4.85	11.92	1473
2	0.52	3.0	0.5	0.5	1.8	26	16.78	5.83	11.47	597
3	0.52	3.0	0	0.5	1.2	26	16.66	5.62	10.71	583
4	0.36	1.9	0	0.5	1.8	24	11.60	4.67	11.82	1867
5	0.52	1.9	0.5	0	1.2	19	12.81	4.68	10.59	1265
6	0.36	3.0	0.5	0	1.8	42	15.44	5.44	11.39	1061
7	0.36	1.9	0.5	0.5	1.2	24	11.22	4.27	10.60	1599
8	0.36	3.0	0	0	1.2	38	17.97	5.76	10.43	490

6.4.1.1 Wet snarling as the response

Test results of yarn wet snarling were analyzed, and a Pareto Chart is shown in Figure 6-1. It is clear that the twist factor and the speed ratio have significant influences on yarn wet snarling at a confidence level of $\alpha = 0.03$. Whereas others such as the installation positions of the device and break draft as well as their interactions have no significant influences on the wet snarling.

Figure 6-2 shows the details of the influences of all the five factors on yarn wet snarling. The twist factor has a dramatic influence on yarn wet snarling. When the twist factor increases from 1.9 to 3.0, yarn wet snarling increases from 22 to 32. Position X and

break draft ratio have a similar tendency, the bigger their values, the greater the wet snarling turns. Whereas the yarn wet snarling is decreased with the increase of speed ratio and position Y, especially for speed ratio, the reduction of snarling is around 8.5 turns/25cm.

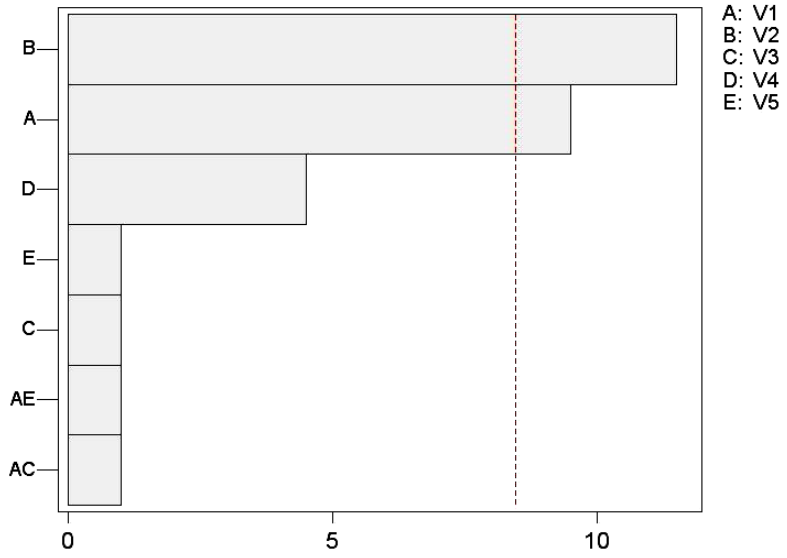

Figure 6-1 Pareto chart of the effects

(response is the number of wet snarling, α = 0.03)

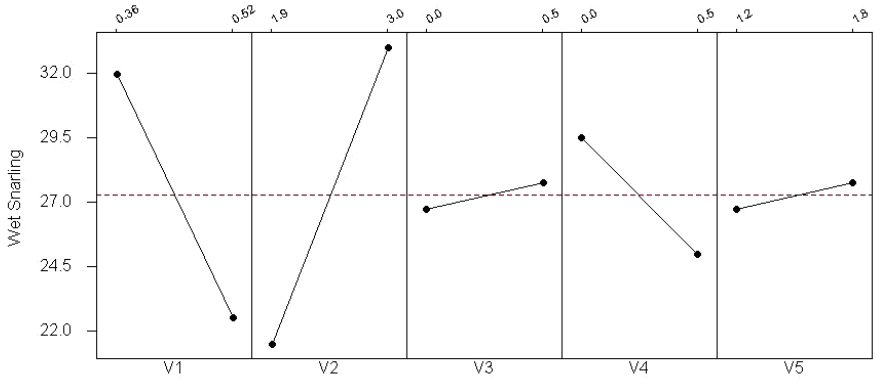

Figure 6-2 Effects plots (data means) for wet snarling

6.4.1.2 Tenacity as the response

Figure 6-3 is a Pareto Chart of the effect of factors on yarn tenacity, showing that the twist factor is the only factor which has significant influences on yarn tenacity at a confidence level of $\alpha = 0.06$ (no factor was identified at a confidence level of $\alpha = 0.03$). Whereas others are statistically insignificant factors.

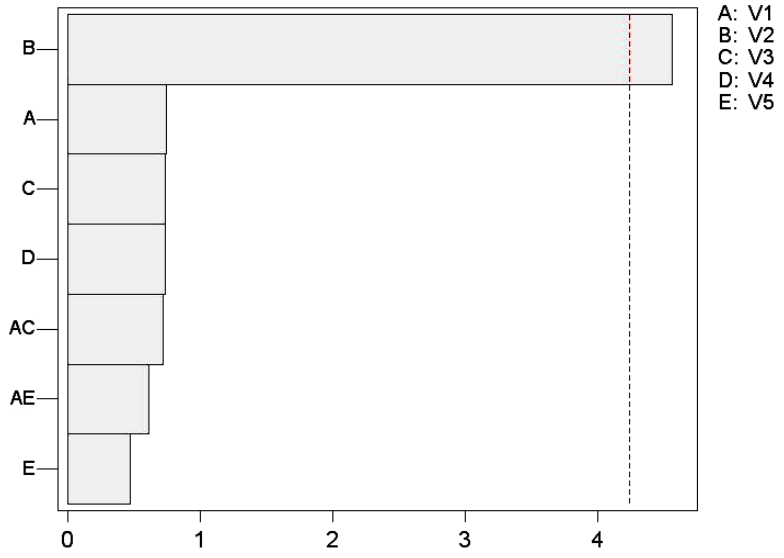

Figure 6-3 Pareto chart of the effects (response is tenacity, $\alpha = 0.06$)

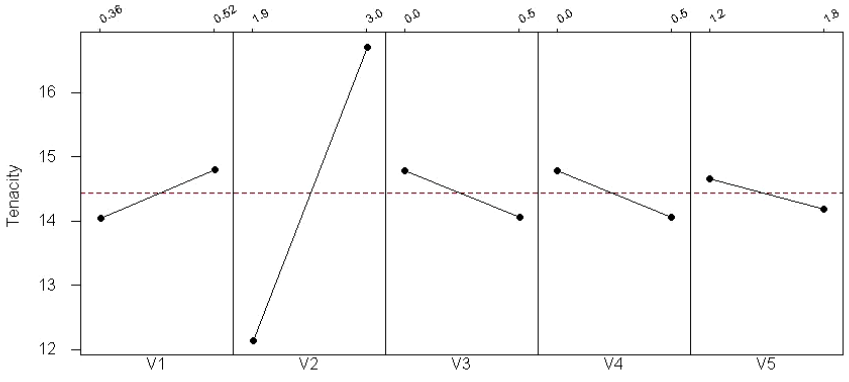

Figure 6-4 Effects plots (data means) for tenacity

Figure 6-4 shows the influences of all the five factors on yarn tenacity. The twist factor has a dramatic influence on yarn tenacity, when the twist factor changes from 1.9 to 3.0; the speed ratio has a similar trend, the bigger the speed ratio value, the higher the yarn tenacity. Other three factors have different influences; yarn tenacity is reduced along with the increase of their values respectively.

6.4.1.3 Other responses

Figure 6-5 shows the influences of all the five factors on yarn elongation. The twist factor has a dominant influence on yarn elongation. Yarn elongation percentage increases with the increase of yarn twist factor. The speed ratio and break draft have similar trends, the bigger the value of the speed ratio and break draft, the greater the yarn elongation. Whereas the positions X and Y have different effects on yarn elongation.

In this case, CVm percentage value is used to evaluate yarn evenness. Figure 6-6 reveals that although all the five factors have influences on it, the effect of the break draft is the most significant. The bigger the break draft ratio, the greater the evenness CVm percentage. This confirms those reported previously in literature, and our earlier experience (Hong Kong Cotton Spinners Association 2000).

Figure 6-7 shows yarn hairiness S3 value. The yarn twist factor has very strong influences on yarn hairiness, as observed by others. Their yarns are not the same type. The higher the yarn twist factor, the lower the yarn hairiness level. Speed ratio and break draft are the secondary factors, increasing speed ratio or decreasing break draft can help

to reduce yarn hairiness. The figure also reveals that the X, Y positions have no significant influences on yarn hairiness.

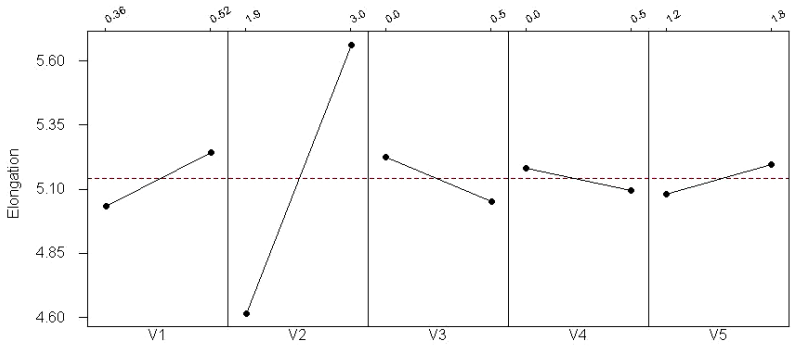

Figure 6-5 Effects plots (data means) for elongation

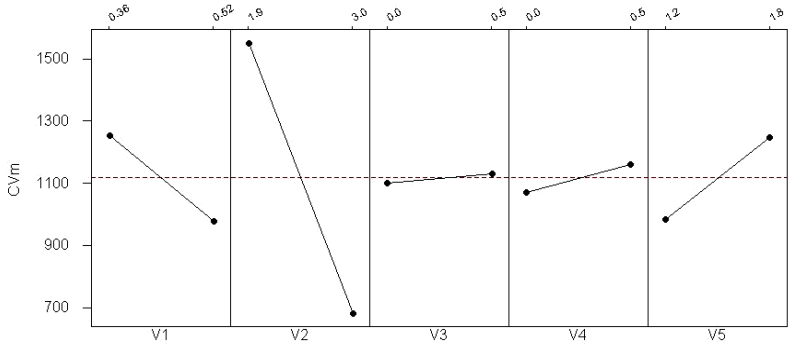

Figure 6-6 Effects plots (data means) for evenness CV%

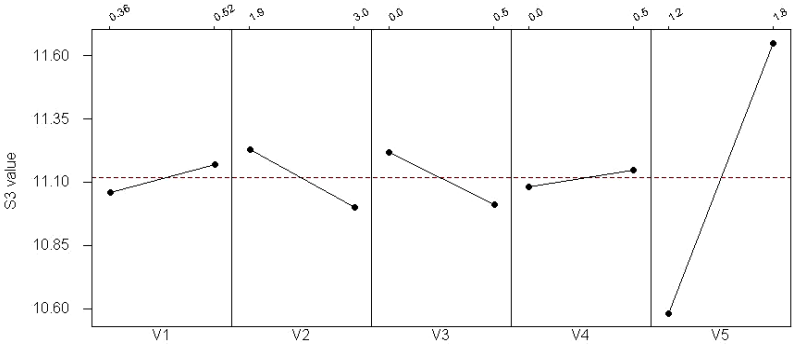

Figure 6-7 Effects plots (data means) for hairiness S3 value

6.4.2 Results from response surface analysis

According to the results of the fractional factorial experiment, two-factor-two-level scheme was adopted. Two significant factors chosen are the twist factor and speed ratio. The twist factor ranges from 1.9 to 3.0, and the range of speed ratio is from 0.36 to 0.52. Table 6-9 shows the actual experimental arrangement and test results.

Table 6-9 Experimental results (20Ne)

Run Order	Twist factor (tpi/ $count^{1/2}$)	Speed ratio	Wet snarling (turns/25cm)	Tenacity (cN/tex)	Elongation (%)	Hairiness (S3 value)
1	2.45	0.44	29	16.37	5.12	1003
2	2.45	0.44	28	16.46	5.09	1020
3	1.90	0.44	21	11.16	4.17	2292
4	2.84	0.38	34	17.65	5.27	683
5	2.45	0.36	30	15.14	4.80	1241
6	2.06	0.50	21	12.70	4.34	1585
7	2.84	0.50	31	16.72	4.89	659
8	2.45	0.52	26	15.85	4.82	870
9	2.45	0.44	30	15.86	4.86	1069
10	2.06	0.38	25	12.42	4.57	1647
11	3.00	0.44	36	17.43	5.59	513
12	2.45	0.44	29	15.47	4.79	959
13	2.45	0.44	30	15.76	4.92	982

Note: Roving C1.

6.4.2.1 Wet snarling as the response

Figure 6-8 is the contour plot of wet snarling. In the contour plot, different curves indicate different wet snarling values. The yarn spun by using the highest twist factor 3.0 and the lowest speed ratio 0.36 has the greater residual torque, its wet snarling is 35 turns/25cm. Whereas the yarn with the lowest twist factor 1.9 and the greatest speed ratio has the least wet snarling, the value is around 18 turns/25cm. The plot also shows that decreasing twist factor is more efficient than increasing speed ratio for reducing yarn wet snarling. The slopes of the reduction of contours are not constant; the slope near the left boundary is steeper than that near the right boundary. It means the same change of twist factor leads to different changes of wet snarling. Therefore, in order to get a lower wet snarling, it is necessary to use lower twist factor and higher speed ratio.

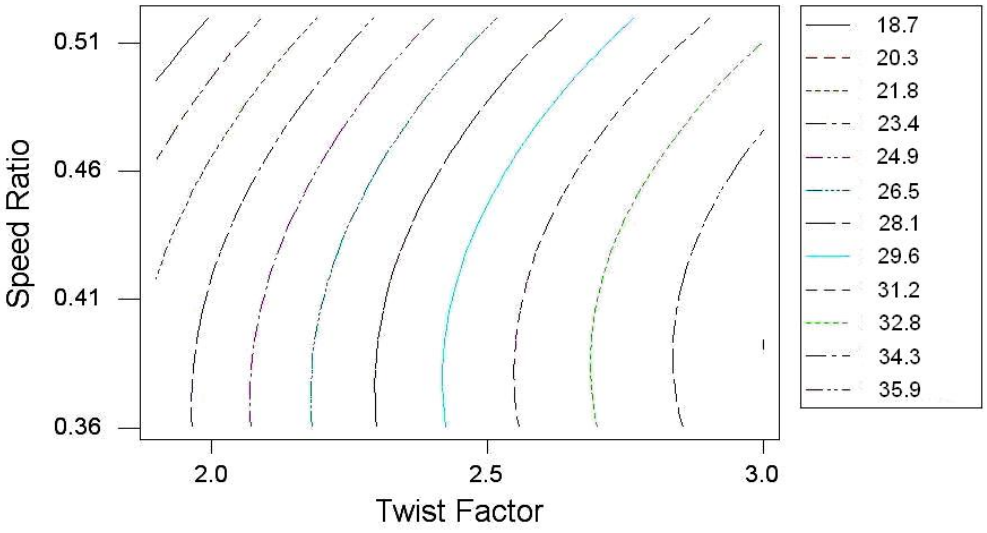

Figure 6-8 Contour plot of wet snarling (20Ne)

6.4.2.2 Tenacity as the response

The contour plot of tenacity is shown in Figure 6-9. In this plot, different curves indicate different tenacities. The twist factor is more sensitive than the speed ratio for influencing yarn tenacity. For the same speed ratio and different twist factors, the slopes of contour grads are different; the one in the high twist section is gentler than the one in the low twist section. Therefore, in the low twist region, using a higher twist factor can help to increase yarn tenacity significantly while the speed ratio has less effect. In addition, it is recommended to avoid using a low twist factor and low speed ratio simultaneously, which leads to a weak yarn.

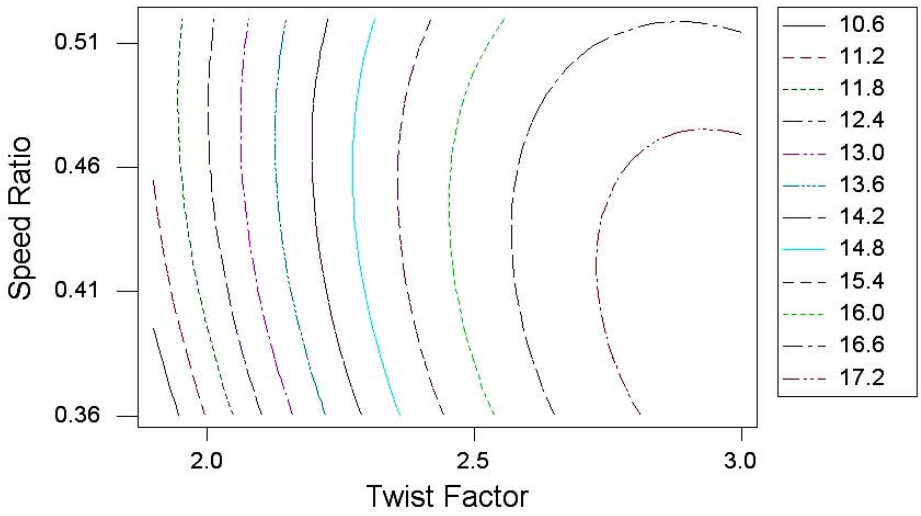

Figure 6-9 Contour plot of tenacity (20Ne)

6.4.2.3 Hairiness as the response

Hairiness is a very important index, especially for knitting yarns. Since the modification process may result in the change of yarn structural hairs, it is necessary to investigate

hairiness of the TBS yarns. Figure 6-10 is the contour plot of yarn hairiness. A low twist yarn possesses more hairs for the conventional ring spun yarns. The TBS yarn follows this trend even though there is not a linear relationship between the twist factor and hairiness. On the other hand, the speed ratio has less influence on yarn hairiness than the twist factor. Generally, a low S3 value occurs when the yarn is spun by using a high twist factor and a high speed ratio. On the contrary, a low twist factor and low speed ratio result in more hairy yarns.

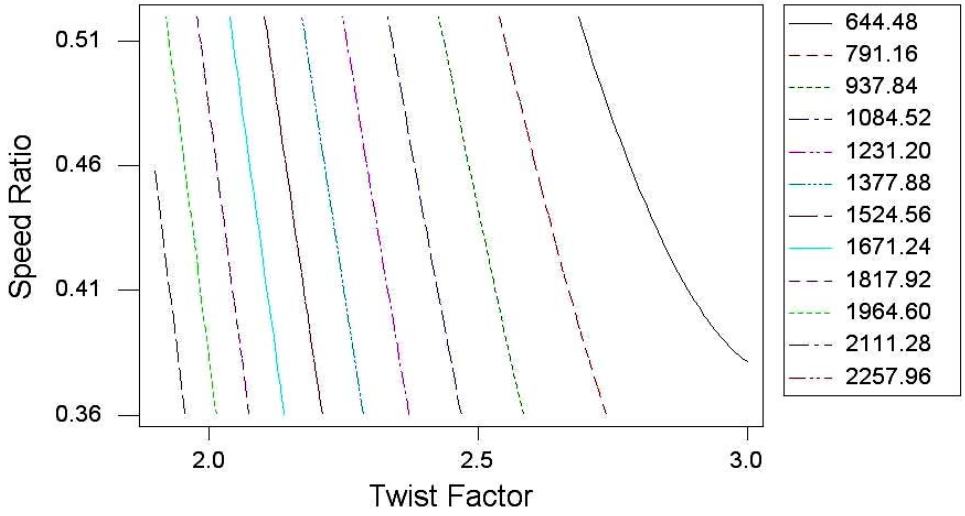

Figure 6-10 Contour plot of hairiness (20Ne)

6.4.2.4 Parameter optimization

With an understanding of relationships between the two factors and three yields respectively, it is possible to identify an optimized region to meet all the requirements. Figure 6-11 shows an example; curves are the set boundaries of wet snarling, tenacity and hairiness, respectively. The white zone is the region which meets all three

requirements, i.e., if a yarn is spun by using the parameters in this zone, it is possible to obtain the desired properties.

Figure 6-12 is another expression of optimization. When targets are defined, it is possible to get a set of parameters in the selected ranges to meet the requirements. The differences between Figure 6-11 and Figure 6-12 are that Figure 6-11 only shows an optimal zone, whereas Figure 6-12 shows the optimal parameters and calculated values of yields. d means an individual desirability, and D is the composite desirability for these three variables.

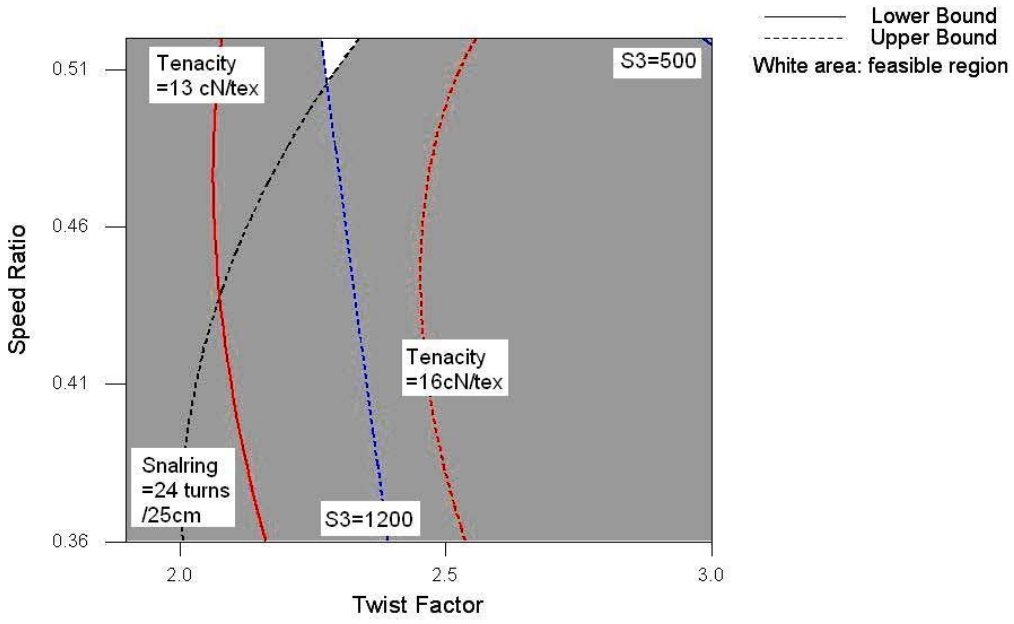

Figure 6-11 Overlaid contour plot of wet snarling, tenacity and hairiness (20Ne)

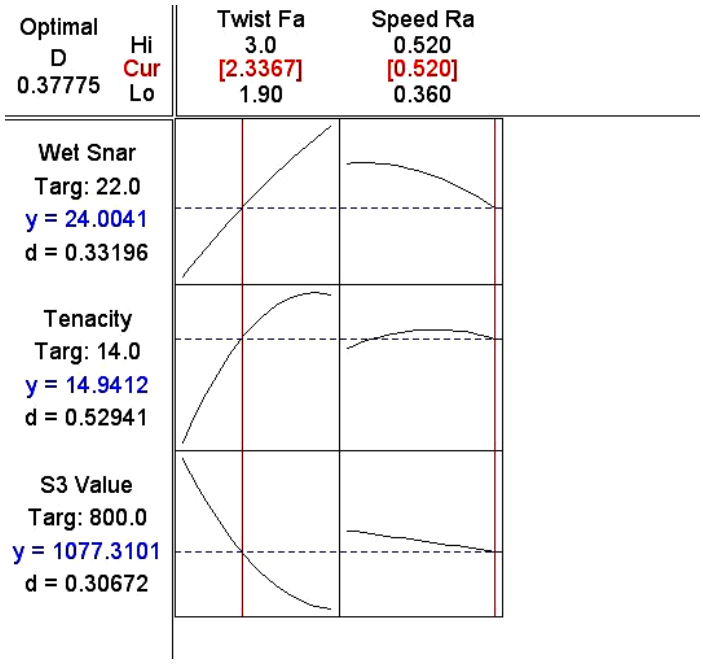

Figure 6-12 Optimal parameters and estimated values (20Ne)

In this example, the boundaries of the wet snarling, tenacity and S3 value are 10 and 24 turns/25cm, 13 and 16 cN/tex, as well as 500 and 1200, respectively. The targets are 22 turns/25cm, 14cN/tex and 800. Figure 6-11 shows that a zone which meets all the requirements exists. Figure 6-12 shows the pairs of optimal parameters and estimated values, i.e., if a yarn is spun by using a twist factor of 2.34 and a speed ratio of 0.52, thus it is possible to meet the desired performances, wet snarling is 24 turns/25cm, tenacity is 14.9 cN/tex and hairiness S3 value is 1077. Although they were the desired parameters in this experimental region, it can provide revelations to our later study.

6.4.2.5 Fitted equations

Based on Equation 6-5, several regresseion equations were established. These equations with R^2 values close to unit would imply that they fit the experimental data very well.

They are listed as follows:

$$S = -36.99 + 23.49X + 124.68Y - 3.12X^2 - 201.39Y^2 + 10.68XY \quad \text{6-12}$$

$$R^2 = 0.982$$

$$T = -58.63 + 37.21X + 98.13Y - 5.22X^2 - 74.69Y^2 - 12.93XY \quad \text{6-13}$$

$$R^2 = 0.978$$

$$H = 12597.5 - 7279.25X - 3018.56Y + 1160.91X^2 + 854.17Y^2 + 405.98XY \quad \text{6-14}$$

$$R^2 = 0.966$$

Where: S: wet snarling (turns/25cm)

T: tenacity (cN/tex), test speed: 5000mm/min, gauge length: 500mm

H: hairiness S3 value (no. of ends which is not shorter than 3mm per 100m)

X: twist factor (tpi/ $count^{1/2}$)

Y: speed ratio

6.4.2.6 Verification experiments

In order to evaluate the validity of these equations, several verification experiments were conducted. The preferred values of wet snarling, tenacity and hairiness S3 are 22 turns/25cm, 14 cN/tex and 1200 ends/100m respectively. Therefore, after the calculation according to the Equations 6-12, 13 and 14, the twist factor was chosen around 2.34 and the speed ratio was 0.52. Furthermore, in order to investigate the applicability of these equations outside the optimization range, two higher speed ratios (0.56 and 0.59) were chosen.

Table 6-10 Test results of the verification experiments (20Ne)

Sample	Twist factor (tpi/ $count^{1/2}$)	Speed ratio	Wet snarl (turns/25cm)			Tenacity (cN/tex)			Hairiness S3 Value (ends/100m)			Remarks
			E	A	Pe (%)	E	A	Pe (%)	E	A	Pe (%)	
1	2.34	0.52	24	23	4.16	14.96	15.50	-4.03	1076	901	16.26	Inside the experimental region
2	2.34	0.56	22	21	4.55	14.45	15.56	-7.68	1030	838	18.64	Outside the experimental region
3	2.40	0.59	20	21	-5.00	14.15	15.57	10.04	903	828	8.31	Outside the experimental region

Note: E — Estimated value based on Equation 6-12, 13 and 14

A — Actual experimental value

Pe — Percentage error, Pe = D/P * 100%

D — Difference between the estimated value and the actual experimental value

P — Estimated value from the fitted model

The results shown in Table 6-10 reveal that Equations 6-12, 13, 14 can be used inside, and in some cases, outside the optimization region. The actual values of wet snarling are very close to their respective estimated values. The tenacity of Sample 3 is underestimated, and the error is 10%. The estimated hairiness S3 values of all samples are higher than actual values and the error can be as high as 18.64%.

Two additional yarns were produced by using different rovings C2 and C3. Test results are listed in Table 6-11. The results show that all errors are higher than those yarns made

from roving C1 except the tenacity of Sample 4. The results reveal that these equations need to be corrected before they are applied to the yarns spun from different fibers.

Table 6-11 Verification by using other rovings (20Ne)

Sample	Twist factor (tpi/ $count^{1/2}$)	Speed ratio	Wet snarl (turns/25cm)			Tenacity (cN/tex)			Hairiness S3 value (ends/100m)			Roving
			E	A	Pe (%)	E	A	Pe (%)	E	A	Pe (%)	
4	2.34	0.56	22	20	9.1	14.45	14.06	2.8	1030	678	34.2	C2
5	2.34	0.56	22	19	13.6	14.45	17.42	-20.6	1030	602	41.6	C3

Note: E — Estimated value based on Equation 6-12, 13 and 14

A — Actual experimental value

Pe — Percentage error, Pe = D/P * 100%

D — Difference between the estimated value and the actual experimental value

P — Estimated value from the fitted model

6.4.3 Effect of yarn counts

6.4.3.1 Response surface experiments of the 16Ne TBS yarns

The optimization experiment of the 16Ne TBS yarns was designed according to the arrangement listed in Table 6-5. A Spin tester was adopted and C1 roving was used. Similar to 20Ne, the optimization trials were conducted for the TBS yarns of 16Ne. Preliminary spinning trials were conducted for the determination of the ranges of spinning parameters. For the 16Ne yarns, after balancing the yarn performance and spinnability, the range of the twist factor was selected from 2.04 to 2.81, and the speed ratio from 0.38 to 0.59. In this region, the TBS yarns can be produced efficiently and smoothly.

Test results are shown in Table 6-12. Figures 6-13 and 6-14 are the surface plots of wet snarling and tenacity. Figure 6-13 shows that the lower wet snarling appears when a yarn is spun by using a lower twist factor and a higher speed ratio. In addition, the speed ratio is more sensitive to yarn wet snarling than the twist factor.

Table 6-12 Experimental results (16Ne)

Run Order	Twist Factor (tpi/ count$^{1/2}$)	Speed Ratio	Wet Snarling (turns/25cm)	Tenacity (cN/tex)
1	2.43	0.49	23	15.63
2	2.43	0.49	25	16.18
3	2.15	0.41	24	12.92
4	2.15	0.56	19	14.11
5	2.70	0.56	23	16.51
6	2.43	0.49	22	15.92
7	2.70	0.41	31	17.29
8	2.81	0.49	27	17.13
9	2.43	0.49	22	16.13
10	2.43	0.59	18	15.27
11	2.04	0.49	19	12.92
12	2.43	0.49	23	16.07
13	2.43	0.38	30	15.47

Note: Roving C1.

As shown in Figure 6-14, a high twist factor leads to a high yarn strength. In the experimental region, using a higher twist factor and a lower speed ratio can obtain a yarn with a higher tenacity, and using a lower twist factor and a lower speed ratio leads to a yarn with a lower tenacity. It is slightly different from the results of 20Ne TBS yarn. The

plot also reveals that the influences of the speed ratio on yarn strength are complicated. Thus it is necessary to properly match the twist factor and speed ratio in order to obtain desired yarn strength.

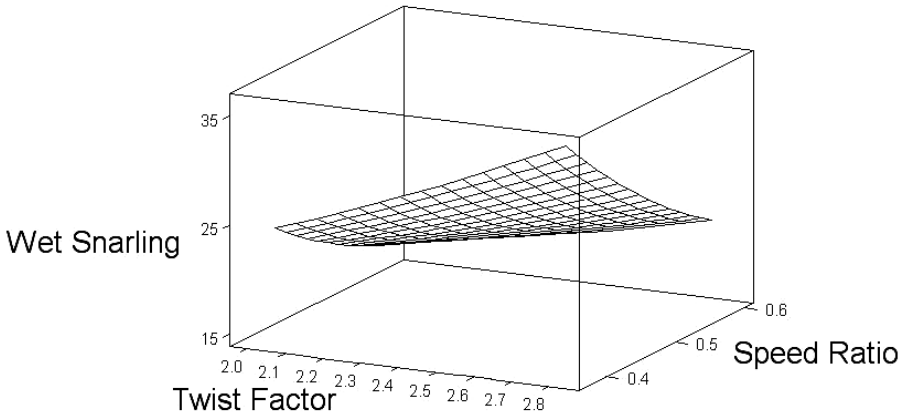

Figure 6-13 Surface plot of wet snarling (16Ne)

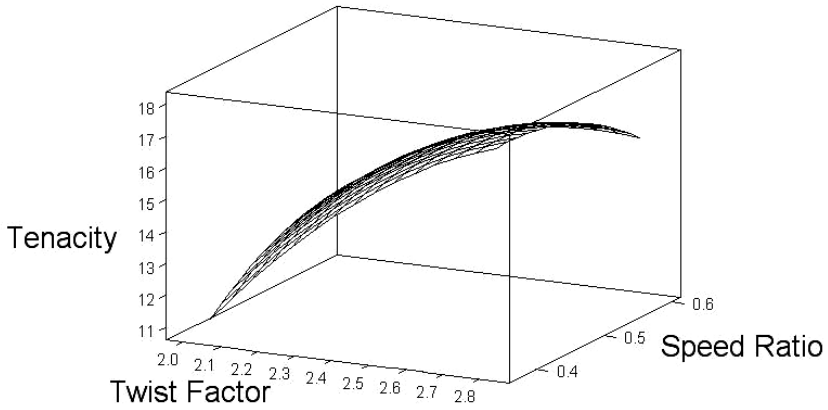

Figure 6-14 Surface plot of tenacity (16Ne)

6.4.3.2 Response surface experiments of 30Ne TBS yarns

The optimization of 30Ne TBS yarns was conducted by using a Toyota RY spinning machine. Since the count of C1 roving was not suitable for producing 30Ne yarns, thus P1 roving of 551tex was used. The range of the twist factor was from 1.9 to 3.0, and the range of the speed ratio was from 0.42 to 0.59.

Table 6-13 Experimental design and test results (30Ne)

Run Order	Twist factor (tpi/ count$^{1/2}$)	Speed ratio	Wet snarling (turns/25cm)	Tenacity (cN/tex)
1	1.90	0.51	22	20.21
2	2.45	0.51	25	25.71
3	2.45	0.51	24	25.39
4	2.45	0.51	26	25.35
5	2.84	0.57	21	25.67
6	2.06	0.45	27	21.37
7	2.06	0.57	18	22.35
8	2.45	0.51	24	25.43
9	2.45	0.51	25	25.27
10	2.84	0.45	33	26.10
11	2.45	0.42	32	24.86
12	2.45	0.59	20	24.53
13	3.00	0.51	28	25.69

Note: Roving P1.

Table 6-13 shows the test results. Figure 6-15 and Figure 6-16 are surface plots of the wet snarling and tenacity, respectively. Figure 6-15 shows that using a higher twist

factor and a lower speed ratio can help to produce a yarn with a higher wet snarling, contrarily; using a lower twist factor and a higher speed ratio will lead to a yarn with a lower wet snarling.

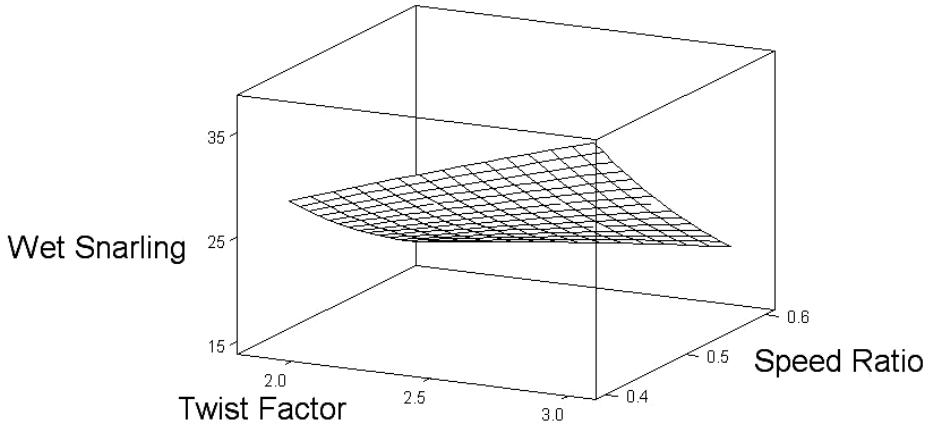

Figure 6-15 Surface plot of wet snarling (30Ne)

Figure 6-16 shows the surface plot of tenacity of 30Ne TBS yarn. The twist factor has dominant influences on the tenacity. In the region of the low twist factor, yarn strength reduces with the decrease of the twist factor. Medium speed ratio helps to increase yarn tenacity.

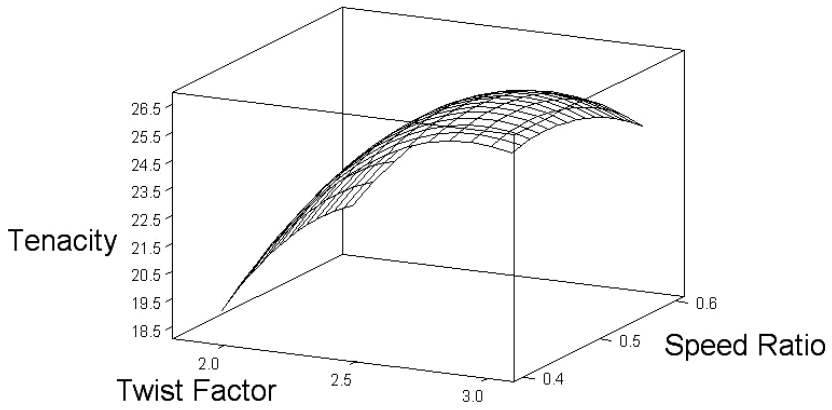

Figure 6-16 Surface plot of tenacity (30Ne)

Table 6-14 Coefficients of the regression equations for 16Ne, 20Ne and 30Ne TBS yarns

Yarn count	Properties	Constant	X	Y	X^2	Y^2	XY	R^2
16Ne	Wet snarling	13.39	21.10	-65.95	1.38	107.41	-36.36	0.954
	Tenacity	-79.25	49.70	115.31	-6.67	-58.96	-23.88	0.984
20Ne	Wet snarling	23.19	15.75	-80.32	2.48	122.22	-36.36	0.962
	Tenacity	-76.17	48.02	110.8	-6.32	-54.31	-23.88	0.978
30Ne	Wet snarling	37.14	24.61	-116.31	-0.58	114.58	-32.05	0.974
	Tenacity	79.66	52.36	137.51	-8.08	-98.96	-15.28	0.994

6.4.3.3 Analysis of the regression equations

Table 6-14 lists the coefficients of the regression equations for 16Ne, 20Ne and 30Ne yarns.

a) Location and nature of the stationary points

The nature of the response surface system (maximum, minimum, or saddle point) depends on the signs and magnitude of the coefficients in Equation 6-5. The second-order coefficients play a vital role. It should be noted that the coefficients used are estimates of β's of Equation 6-5.

An analysis of this response function would determine the location of the stationary point and the natural of the response system. Because two factors were used in this case, the stationary point can be calculated by using Equation 6-15.

$$\frac{\partial \hat{y}}{\partial x_1} = \frac{\partial \hat{y}}{\partial x_2} = 0 \qquad \text{6-15}$$

After obtaining the coordinates of the stationary points, it is easy to calculate the yield of this point.

Table 6-15 shows the location and nature of the stationary points and the yield at this point. It is obvious that all of the stationary points were located outside the experiment regions. The nature of the stationary point is determined from the signs of the eigenvalues of the matrix of the second-order coefficients $\hat{\boldsymbol{B}}$ (Myers and Montgomery 2002). It turns out that the relative magnitudes of these eigenvalues can be helpful in the total interpretation. Equation 6-16 describes the nature of the stationary point and the nature of the system around the stationary point.

$$\hat{y} = \hat{y}_s + \sum_{i=1}^{k} \lambda_i w_i^2 \qquad 6\text{-}16$$

Where $\hat{y}_s$ is the estimated response at the stationary point, and $\lambda_1, \lambda_2, \cdots, \lambda_k$ are the eigenvalues of $\hat{\boldsymbol{B}}$. The variables $w_1, w_2, \ldots, w_k$ are canonical variables. Myers (Myers and Montgomery 2002) stated that if $\lambda_1, \lambda_2, \cdots, \lambda_k$ are all negative, the stationary point is a maximum response; if $\lambda_1, \lambda_2, \cdots, \lambda_k$ are all positive, the point is a minimum response; and if $\lambda_1, \lambda_2, \cdots, \lambda_k$ are mixed in sign, the point is a saddle point.

The nature of every response is also listed in Table 6-15. The results show that different yarn counts and responses possess different natures of the stationary points. Most of them are the maximum point and the other two are saddle shape. The response surface is not always symmetrical in all directions. A smaller value indicates a faster change of the response in that direction.

For the wet snarling, the twist factors and speed ratios of the stationary points of the 16Ne, 20Ne and 30Ne TBS yarns are 2.92 and 0.8, 4.50 and 0.43, as well as 2.79 and 0.48, respectively. Comparing the yarns of 16Ne and 20Ne, which were produced on the same machine and using the same roving, at the stationary point of the 16Ne yarn, its twist factor and speed ratio are smaller and higher respectively than those of the 20Ne yarns. In other words, along with the increase of yarn count, the location of the stationary point will move to a point with a lesser twist factor and higher speed ratio. The results also indicate that the yield of the stationary point of the 20Ne yarn is much

higher than that of the 16Ne yarn. The nature of the stationary point revealed that the nature of the 16Ne yarn is a saddle shape, i.e., it is a combination of the lowest and highest point in two directions respectively. While the 20Ne yarn reached its maximum value at its stationary point. Since the stationary points of both yarns are not in their experimental regions, and can not give us the minimum values of wet snarling, therefore it is necessary to limit the analysis boundaries.

For the tenacity, the twist factors and speed ratios of the stationary points of the 16Ne, 20Ne and 30Ne TBS yarns are 3.10 and 0.35, 3.08 and 0.0.39 as well as 1.48 and 0.71, respectively. The comparison between 16Ne and 20Ne TBS yarns demonstrates that the yarn tenacity is not as sensitive to the change of yarn count. The results also reveal that the stationary points for the responses of wet snarling and tenacity are not located on the same point. That means it is impossible to achieve the extremum of wet snarling and tenacity at the same time. Therefore, a balance between the parameters and responses is necessary. The stationary point of 20Ne TBS yarn for the response of tenacity is slightly lesser in the twist factor and greater in the speed ratio if compared with the 16Ne TBS yarn. The stationary point for the response of wet snarling follows a reverse tendency. For the 30Ne TBS yarns, its stationary point of wet snarling is located adjacent to the experiment region. The results imply that the range of the speed ratio is sufficient for the determination of the stationary point; it is possible to get the stationary point by extending the range of the twist factor. The stationary point of wet snarling is located in the experiment region, but it is not the lowest point rather than the highest point. Therefore, it also needs to balance its two properties.

Table 6-15 Results of the analysis of the stationary points and the nature of the stationary point of different yarn counts

Yarn		Nature of the stationary point			Stationary point		
Count	Properties	λ_1	λ_2	Shape	x_1	x_2	Yield
16Ne	Wet snarling	110.43	-1.65	Saddle	2.92	0.80	17.78
	Tenacity	-4.07	-61.56	Maximum	3.10	0.35	17.98
20Ne	Wet snarling	-2.98	-201.53	Maximum	4.50	0.43	42.58
	Tenacity	-4.63	-75.29	Maximum	3.08	0.39	17.84
30Ne	Wet snarling	115.57	-1.65	Saddle	1.48	0.71	13.79
	Tenacity	-7.24	-99.79	Maximum	2.79	0.48	185.60

b) Desirable region and points

Since yarns' stationary points of wet snarling and tenacity are not in the same point, and most of them are out of the experiment region, as well as their natures was not what we wanted. For example for the wet snarling of the 20Ne yarn, there is a maximum value in the experimental region, however, the lowest value is our favourite. Therefore it is necessary to find an optimum zone in the experimental region. Thus we can obtain a yarn with lower wet snarling and relatively higher tenacity simultaneously. In this study, wet snarling was firstly considered, and then is the tenacity. Finally, yarn spinnability was also included. According to our experience on the relationship between the yarn wet snarling and the spirality of plain knitted fabrics, the twist factor was chosen around 2.3 to 2.5, and the speed ratio was selected as high as possible in the experimental region. In practice, however, we can reduce the speed ratio for improving yarn spinnability.

6.4.4 Effect of spinning machines

In order to evaluate the adaptability of the modification device to different spinning machines and the yarn performance, two sets of optimization were conducted by using two spinning machines (Toyota RY and Zinser 319SL), respectively. 20Ne yarns were produced, and the results of the Spin tester were also included for comparison.

The geometries of these spinning machines differ from that of the Spin tester, leading to some small changes of the installation positions of the device. Preliminary investigations were conducted before the optimization experiments to determine the boundaries of parameters based on spinning performance and previous experience. For the Toyota RY, the twist factor ranged from 2.1 to 2.7, and the speed ratio ranged from 0.39 to 0.59. For the Zinser 319SL, the range of the twist factor was from 2.2 to 2.5, and the speed ratio ranged from 0.39 to 0.59. C1 roving was used for both experiments.

6.4.4.1 Response surface experiments of different machines

Table 6-16 shows the experiment arrangement and results of the yarns produced by using the Toyota RY, Zinser 319 SL and Spin tester.

Table 6-16 Optimized results of the TBS yarns spun by using the Toyota RY, Zinser 319SL and Spin tester

Run Order	Toyota RY				Zinser 319SL				Spin tester			
	Twist Factor (tpi/ count$^{1/2}$)	Speed Ratio	Wet Snarling (turns /25cm)	Tenacity (cN/tex)	Twist Factor (tpi/ count$^{1/2}$)	Speed Ratio	Wet Snarling (turns /25cm)	Tenacity (cN/tex)	Twist factor (tpi/ count$^{1/2}$)	Speed ratio	Wet snarling (turns /25cm)	Tenacity (cN/tex)
1	2.60	0.49	24	16.48	2.35	0.49	20	15.18	2.45	0.44	29	16.37
2	2.53	0.42	29	16.22	2.35	0.39	24	13.91	2.45	0.44	28	16.46
3	2.35	0.59	18	15.40	2.20	0.49	19	14.11	1.90	0.44	21	11.16
4	2.53	0.56	19	16.36	2.24	0.56	17	14.59	2.84	0.38	34	17.65
5	2.35	0.49	22	15.25	2.24	0.42	22	13.29	2.45	0.36	30	15.14
6	2.35	0.39	27	13.42	2.35	0.49	20	15.36	2.06	0.50	21	12.70
7	2.35	0.49	21	14.86	2.50	0.49	21	16.28	2.84	0.50	31	16.72
8	2.17	0.56	18	14.31	2.35	0.59	18	15.32	2.45	0.52	26	15.85
9	2.35	0.49	22	14.95	2.46	0.56	19	15.52	2.45	0.44	30	15.86
10	2.35	0.49	22	14.61	2.35	0.49	20	15.31	2.06	0.38	25	12.42
11	2.10	0.49	22	13.24	2.46	0.42	25	15.02	3.00	0.44	36	17.43
12	2.35	0.49	23	15.05	2.35	0.49	21	15.19	2.45	0.44	29	15.47
13	2.17	0.42	26	12.87	2.35	0.49	20	15.23	2.45	0.44	30	15.76

Note: Roving C1.

6.4.4.2 Analysis of regressed equations

Some regressed equations were established. These equations with R^2 values close to unit would imply that they fit the experimental data very well.

Table 6-17 Coefficients of the regression equations for the TBS yarns spun by using the Toyota RY and Zinser 319SL ring spinning machines

Machine	Properties	Constant	X	Y	X^2	Y^2	XY	R^2
Toyota RY	Wet snarling	103.24	-57.41	-24.11	17.36	63.78	-39.68	0.957
	Tenacity	-38.39	14.60	106.59	1.06	-38.93	-25.79	0.958
Zinser 319SL	Wet snarling	-15.50	39.37	-50.99	-3.10	94.39	-32.47	0.961
	Tenacity	-100.30	59.83	146.71	-8.64	-80.51	-25.97	0.969
Spin tester	Wet snarling	-36.99	23.49	124.68	-3.12	-201.39	10.68	0.982
	Tenacity	-58.63	37.21	98.13	-5.22	-74.69	-12.93	0.978

a) Location and nature of the stationary points

It is easy to locate the stationary point and calculate the yield at the stationary point by using the Equation 6-14. Similar with the case of the effect of different yarn counts, the location and nature of every response were calculated and the results are listed in Table 6-18. The results show that the geometry of a spinning machine has influences on the natures of the stationary points of the yarn. The natures of them are minimum, maximum and saddle. The response surface is not always symmetrical in all directions. A smaller value indicates a faster change of the response in that direction. In addition, the results show that all of the stationary points were located outside the experiment regions. For the wet snarling, the twist factors and speed ratios of the stationary points of the yarns produced by using the Toyota, Zinser and Spin tester were 2. 90 and 1.09, 2.59 and 0.72 as well as 4.50 and 0.43, respectively. For the tenacity, the twist factors and speed ratios of the stationary points of the yarns produced by using the Toyota, Zinser and Spin tester were 1.94 and 0.73, 2.76 and 0.47, as well as 3.08 and 0.39, respectively. Comparing the

Zinser TBS yarn with the other two TBS yarns, it exhibits the best properties (lower wet snarling and relatively higher tenacity) if compared with the other yarns at their stationary points.

Table 6-18 Results of the analysis of the stationary points and the nature of the response of different machines

Yarn		Nature of the stationary point			Stationary point		
Count	Properties	λ_1	λ_2	Shape	x_1	x_2	Yield
Toyota RY	Wet snarling	71.10	10.06	Minimum	2.90	1.09	18.19
	Tenacity	4.86	-42.73	Saddle	1.94	0.73	14.45
Zinser 319SL	Wet snarling	97.02	-5.73	Saddle	2.59	0.72	17.35
	Tenacity	-6.36	-82.78	Maximum	2.76	0.47	16.52
Spin Tester	Wet snarling	-2.98	-201.53	Maximum	4.50	0.43	42.58
	Tenacity	-4.62	-75.29	Maximum	3.08	0.39	17.84

The comparison among these three yarns also reveals that their coordinates and the yield of the stationary points are different. Since these three yarns have the same yarn count and produced by using the same roving, the only difference is the machine used. Therefore, the variables related to the sinning machine may be the reasons resulting in these differences. The Toyota RY and Zinser 319SL are two types of spinners for industrial use. They are stable and have similar geometries. Whereas the Spin tester differs from them; it is a mini-frame for laboratorial trial. Its geometry is different from those of the other two machines, and not as stable as them. These may explain the differences of the location and yield of the stationary point between the yarns made by using these three machines.

c) Desirable region and points

Similar with the case of the effect of different yarn counts, stationary points of wet snarling and tenacity of these yarns are not in the same point, and most of them are out of the experiment region, and their natures were not what we wanted. Therefore, we need to find an optimum zone in the experimental region. The sequence of our consideration is wet snarling, tenacity and spinnability. After considering and balancing these properties and requirement, the twist factor was chosen around 2.4 to 2.5, and the speed ratio was selected as high as possible in the experimental region. In practice, we can also decrease the speed ratio for further improving yarn spinnability.

6.5 Summary and Conclusions

In this chapter, several optimization experiments were carried out. The optimization was divided into two stages, i.e., fractional factorial experiment and response surface experiment. In the first stage, five factors were chosen as the candidates. They were yarn twist factor, speed ratio, break draft as well as the installation position of the modification device X and Y. The experiment identified that the twist factor and speed ratio are the two most important factors which have significant influences on yarn wet snarling, tenacity and hairiness. Others are the secondary factors or can be neglected.

In the second stage, response surface experiment of 20Ne TBS yarn was conduced. Several 2^{nd} order response surface equations were derived for predicting wet snarl, tenacity, and hairiness of yarns. R square values indicate they were well fitted. The

verification experiments showed that the actual values of yarn wet snarling and tenacity were close to their predicted values if the yarns were spun by using the same material. However, the errors for hairiness S3 value were bigger. For different fibers, the yarn properties predicted directly by using the equations regressed from a different fiber deviated from the prediction, thus correction may be needed.

The optimizations of yarns of three counts were carried out, and the results reveal that the modification device can be used for producing TBS yarns in the range of 16Ne to 30Ne. The analyses of 2^{nd} order equations indicate that the yarn count has influences on the location, yield as well as the nature of the stationary points.

The TBS yarns were also spun by using three different spinning machines. The response surface analyses indicate that the spinning geometry affects not only the range of the parameter selection and yarn performance, but also the location, yield and the nature of the stationary point.

CHAPTER 7

PERFORMANCE OF PLAIN KNITTED FABRICS MADE FROM TORQUE –BALANCED SINGLES RING SPUN YARNS

7.1 Introduction

After the investigation on yarn structure and spinning mechanism, as well as the establishment of the torsional model of the TBS yarn, it is necessary to examine the properties and performance of the yarns and fabrics. Besides the residual torque and fabric spirality, tenacity and hairiness of the yarn, bursting strength, dimensional stability, pilling and weight of the fabric were also measured.

7.2 Experimental

In the present study, the experiments were divided into two parts. The first part was related to the yarns, and the second part was associated with the fabrics. In the yarn part, 20Ne TBS yarns and control yarns (conventional ring spun yarns) were spun. After spinning and winding, some greige yarns were used for knitting directly, and others were package dyed. In the second part of fabric experiments, single jersey knitted fabrics were produced by using multi-feeder knitting machines in a factory. Then fabrics were piece dyed and finished. The measurements of the yarn and fabric properties were conducted in the standard environment. For comparison and reference, fabric properties were also evaluated by the factory.

7.2.1 Yarn production

7.2.1.1 Material

Cotton rovings of C1, C3 and P1, and their specifications are listed in Table 6-1.

7.2.1.2 Machine used

Yarn production was conducted by using a Zinser 319 spinning machine （60 spindles）in our workshop. Apart from the TBS yarn, conventional ring spun yarns were also produced by using the same roving.

7.2.1.3 Spinning parameters

Hundreds of pounds of 20Ne TBS yarns were produced for evaluating the performance of the yarn and the resultant fabric. The spindle speed of the spinning machine was 10,000rpm. Table 7-1 shows some of the spinning parameters. For the TBS yarns, 2.34 is the optimized twist factor and 2.5 is a twist factor recommended by the factory after evaluating the production cost. For the twist factors of conventional 20Ne knitting yarns, 3.0 is the lowest twist factor and 3.6 is the normal twist factor used in spinning factories.

Table 7-1 Spinning parameters for the production of 20Ne yarns

Yarn type	Yarn count	Twist factor	Speed ratio	Purpose	Roving
TBS	20	2.34, 2.5	0.59	Production	C3
Conventional	20	3.0, 3.6	-	Comparison	C3

7.2.2 Fabric production

Fabric productions were carried out in a factory. The aim of these production trials is to evaluate (1) the knitting capability of the TBS yarn under commercial production conditions, (2) the influences of knitting variables on the fabric spirality and (3) other fabric properties.

7.2.2.1 Knitting machines

Multi-feeder circular knitting machines were used for production trials (in factories). Figure 7-1 shows a Fukuhara FXC-Z/3S multi-feed circular knitting machine used in this study; Fukuhara VXC-3SRE is similar but running in the opposite direction. Main features of the machines are listed in the Table 7-2.

Table 7-2 Knitting machine used

Machine type	Multi-feeder	Multi-feeder
Brand and type	Fukuhara FXC-Z/3S	Fukuhara VXC-3SRE
Diameter of cylinder (in)	30	30
No. of feeder	90	90
No. of needle	2268	2268
Speed (rpm)	30	30
Gauge (npi)	24	24
Knitting tension (g)	6-8	6-8
Yarn supply	Positive	Positive
Rotational direction	Clockwise	Counter-clockwise
Purpose	Production trial	Production trial

Figure 7-1 Fukuhara FXC-Z/3S multi-feed circular knitting machine (the same type as the machine used in this study)

It has been known that the numbers of feeder and needle, gauge, cylinder diameter, and rotational direction of the machine can affect the fabric spirality (Araujo and Smith 1989; Dias and Lanarolle 2002; Primentas 2003), the machines selected cover these factors.

7.2.2.2 Fabric making

A TBS yarn, a singles control yarn and a plied yarn of the same resultant count were produced by using the same cotton for the fabric production trial in a factory. The factory also provided one singles yarn and one plied yarn for comparison. Table 7-3 shows the yarns for the knitting trial in the factory.

Table 7-3 Yarns specifications for knitting the production trial

Yarn count (Ne)	1/20	1/20	2/40	1/20	2/40
Roving used	C1	C1	C1	--	--
Yarn type	TBS	Singles control	Plied	Singles control	Plied
Provider	PolyU	PolyU	PolyU	Factory	Factory
Yarn code	TBS	P1/20	P2/40	F1/20	F2/40

For 20Ne yarns, according to factory's suggestion, 0.32cm was chosen as the loop length in order to obtain a required fabric tightness factor, around 17 $tex^{-1/2}$/cm.

After knitting, all fabrics were divided into two parts; one part was sent back to our lab for the evaluation of properties of greige fabric, the other part was piece dyed under the industrial conditions. For the dyed fabrics, half of them were sent back to our lab for evaluating the properties; the other halves were finished in the factory and sent back to our lab for testing and measurement.

Yarn dyed stripe fabrics were also produced for the knitting trials. Yarns were package dyed in the factory. In the present study, fabrics were knitted in the counter-clockwise direction. The knitted fabrics were then finished. And finally the finished fabrics were taken back to our lab for properties evaluation.

The aim of the production is to evaluate the improvement of the yarn and the resultant fabrics by comparing with the control yarns and fabrics produced under the same conditions. Since the dyeing and finishing processes were conducted in a factory, the

dyeing and finishing conditions as well as production route are not provided due to commercial reasons.

7.2.3 Test

7.2.3.1 Yarn test

All yarns were conditioned at 65±2%RH and 20±2ºC for at least 24 hours before test. Yarn properties including wet snarling, tenacity, elongation, hairiness, and evenness were measured by using the methods listed in Table6-2.

7.2.3.2 Fabric test

Fabric tests include spirality, dimensional shrinkage, fabric weight, bursting strength and pilling resistance. Measurements were conducted according to the methods and standards shown in Table 7-4.

Fabric tightness factors were calculated from the measured value of yarn loop length and linear density. The spirality angle between the inclined wales and the lines parallel to the fabric edge was measured after three 5-A washing and tumble-dry cycles according to IWS TM 276 method. Fabric dimensional stability was also evaluated. Figure 7-2 demonstrates a square ABCD which has a side length of 250mm. The method is to measure the dimensional change of each side and two diagonals before and after three washing and tumble-dry cycles. Fabric weight and bursting strength were also tested in this investigation. The targets of this investigation are that the spirality angle of the TBS fabric is less than 3 degrees after three 5-A washing and tumble dry cycles, and other

properties such as fabric shrinkage, weight, bursting strength, and pilling resistance etc. are similar to those of their control fabrics.

Table 7-4 Fabric test methods and standards

Test / Evaluation	Standard	Equipment used
Spirality measurements (Before and after three washes)	IWS 276 (modified) / AATCC 135-1995	Template, Ruler
Loop length	ASTM D 3883-90	Shirley crimp tester
Fabric weight	ASTM D 3776-96	Electronic balance
Bursting strength	ASTM D 3787-01	Mullen burst tester
Pilling (Before and after three washes)	ASTM D 3512-02/ AATCC 135-1995	Random tumble pilling tester

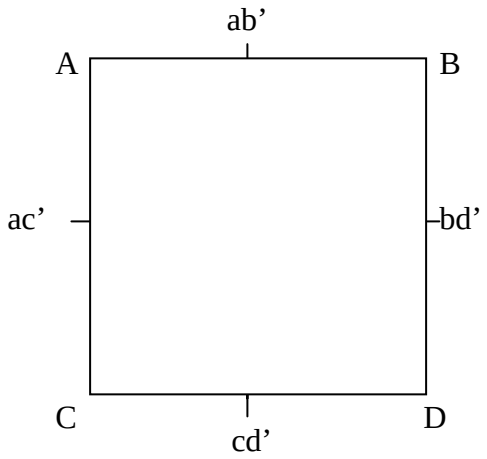

Figure 7-2 Method for evaluate fabric dimensional stability

In this study, all fabrics were conditioned at 65±2%RH and 20±2ºC for at least 24 hours before tests. Full relaxation is very important for evaluating fabric geometrical properties (Munden 1959; Postle 1968; Heap et al. 1983, 1985; Quaynor et al. 1999).

Therefore, to obtain the full relaxation state, the samples were treated using three 5-A washing (60°C) and tumble-dry cycles according to the AATCC test method 124-1996.

7.3 Results and Analysis

7.3.1 Yarn test results and analysis

7.3.1.1 20Ne greige yarns

Table 7-5 shows test results of the 20Ne TBS yarn and conventional control yarns. These results reveal that the TBS yarn has around 50 percent reduction in wet snarling; meanwhile its tenacity is 15 percent lower than that of conventional yarn of TF=3.6, but higher than that of the yarn of TF=3.0. Since they were produced by using the same C1 roving, this means the mass variation of the TBS yarn is the least among the three yarns. The possible explanation is that the higher twist of the part above the torque reduction device shortens the length of spinning triangle, increases fiber migration and reduces fiber flies, leading to the reduction of mass. However, the change of spinning triangle may affect the hairiness of the resultant yarns (Stalder 2000). Moreover, the low twist used may be another reason resulting in higher yarn hairiness (Barella and Manich 1988). In summary, the 20Ne TBS yarn has a lower twist, lower wet snarling and higher mean tenacity as well as better evenness performance if compared with the control yarn of TF=3.0.

Table 7-5 Properties of the 20Ne greige yarns

Yarn type	Control		TBS
	High twist	Low twist	
Twist multiplier	3.6	3.0	2.34
Yarn mean tenacity (cN/tex) [CV%]	18.16 [7.1]	14.98 [6.6]	15.50 [6.8]
Yarn elongation (%) [CV%]	5.01 [10.2]	4.49 [8.8]	4.65 [7.9]
Wet snarling (No. of turns/25cm) [CV%]	49 [5.9]	45 [6.1]	23 [8.9]
Yarn evenness CVm % [CV%]	11.58 [1.0]	12.08 [7.1]	10.90 [1.2]
Yarn hairiness S3 value [CV%]	870 [43.0]	728 [44.5]	901 [32.8]

7.3.1.2 20Ne dyed yarns

Knitters use dyed yarns to produce knitted goods such as stripe fabrics or sweaters (Spencer 2001). Yarns can be dyed in many manners, and package dyeing is often used in factories, especially for striping pattern and color jacquard. It is carried out in a closed vessel. The yarn is wound loosely on a special cone. Dye liquid is injected in order to penetrate the yarn package (Wynne 1997). Thus the yarn needs to have higher strength.

One TBS yarn (TF=2.5) and one control yarn (TF=3.6) were compared. Figure 7-3 demonstrates that the wet snarling of both the TBS and the control yarns decreased after dyeing due to partial removal of yarn residual torque, especially for the control yarn, the reduction was more than 40 percent, while the reduction of the TBS yarn was around 15 percent. After dyeing, yarn strengths are slightly increased for both TBS and control yarns (see Figure 7-4). This may be explained that the wet process increases the friction

between fibers. This increase was bigger than the loss of strength due to high-pressure flow, leading to a slight increase of strength.

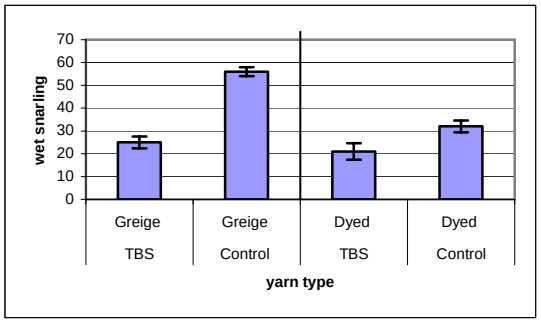

Figure 7-3 Yarn wet snarling before and after dyeing

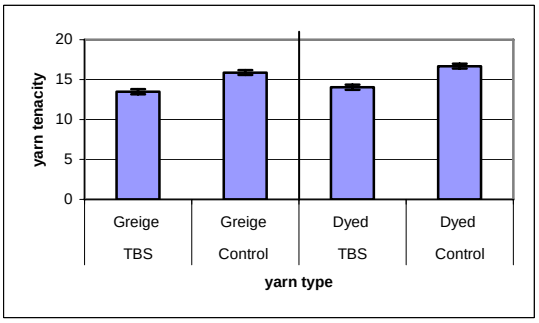

Figure 7-4 Yarn tenacity before and after dyeing

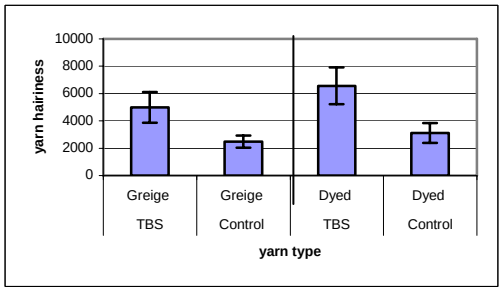

Figure 7-5 Yarn hairiness performance (S3 value) before and after dyeing

Figure 7-5 shows yarn hairiness S3 values before and after the dyeing process. The results demonstrate that the TBS yarn is more hairy than the control yarn for both dyed and greige yarns. The lower twist factor of the TBS yarn (2.34) may be responsible for this result.

7.3.1.3 Effect of winding and cleaning processes

Winding process has influences on yarn properties (Grosh et al. 2001; Ma et al. 2001; Krol and Przyby 2002), such as yarn tensile properties, yarn hairiness and other properties. Therefore investigating the effect of winding process on the properties of the TBS ring yarns is very important.

One 20Ne TBS (TF=2.5) yarn and one control yarn (TF=3.6) were produced by using the C1 roving. Two winders with different configurations were used, Winder A: a Mettler SPE winding machine, and Winder B: one Murata 7V-II winding machine. In this study, yarns were wound using both machines at a speed of 800 m/min. Before and after winding, yarn properties were evaluated and compared.

Figures 7-6 to 7-9 show the effects of winding on yarn properties. For wet snarling, Figure 7-6 shows that after winding using winder B, the wet snarling of the TBS yarn is increased slightly. Extra winding tension may be one of the reasons (Price 1983). Yarn tension of Winder B is higher than that of Winder A. Bigger tension and different winding geometry may be the reasons resulting in the slight increase of torque even though the same winding speeds were adopted.

Figure 7-7 demonstrates the effect of winding on yarn tenacity. After winding, yarn tenacities have no significant changes. The influences of winding on yarn evenness are shown in Figure 7-8. The results indicate that after winding, yarn evenness CVm % values increase slightly for both yarns. This may be due to the extra drawing during the winding process. The results shown in Figure 7-9 reveal that the winding geometry has

influences on the change of hairiness. Winder B has a more straight (vertical) and smoother path compared with Winder A, the differences of yarn hairiness S3 values reflect it.

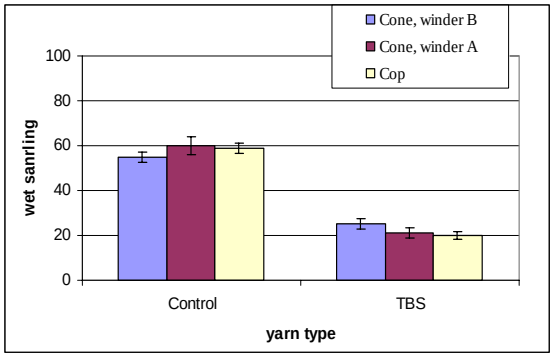

Figure 7-6 Effect of winding on snarling

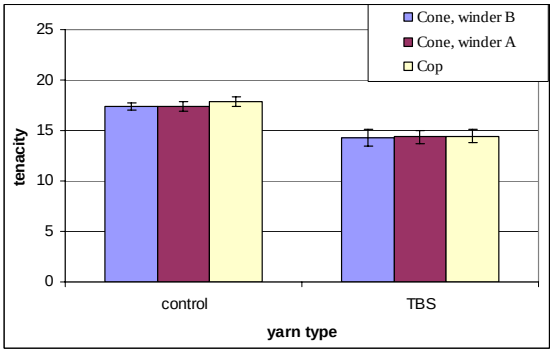

Figure 7-7 Effect of winding on tenacity

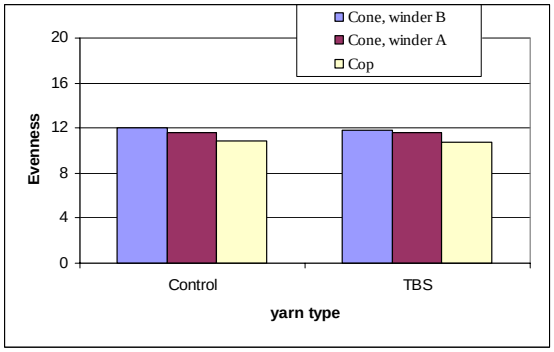

Figure 7-8 Effect of winding on evenness

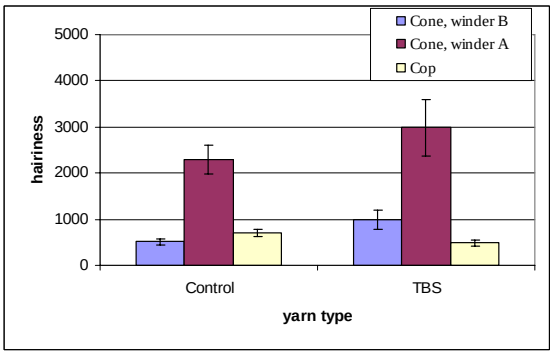

Figure 7-9 Effect of winding on hairiness

7.3.1.4 Splicing strength

The package of cop is unsuitable for the knitter, thus splicing process is needed during winding and cleaning. It was completed by using air flow on a Murata 7V-II winding machine. The length is around one inch. The strength was evaluated by measuring the strength of the yarn and the joint point. The percentage of the strength of the joint point over the yarn was compared between the TBS yarn (TF=2.5) and conventional yarn

(TF=3.6). Figure 7-10 shows the results of the splicing strength of the 20Ne TBS and conventional yarns with water treatment. The joint point can remain more than 80% of the strength for the TBS yarn, and more than 95% for the conventional yarn. If without water treatment, the TBS yarn can keep 70% of the strength.

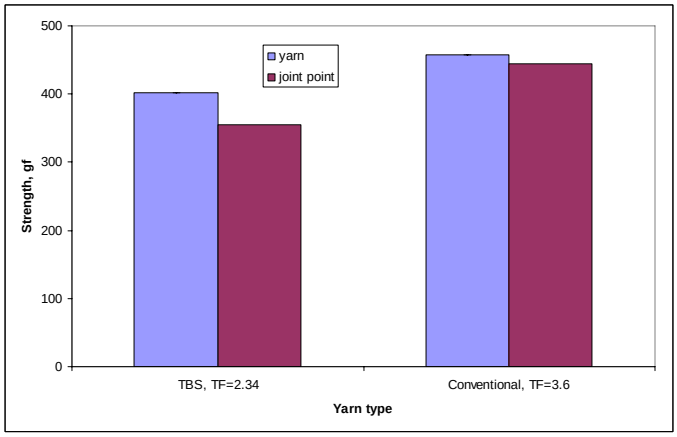

Figure 7-10 Splicing strength of 20Ne yarns

7.3.1.5 Cleaning and classimat test

Yarn faults were cleaned on the Murata 7V-II winding machine and the records are shown in Table 7-6. The TBS yarn is a little worse than the conventional ring spun yarn in all items but the long slub L (length >8cm). The classimat test was conducted by using a Keisokki CFT-11 detector at a speed of 700m/min. The results listed in Table 7-7 indicate that the TBS yarn has similar or slightly better performances than the conventional yarn. The operators thought that these two yarns have similar quality in yarn fault statistic.

Table 7-6 Records of cleaning process

Yarn type	TBS (TF=2.5)	Conventional (TF=3.6)
Y	141	114
N	55.7	52.3
S	59.6	44.8
L	7.6	16.7
LL	18.2	0.7
T	0	0

Note: Y: No. of cleaning per 100 km length.

N: Short slub, length < 1cm.

S: Short slub, length from 1 to 8cm.

L: long slub, length > 8cm.

LL: Long slub, length >50cm.

T: Thin place.

Table 7-7 Records of classimat test

	TBS (TF=2.5)	Conventional (TF=3.6)
A1	239.2	215.5
A2	39.3	47.2
A3	0	3.5
A4	0	0
B1	3.3	6.5
B2	9.8	6.1
B3	0	3
B4	0	0.4
C1	0	0
C2	0	0
C3	0	0
C4	0	0
D1	0	0
D2	0	0

Table 7-7 Records of classimat test (continued)

D3	0	0
D4	0	0
E1	0	0
E2	0	0
E3	0	0
E4	0	0
F1	0	2.6
F2	0	1.3
G1	0	2.6
G2	0	0.4
H1	0	0.4
H2	0	0
I1	0	0
I2	0	0
J1	0	0
J2	0	0
K1	0	0.4
K2	0	0
L1	0	0
L2	0	0
M1	0	0
M2	0	0
N1	0	0
N2	0	0
O1	0	0
O2	0	0

7.3.2 Fabric test results and analysis

7.3.2.1 Properties of the greige fabrics

- *Fabric spirality*

The spirality angles of greige fabrics were measured in our lab after three 5-A washing and dry cycles according to the method mentioned in 7.2.3.2. Results are plotted as a function of the snarling turns of the yarns and the spirality angles of the resultant fabrics in Figure 7-11 and Figure 7-12. Every point is the mean value of five samples.

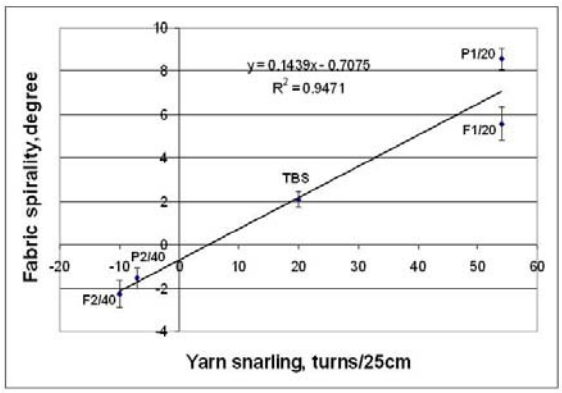

Figure 7-11 The relationship between wet snarling of the yarn and the spirality angle of the resultant greige fabrics knitted in clockwise direction

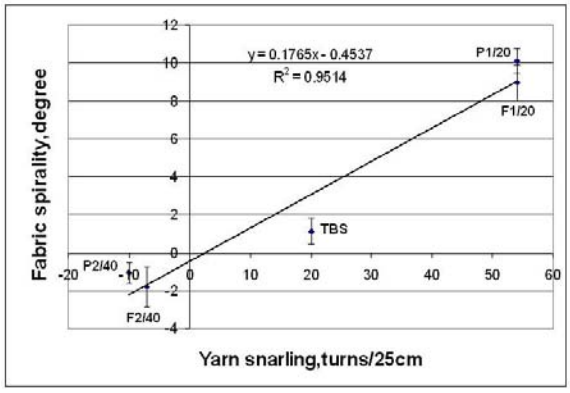

Figure 7-12 The relationship between wet snarling of the yarn and the spirality angle of the resultant greige fabrics knitted in counter-clockwise direction

Fabrics in Figure 7-11 were knitted by using a knitting machine rotating in the clockwise direction. There is a linear relationship between yarn snarling and fabric spirality. $R^2 = 0.94$ represents that the equation is fitted very well. For the case of the fabrics knitted in counter-clockwise direction shown in Figure 7-12, the equation was also fitted very well.

These two diagrams demonstrate that fabric spirality angle is increased linearly with the increase of yarn wet snarling, i.e., the higher the yarn wet snarling, the greater the fabric

spirality. For the TBS fabrics, both fabrics have minor spirality. They are less than 3 degrees, reaching the target of this study. The diagrams also show that the two fabrics have different spirality angles even though they were knitted from the same yarn. The difference of the spirality of the two TBS fabrics is around 0.5 degree. In this case, the counter-clockwise fabric has slightly greater spirality angle than the clockwise fabric due to the influences of multi-feeder machine used. This is in agreement with the statement that the wale will be inclined to the right, giving a Z-skew in machines that rotate counterclockwise (Araujo and Smith 1989). The two plied yarn fabrics also have minor spirality angles which incline to the opposite direction. The spirality angles of the other two control fabrics are greater than 6 degrees, far away from the required 3 degrees.

- *Fabric dimensional stability*

Table 7-8 shows the fabric dimensional properties of the greige fabrics. It is obvious that for the greige fabrics knitted in the clockwise direction, the fabric dimension changes after 3 cycles of washing in the horizontal direction are 5 to 6 times greater than their vertical changes for all yarn types. That means after washing and drying treatments the fabrics became relatively narrower and longer, partially balancing the spirality caused by the relaxation of yarn residual torque. Whereas for the fabrics knitted in the counter-clockwise, the shrinkage rates in horizontal and vertical directions are closer to each other. That means the counter-clockwise fabrics have better shape stability. In addition, the greige TBS fabrics have similar dimensional performance with their control fabrics in both directions.

Table 7-8 Dimensional stability of greige fabrics

Fabric code	Horizontal shrinkage % [CV%]	Vertical shrinkage % [CV%]	Diagonal Change % skewness [CV%] + = LH skew - = RH skew
Clockwise			
TBS	19.8[3.3]	3.1[49.0]	-2.5 [106.0]
P 1/20	18.9[5.8]	4.3[23.5]	4.2 [42.3]
P 2/40	20.0[4.2]	3.0[27.9]	-5.2 [40.8]
F 1/20	19.5[5.0]	4.4[26.1]	-0.1[713.0]
F 2/40	21.0[-4.1]	2.9[38.0]	-5.1[30.7]
Counter-clockwise			
TBS	16.6[5.2]	10.0[12.4]	5.0[33.7]
P 1/20	15.2[11.0]	10.8[8.6]	11.6[10.7]
P 2/40	16.1[5.5]	9.1[12.0]	1.3[131.9]
F 1/20	16.2[4.4]	11.7[13.5]	9.2[20.1]
F 2/40	16.3[3.8]	9.3[13.3]	-6.6[263.3]

- *Other properties of greige fabrics*

Mean values of fabric weight and bursting strength shown in Table 7-9 reveal that the TBS fabrics have significant higher bursting strength if compared with their control fabrics made from plied yarns, and slightly higher than those of the fabrics made from singles yarns. The TBS fabric weights are similar to or slightly higher than controls.

Table 7-9 Other properties of the greige fabrics

Fabric code	Mean Fabric Weight g/m^2 [CV%]	Mean Bursting Strength lb/sq. inch [CV%]
Clockwise		
TBS	176[0.7]	108[7.7]
P 1/20	172[0.6]	102[12.8]
P 2/40	166[1.47]	70[14.3]
F 1/20	173[0.3]	101[8.9]
F 2/40	170[1.2]	76[11.8]
Counter-clockwise		
TBS	163[1.4]	97[11.3]
P 1/20	157[1.0]	90[7.9]
P 2/40	154[1.4]	85[5.9]
F 1/20	164[1.8]	98[16.8]
F 2/40	155[2.8]	82[16.5]

(a) TBS fabric (b) P1/20 fabric (c) P2/40 fabric

Figure 7-13 Appearance of greige fabrics (counter-clockwise)

Figure 7-13 illustrates the appearances of these greige fabrics. The greige TBS fabrics and P2/40 fabric have little spirality. Whereas the wales of the P1/20 fabric incline to the right, the angle is far away from the requirement. The TBS fabric has clear surface, vertical wale lines and symmetrical loops; the plied yarn fabric has similar appearance. The singles yarn control fabric has asymmetrical loops and wales incline to the right.

7.3.2.2 Properties of the dyed fabrics

- *Fabric spirality*

Similar to the greige fabrics, ten piece-dyed fabrics have linear relationships with their yarn wet snarling respectively. Each point is the mean value of five samples. The equations are $Y = 0.1472X - 1.1677$ for the clockwise case and $Y = 0.1483X - 1.5345$ for the counter-clockwise case (Figures 7-14 and 7-15). Both equations were fitted quite well. The spirality angles of these two TBS fabrics are less than 3 degrees, meeting the requirement of this investigation. The two diagrams also reveal that there is no significant difference between the machines rotating in two directions. Araujo and Smith (1989), as well as Primentas (2003) investigated the difference and gave the same conclusions. Similar with the greige fabrics, the dyed plied yarn fabrics also possess smaller inclination angles if compared with the singles yarn fabrics.

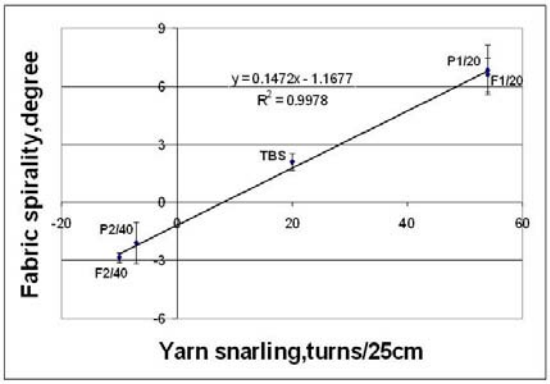

Figure 7-14 The relationship between wet snarling of the yarn and the spirality angle of the resultant dyed fabrics knitted in clockwise direction

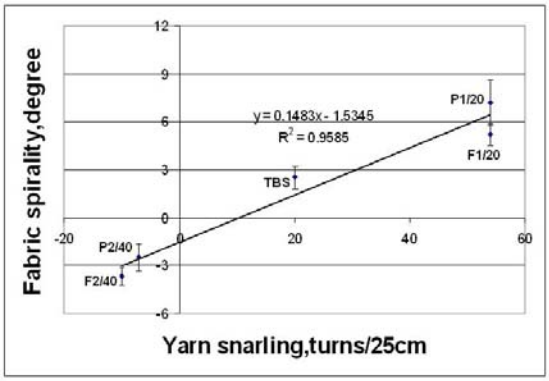

Figure 7-15 The relationship between wet snarling of the yarn and the spirality angle of the resultant dyed fabrics knitted in counter-clockwise direction

- *Fabric dimensional stability*

Table 7-10 shows the fabric dimensional properties of the piece dyed fabrics. All the fabrics have similar tendency. The washed fabrics are narrower and longer than their original fabrics. Since the change of fabric dimensions may affect fabric loop shape, this leads to the change of fabric spirality (Tao et al. 1997). Generally speaking, the piece dyed TBS fabrics have similar dimensional performance with their control fabrics.

Table 7-10 Dimensional stability of piece dyed fabrics

Fabric code	Horizontal change % [CV%]	Vertical change % [CV%]	Diagonal Change % skewness [CV%] + = LH skew - = RH skew
Clockwise			
TBS	3.6[26.6]	-4.2[18.4]	0.5[329.6]
P 1/20	2.3[54.1]	-4.3[26.4]	3.4[47.5]
P 2/40	3.5[27.8]	-4.0[57.3]	1.6[171.9]
F 1/20	3.9[29.7]	-4.9[24.4]	0.9[292.5]
F 2/40	2.8[34.1]	-4.2[20.7]	0.7[410.5]
Counter-clockwise			
TBS	2.2[46.8]	-6.1[11.5]	1.1[307.2]
P 1/20	1.3[65.9]	-7.4[11.4]	2.9[153.3]
P 2/40	1.6[71.6]	-6.4[20.3]	-1.4[-112.4]
F 1/20	0.6[123.1]	-6.9[12.9]	-1.5[-315.3]
F 2/40	0.7[131.6]	-5.2[11.6]	-0.2[-856.7]

Table 7-11 Other properties of piece dyed fabrics

Fabric code	Mean Fabric Weight g/m^2[CV%]	Mean Bursting Strength lb/sq. inch[CV%]
Clockwise		
TBS	212[0.3]	70[16.8]
P 1/20	201[1.4]	84[11.4]
P 2/40	203[0.8]	43[54.3]
F 1/20	194[0.8]	85[14.4]
F 2/40	204[0.7]	64[10.2]
Counter-clockwise		
TBS	200[0.5]	77[8.7]
P 1/20	194[0.3]	83[10.1]
P 2/40	191[1.0]	64[26.1]
F 1/20	194[0.3]	86[21.1]
F 2/40	199[0.5]	65[22.4]

- *Other properties of dyed fabric*

The results shown in Table 7-11 reveal that the TBS fabrics have bigger fabric weight if compared with its control fabrics. For bursting strength, the TBS fabrics are stronger than their plied yarn control fabrics, but weaker than singles yarn control fabrics.

Figure 7-16 illustrates the appearances of three piece dyed fabrics. It is obvious that the piece dyed TBS fabrics have less spirality angle and clearer appearance if compared with the other two fabrics. Its wales are vertical, and loops are clear, whereas the P1/20 fabric possesses obvious fabric spirality. For the P2/40 fabric, its appearance is the blurriest among these fabrics even it has little spirality.

(a) TBS fabric (b) P1/20 fabric (c) P2/40 fabric

Figure 7-16 Appearance of some dyed fabrics (counter-clockwise)

7.3.2.3 Properties of the yarn dyed stripe fabrics

- *Fabric spirality*

Five yarn dyed stripe fabrics were produced by using the dyed yarns and the machine running in the counter-clockwise direction (Figure 7-17). Each point is the mean value of five samples. The fitted equation is $Y = 0.2545X - 2.7362$. $R^2 = 0.9151$ means that the equation was fitted very well. The results also show that the TBS stripe fabric has a much reduced spirality angle (less than 2 degrees). Whereas the spirality angles of other four fabrics are greater than the angle of the TBS fabric.

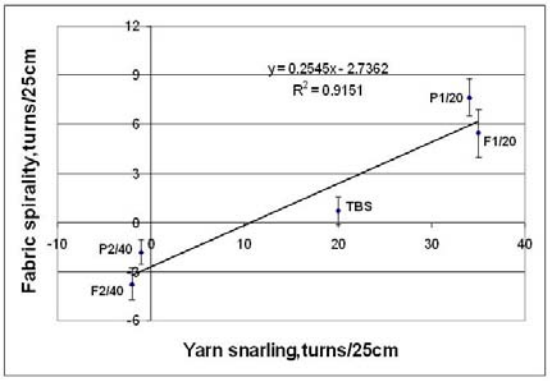

Figure 7-17 The relationship between wet snarling of the yarn and the spirality angle and resultant stripe fabrics knitted in counter-clockwise

- *Fabric dimensional stability*

Table 7-12 shows the fabric dimensional properties of the yarn dyed stripe fabrics. The TBS fabric has similar dimensional performance with the other fabrics. The table reveals that the fabric dimension changes in horizontal directions are 3 to 4 times greater than their vertical changes. That means after washing and drying treatments the fabrics became relatively narrower and longer, partially balancing the spirality caused by the relaxation of yarn residual torque.

Table 7-12 Dimensional stability of stripe fabrics

Fabric code	Horizontal change % [CV%]	Vertical change % [CV%]	Diagonal Change % skewness [CV%]
Counter-clockwise			
TBS	14.9[8.1]	4.5[19.1]	3.0[56.6]
P 1/20	15.4[8.5]	5.1[20.4]	10.6[13.8]
P 2/40	16.8[3.2]	3.8[29.8]	0.4[466.2]
F 1/20	16.5[5.9]	4.9[15.2]	9.5[13.1]
F 2/40	17.2[6.1]	4.0[28.1]	-1.3[-148.7]

- *Other properties of stripe fabrics*

Fabric weight and bursting strength of these five fabrics were measured and tested in our lab. Table 7-13 reveals that the TBS fabric has the fabric weight similar to other fabrics. For the bursting strength, the TBS fabric is stronger than fabrics made from two plied yarns, but weaker than those made from two singles yarns.

Table 7- 13 Other properties of stripe fabrics

Yarn code	Mean Fabric Weight g/m^2[CV%]	Mean Bursting Strength lb/sq. inch[CV%]
TBS	166[1.5]	67[10.0]
P 1/20	162[2.9]	74[15.4]
P 2/40	162[2.2]	60[10.2]
F 1/20	166[0.9]	84[10.6]
F 2/40	161[0.9]	56[9.8]

Generally, combining with fabric spirality, it is clear that the yarn dyed stripe TBS fabric has good performances in spirality and other fabric properties. Figure 7-18 illustrates the appearances of the TBS stripe fabrics. The fabric has symmetrical loops and clear surface.

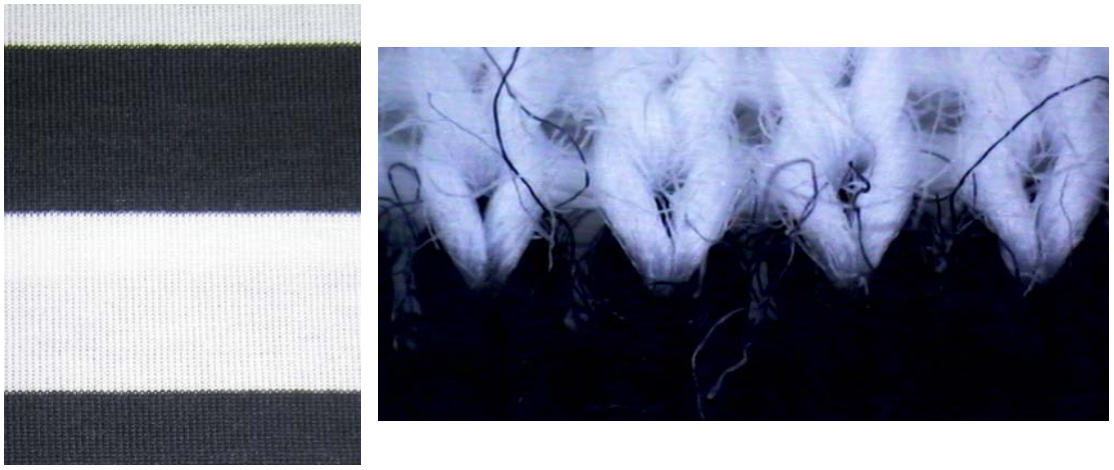

(a) Fabric Appearance (b) Loop Shape

Figure 7-18 Appearance of the TBS stripe fabric

d) Feedbacks from the factory

Feedbacks were obtained from the factory. The operators and managers generally gave positive feedbacks and satisfied the knitting operation and productivity of the TBS fabrics. The only problem encountered was during the knitting of the yarn dyed fabric. Its value of number of stops was bigger than their requirement. Therefore, solving this problem is our future target. The operators and managers also evaluated and compared the TBS fabrics with other fabrics. They thought the problem of spirality of plain knitted fabric can be solved by using the newly developed TBS yarns. They tested the fabrics and the test results are shown in Table 7-12; it should be noted that the factory uses inclination percentage to represent spirality. After knitting, dyeing and mechanical finishing, the TBS fabrics and other two fabrics made from plied yarns have minor wale inclinations in both running directions. The inclination percentages range from 1.00% to 4.00% for the clockwise direction, and range from 1.33% to 5.00% for the counter-clockwise direction. Whereas, the fabrics made from the conventional singles ring spun yarns, all of them possess greater spirality due to the greater residual torque stored in the yarns. In addition, the TBS fabrics and other fabrics have similar physical and mechanical properties. Table 7-14 also shows that the TBS fabrics have the pilling resistance performances and appearances similar to the plied yarn fabrics after 20 cycles of washing.

Table 7-14 Properties measured by a factory (Part I, greige and piece dyed fabrics)

Yarn code	Inclination (greige) %	Inclination (dyed tubular) %	Fabric weight (greige) g	Inclination (finished) %	Fabric weight (finished) g	Fabric bursting strength (finished) psi	After 20 washes	
							Pilling	Hairiness
Clockwise								
TBS	5.67	3.33	164	4.00	187	111	2-3	3-4
P 1/20	11.67	10.00	166	10.67	178	122	2	3-4
P 2/40	5.00	3.33	165	1.67	176	110	2	3-4
F 1/20	11.67	8.33	164	13.33	175	130	1-2	3
F 2/40	1.67	3.33	165	1.00	182	110	2-3	4
Counter-clockwise								
TBS	3.33	7.33	165	3.33	178	118	2-3	3-4
P 1/20	6.67	10.00	163	16.67	176	115	2	3-4
P 2/40	3.33	3.33	162	5.00	172	110	2-3	3-4
F 1/20	6.67	11.67	162	9.33	172	130	1-2	3
F 2/40	5.00	1.67	162	1.33	176	109	2-3	3-4

For the yarn dyed stripe fabrics, the TBS fabric has a spirality inclination percentage similar with the two plied control yarns. Other properties of the TBS fabric are also similar with those of the two plied yarns (Table 7-15). That is to say, the TBS yarn can replace plied yarns for producing the yarn dyed fabrics.

Table 7-15 Properties measured by a factory (Part II, stripe yarn dyed fabrics)

Yarn code	Inclination (greige) %	Fabric weight (greige) g	Inclination (finished) %	Fabric weight (finished) g	Fabric bursting strength (finished) psi	After 20 washes	
						Pilling	Hairiness
TBS	3.33	160.00	1.67	176	100.00	2	4
P 1/20	9.00	160.00	10.00	175	95.00	2	4
P 2/40	3.33	161.00	1.67	174	90.00	3	4
F 1/20	8.33	160.00	6.67	175	115.00	2	4
F 2/40	5.00	161.00	1.67	179	95.00	3	4

If comparing our test results with the feedbacks from the factory, we can find that there is a difference of bursting strength between the results measured by PolyU and the factory. Through communicating with the operators and technicians, the difference may be due to the different range of the tester used. Despite of this difference, both of them confirm that the TBS can be used for solving the problem of fabric spirality, other properties are similar with or better than their control fabrics made from singles and pied yarns.

7.4 Summary and Conclusions

Before knitting process, some properties of the TBS yarn were tested and measured. Two other conventional ring spun yarns with different twist factors were also included for comparison. The results reveal that the TBS yarn has a lower wet snarling and a relatively high strength if compared with the other two conventional yarns. The results also imply that the TBS yarn has very good evenness CVm percentage. Effect of

package dyeing process on yarn properties was evaluated in this study. The results show that the wet snarling of both the TBS and control yarns are decreased after dyeing process; and the reduction of the TBS yarn was smaller than that of the conventional yarn. At the same time, yarn strengths are slightly increased for both TBS and control yarns because the wetting treatment increases the entanglement, binding and friction between fibers within the yarn. For yarn hairiness, the TBS yarn is more hairy than the control yarn for both dyed and greige yarns. This can be explained by the lower twist used. Winding and splicing processes were evaluated. The results indicate that winding conditions have influences on yarn properties such as wet snarling, tenacity, and evenness CVm% as well as hairiness S3 value. Yarn torque is sensitive to winding tension; higher winding tension leads to higher wet snarling. Winding geometry has more influences on yarn evenness CVm percentage. The friction along the winding path may mainly affect the yarn hairiness S3 value. In addition, the winding conditions have no significant influences on yarn tenacity. For winding the TBS yarn, it is recommended to use a winder with lower, stable speed and tension, as well as optimal geometry and smooth yarn path. The statistic of cleaning and classimat test indicates that the TBS yarn has a quality similar with the conventional ring spun yarn in yarn fault statistics.

Single jersey knitted fabrics were produced for evaluating the knittability and fabric properties. The production was conducted by using multi-feeder knitting machines under industrial conductions. The greige TBS knitted fabric has a lower spirality after 3 washing and dry cycles if compared with the fabrics knitted by using the conventional singles ring spun yarns. Other properties such as fabric dimensional stability, fabric weight and bursting strength etc were better than or similar with those of the control

fabrics. The results of the piece dyed fabrics has similar tendency: the piece dyed TBS fabric has a little spirality after 3 washing and dry cycles; other properties are better than or similar with those of the piece dyed fabrics made from singles and plied conventional yarns. In addition, some fabrics were produced by using the package dyed yarns. It was also confirmed that spirality of the knitted fabric could be dramatically reduced by using the package dyed TBS yarn. Other properties are similar with those of the control fabrics.

The knitting trials were conducted in a knitting factory. After testing and measuring fabric properties, the factory confirmed that the TBS yarn could help improve fabric spirality. All fabric properties can meet their commercial requirements. The operators and managers also satisfied the knitting process and productivity of the greige and piece dyed TBS fabrics. A relatively higher yarn break rate was the only problem encountered during the knitting of yarn dyed fabric. To solve it is one of the targets of our further work.

CHAPTER 8

CONCLUSIONS AND RECOMMENDATIONS FOR FUTURE WORK

8.1 Conclusions

8.1.1 Yarn modification process

Previous research has demonstrated that it is possible to obtain a yarn with lower residual torque and relatively high strength simultaneously by modifying its structure. The mechanisms of modification were identified as internal fiber migration and entanglement. The fiber migration was mainly introduced in the spinning triangle during the formation of the yarn; the shape of the spinning triangle was modified by inserting an extremely high twist. The extremely high twist not only increased the tension variation, leading to an increase of fiber migration, but also locked the migrated fibers and set the shape of the migrated fibers by applying a greater tensile strain. Then a reverse twist was applied to remove the extremely high twist introduced in the spinning triangle. Because the fibers were not at the same twist level due to fiber migration, some twists would be remained in the yarn after the de-twisting process. These remained twists would result in a reverse torque to balance the torque generated from the positive twist.

The modification was achieved by a false-twister. It was installed between the front rollers and yarn guide on a conventional ring spinning frame. Thus the yarn path was

divided into several parts. The false-twister not only provided extremely high twist to the spinning triangle in the part above it, but also gave the reverse twist to the formed yarn in the lower part for de-twisting the extra-twists introduced in the spinning triangle.

8.1.2 Yarn structure

The structure of the TBS yarn was examined. Most fibers followed helical paths with lower twist angles if compared with conventional yarns. Some wrapping fibers were found on the surface of the TBS yarn. This may be the result of the de-twisting process. These fibers tightly wound on the yarn body that possessed a ring yarn appearance in an opposite direction to the yarn twist. The wrapping fibers contributed not only the reduction of the yarn torque, but also the reinforcement of yarn strength.

The TBS yarn possessed radial fiber distribution patterns different from conventional ring yarns. The TBS yarn had a relatively high packing density than the conventional ring yarns with the same or slightly higher twist. Its central packing density was the highest among all annular areas, meaning it having a “harder” or “more compact” core, whereas the core of the conventional yarn was slightly “softer” or “looser” than its adjacent annular region. This is a major feature of the cross-sectional structure of the TBS yarn, and it can be explained by using the mechanism of the wrapping-ribbon-form twist and the mechanism of fiber migration due to tension variation.

The fiber path within a TBS yarn was examined by using the tracer fiber technique. The TBS yarns did not migrate uniformly inside the yarn. The FFT analysis implied that the envelop of the TBS yarn can not be expressed by using one sinusoid function; it may be

a combination of many functions. The 3-D analysis revealed that a fiber was formed by many segments rotating in different directions; the projections of their torques to the yarn axis may partially counteract each other, leading to the reduction of yarn residual torque.

8.1.3 Yarn modeling

Based on the results of the yarn structural investigation and assumptions that the fibers were elastic and no inter-fiber friction and viscosity, a modified cylindrical helix structural model was introduced. An energy method and the discrete-fiber-modeling principle were adopted. A series of sinusoidal functions was used for simulating the fiber migration, and a changeable radial packing density was adopted for representing the fiber distribution in the yarn cross-section

The originality of this model is the introduction of fibre migration by using a series of the sinusoidal functions. The analysis of the yarn geometrical expression showed that the fiber path can be represented by using a series of sinusoidal functions, and different combinations of the coefficients expressed various migration patterns. The theoretical results demonstrated that it is possible to further reduce yarn torque by introducing an appropriate fiber migration pattern.

8.1.4 Optimization of spinning parameters

Several optimization experiments were conducted before the production of the TBS yarns by using the response surface methodology. A two-step scheme was adopted, i.e., fractional factorial experiment and response surface experiment. In the first stage, five

factors were chosen as the candidates. They were the yarn twist factor, speed ratio, break draft as well as the installation position of the modification device X and Y. The experiment identified that the twist factor and speed ratio were the two most important factors. Others were the secondary factors or can be neglected. In the second stage, response surface experiments for 16Ne, 20Ne and 30Ne yarns were carried out, and optimal conditions were determined. A comparison was carried out between the optimizations of the yarns with different yarns counts (16Ne, 20Ne and 30Ne). These three yarns had different stationary points and natures. Thus an optimization was necessary before the production of a yarn in a new count or with a new material. The effect of spinning machines on the properties of the TBS yarns was evaluated by conducting three optimizations of the 20Ne yarn on Spin tester, Zinser 319SL and Toyota RY spinning machines. The differences of the geometries of these machines affect the installation position of the device and the yarn spinnability, leading to the differences of stationary point, nature as well as yarn properties.

8.1.5 Properties of yarns and resultant fabrics

TBS yarns and plain knitted fabrics were produced for evaluating the effect of the modified spinning system on the performance of the yarn and resultant fabrics. The results showed that the TBS yarn had a very lower residual torque and relatively high strength simultaneously. Others such as hairiness and evenness were similar with or not worse than their corresponding conventional ring spun yarns. Plain knitted fabrics were produced by using greige yarns and package dyed yarns on two commercial circular knitting machines in a factory. The measurements of the greige, piece dyed and yarn dyed stripe fabrics showed that the fabric spirality could be dramatically reduced by

using the TBS yarns. Compared with their control fabrics, the TBS fabrics had better or similar properties in dimensional stability, fabric weight, bursting strength and pilling resistance etc. These conclusions were in agreement with the feedback from a knitting factory.

8.2 Limitations of the Study and Recommendations for Future Work

In this study, although we successfully developed a novel ring spun yarn with low residual torque and relatively high strength, as well as other acceptable properties, some limitations were found out. For instance, since relatively higher strength of the TBS yarns mainly results from the greater fiber migration and entanglement, it may encounter some problems when producing a finer yarn. Another limitation is that the fiber migration cannot be controlled accurately, thus after de-twisting process, the final yarn may possess an unstable twist expressing a structure of some parts slightly looser or some parts slightly tighter. This may lead to an increase of twist and strength variation.

At this stage, the investigation mainly focuses on the modification of cotton fibers. Tencel and Rayon fibers were used for verifications of spinning mechanism and yarn structure. In the future, a much wider selection of fibers might be exploited in order to evaluate how these fibers would behave under the modification. Among these fibers, Polyester blend fibers may be adopted. Some other treatments can also be combined with the modification system. For example the modification system can be used with the core spun, sirospun and solospun as well as other techniques.

The investigation of yarn structure was conducted based on limited samples. In the future, more samples will be examined for obtaining more yarn structural information, increasing the accuracy of the re-construction of the yarn structure. In the yarn modeling, since the model was established based on some assumptions such as yarns are elastic and no inter-fiber friction and viscosity, etc, these limited the accuracy of the computation. In addition, the neglects of the loss of energy due to friction, etc affect the conversation of energy, leading to the reduction of the accuracy of the computation. In the future, some improvements will be carried out for increasing the simulation accuracy of the model. Since yarn residual torque is very important, the relationship between yarn torque and residual torque will also be studied.

REFERENCES

Araujo M. D. D. and Smith G. W. (1989). "Spirality of knitted fabrics, Part I: The nature of spirality." Textile Research Journal 59, 247-256.

Araujo M.D.D. and Smith G.W. (1989)."Spirality of knitted fabrics, Part II: The effect of yarn spinning technology on spirality." Textile Research Journal 59,350-356.

Backer S. and Thwaites J.J. (1976). "Transient Phenomena during false-twist texturing." Journal of the Textile Institute 67, 218-221.

Balakrishna I.K. and Phatarfod R.M. (1965). "Some aspects of yarn structure." Journal of the Textile Institute 56, 225-247.

Barella A. and Manich A.M. (1988). "Influence of the spinning process, yarn linear density, and fiber properties on the hairiness of ring-spun and rotor-spun cotton yarns." Journal of the Textile Institute 79, 189-197.

Beck J.V. and Arnold K.J. (1977). Parameter estimation in engineering and science, John Wiley & Sons Inc.

Bennett J. M. and Postle R. (1979). "A study of yarn torque and its dependence on the distribution on fiber tensile stress in the yarn, Part I: Experimental." Journal of the Textile Institute 70, 133-150.

Bennett J. M. and Postle R. (1979). "A study of yarn torque and its dependence on the distribution on fiber tensile stress in the yarn, Part I: Theoretical analysis." Journal of Textile Institute 70, 121-151.

Bennett J. M. and Postle R. (1981). "Fibre torsional hysteretic and its contribution to

yarn torque." Journal of the Textile Institute 72, 231-236.

Box G. E. P. and Wilson K. B. (1951). "On the experimental attainment of optimum conditions." Journal of the Royal Statistical Society Series B 13, 1-38.

Carnaby G.A. and Grosberg P. (1976). "The tensile behavior of staple-fiber yarns at small extensions." Journal of the Textile Institute 67, 299-308.

Carnaby G.A. and Postle R. (1991). "Discrete fibers versus continuum models in the mechanics of staple yarns." Journal of the Applied Polymer Science: Applied Polymer Symposium 47, 341-354.

Ceken F. "The spirality of the single-jersey fabrics and its effect on the garments." http://www.ft.vslib.cz/indoczech-conference/conference_proceedings/fulltext/Turkey_02.pdf.

Chen Q. H., Au K. F., Yeun C. W. M. and Yeung K. W. (2002). "Dimensional stability of plain wool knits." Textile Asia (8): 51-57.

Chen Q. H., Au K. F., Yeun C. W. M. and Yeung K. W. (2002). "Relaxation shrinkage characteristics of steamed-ironed plain knitted wool fabrics." Textile Research Journal 72, 463-467.

Cheng K.P.S. and Li C. H. L. (2002). "JetRing spinning and its influence on yarn hairiness." Textile Research Journal 72, 1079-1087.

Cheng K.P.S. and Yu C. (2003). "A study of compact spun yarns." Textile Research Journal 73, 345-349.

Choi K.F. "Private communication": Institute of Textile and Clothing, the Hong Kong Polytechnic University. tckfchoi@inet.polyu.edu.hk.

Choi K.F., Carnaby G.A., et al. (1998). "A theoretical torsional model of singles yarn." Journal of Hong Kong Institution of Textiles and Apparel 2, 1-12.

Choi K.F., Lam Y.L., Wong Y.W. and Luo Z.X. (2003). "Measuring the distribution of yarn density by using the CT principle." Textile and clothing 15(3): 72-75.

Choi K.F. and Lo T.Y. (2003). "An energy model of plain knitted fabrics." Textile Research Journal 73, 739-748.

CSIRO textile and fiber technology. Corner Princes Hwy and Henry Street, Belmont, Geelong, Victoria, Australia. http://www.tft.csiro.au/achievements/solospun.html.

CSIRO textile and fiber technology. Corner Princes Hwy and Henry Street, Belmont, Geelong, Victoria, Australia. http://www.tft.csiro.au/achievements/sirospun.html.

Demir A. (1996). "Torque-free false-twist textured yarns and de-torque mechanism." Chemical fibers international 46, 361-363.

Demiroz A. and Dias T.A. (2000). "A study of the graphical representation of plain-knitted structure, Part I: Stitch model for graphical representation of plain-knitted structure." Journal of the Textile Institute 91, 463-480.

Denton M.J. (1975). "Twisting-rate variation in the false-twist threadline, Part I: Background and the effect of a step change in the twisting rate." Journal of the Textile Institute 66, 282-288.

Denton M.J. (1975). "Twisting-rate variation in the false-twist threadline, Part II: The effect of a 'rectangle-pulse' transient change and a sinusoidal variation in the twisting rate." Journal of the Textile Institute 66, 289-296.

Dhingra R.C. and Postle R.(1974). "The measurement of torque in continuous-filament yarns, Part I: Experimental techniques." Journal of the Textile Institute 65, 126-132.

Dhingra R. C. and Postle R. (1975). "Torsional and recovery properties of worsted yarns." Journal of Textile Institute 66, 407-412.

Dias T. and Lanarolle G. (2002). "Stitch length variation in circular knitting machines due to yarn winding tension variation in the storage yarn feed wheel." Textile Research Journal 72, 997-1001.

Dogu I. (1972). "The distribution of transverse pressure in a twisted yarn allowing for the fiber migration and variation of fiber packing density." Textile Research Journal 42, 726.

Doyle P.J. (1952). "Some fundamental properties of hosiery yarns and their relation to the mechanical characteristics of knitted fabrics." Journal of the Textile Institute 43, 19-35.

Doyle P.J. (1953). "Fundamental aspects of the desifn of knitted fabrics." Journal of the Textile Institute 44, 561-578.

Ghosh T. K., Batra S. K. and Murthy A. S. (2001). "Dynamic analysis of yarn unwinding from cylindrical packages, Part I: Parametric studies of the two-region problem." Textile research Journal 71, 771-778.

Gowda R.V.M., Sivakumar M. and Kannan M.S.S. (2004). "Influence of process variables on characteristics of modal siro-spun yarns using Box-Behnken response surface design." Indian Journal of Fiber and Textile Research 29, 412-418.

Greenwood K. (1975). "The present situation and future prospects of the false-twist process." Journal of the Textile Institute 66, 420-425.

Greenwood K.(1977)."An apparent friction paradox." J.Phys.D:bAppl.Phys.10(5), 53-58.

Grishanov S.A., Lomov S.V. and Harwood R.J. (1997). "The mechanical simulation of the geometry of a two-component yarn, Part II: Fiber distribution in the yarn cross section." Journal of the Textile Institute 88, 352-372.

Heap S.A., Greenwood P.F., Leah R.D., Eaton J.T., Stevens J.C. and Keher P.(1983). "Prediction of finished weight and shrinkage of cotton knits- The starfish project, Part I:Introduction and general overview."Textile research journal 53, 109-113.

Heap S.A., Greenwood P.F., Leah R.D., Eaton J.T., Stevens J.C. and Keher P.(1985). "Prediction of finished relaxed dimensions of cotton knits-The starfish project, Part II:Shrinkage and the reference state."Textile Research Journal 55, 211-222.

Hearle J.W.S. and Bose O. N. (1965). "Migration of fibers in yarns, Part II:A geometrical explanation of migration." Textile Research Journal 55, 693-699.

Hearle J.W.S. and Bose O.N. (1966). "The form of yarn twisting, Part I: Ideal cylindrical and ribbon-twisted forms." Journal of the Textile Institute 56, 294-307.

Hearle J.W.S., Grosberg P. and Backer S. (1969). Structural mechanics of fibers, yarns, and fabrics, John Wiley & Son, Inc.

Hearle J.W.S., Gupta B. S. and Goswami B.C. (1965). "Migration of fibers in yarns, Part V: The combination of mechanisms of migration." Textile Research Journal 35, 972-978.

Hearle J.W.S., Gupta B. S. and Merchant V.B. (1965). "Migration of fibers in yarns, Part I: Characterization and idealization of migration behavior." Textile Research Journal 35, 329-334.

Hearle J.W.S. and Gupta B.S. (1965). "Migration of fibers in yarns, Part III: A study of migration in staple fiber rayon yarn." Textile Research Journal 35, 788-795.

Hearle J.W.S. and Merchant V.B. (1962). "Interchange of position among the components of a seven-ply structure: mechanism of migration." Journal of the Textile Institute 53, 537-552.

Hearle J.W.S., Thwaite J.J. and Amirbayat J. (1980). Mechanics of flexible fiber

assemblies. Sinjhoff and Noordhof .

Hickie T.S. and Chaikin M.(1960)."The configuration and mechanical state of single fibers in woollen and worsted yarns." Journal of the Textile Institute 51, 1120-1129.

Hickie T.S. and Chaikin M. (1974). "Some aspects of worsted-yarn structure, Part III: The fiber-packing density in the cross-section of the worsted yarns." Journal of the Textile Institute 65, 433-437.

Hickie T.S. and Chaikin M. (1974). "Some aspects of worsted-yarn structure, Part IV: The application of fourier analysis to the study of single-fiber configurations in a series of worsted yarns." Journal of the Textile Institute 65, 537-545.

Hong Kong Cotton Spinners Association (2000). Textile Hoodbook.

Hua T. "Prravite communication": Institute of Textile and Clothing, the Hong Kong Polytechnic University. trthua@inet.polyu.edu.hk.

Huh Y., Kim Y.R. and Oxenham W.(2002). "Analyzing structural and physical properties of ring, rotor, and friction spun yarns." Textile Research Journal 72, 156-163.

Ishtiaque S.M., Rengasamy R.S. and Ghosh A. (2004). "Optimization of ring frame process parameters for better yarn quality and production." Indian Journal of Fiber and Textile Research 29, 190-195.

Jasper W.J., Gunay M. and Suh M. W. (2005). "Measurement of eccentricity and twist in spun and plied yarns." Journal of the Textile Institute 96, 93-97.

Jiang X. Y. (2003). Tensile drawing behavior of rotor spun yarn. PhD Thesis. Institute of textile and clothing. The Hong Kong Polytechnic University.

Jiang X. Y., Hu J. L., Cheng K. P. S. and Postle R. (2004). "Determining the cross-

sectional packing density of rotor spun yarns." Textile Research Journal 74, 233-239.

Jiang X. Y., Hu J. L. and Postle R. (2002). "A new tensile model for rotor spun yarns." Textile Research Journal 72, 892-898.

Kilby W.F. (1964). "The mechanical properties of twisted continuous-filament yarns." Journal of the Textile Institute 55, 589-632.

Koch K.R. (1999). Parameter estimation and hypothesis testing in linear models (second edition), Spiringer-Verlag.

Krol B. and Przyby K. (2002). "Influence of yarn kind on the dynamic of the twisting-and-winding system of the ring spinning machine." AUTEX Research Journal 2, 144-152.

Lau Y. M., Tao X.M. and Dihingra R. C. (1995). "Spirality in single-jersey fabrics." Textile Asia (8): 95-102.

Lau Y.M. and Tao X. M. (1997). "Torque-balanced singles knitting yarns spun by unconventional systems, Part II: Cotton friction spun DREF III yarn." Textile Research Journal 67, 815-828.

Leaf G. A. V. (1960). "Models of the plain knitted loop." Journal of the Textile Institute 51, 49-58.

Leaf G. A. V. (1961). "The stresses in the plain knitted loop." Journal of the Textile Institute 52, 587-605.

Ma X. F., Ghosh T. K., and Batra S. K. (2001). "Dynamic analysis of yarn unwinding from cylindrical packages, Part II: The three-region analysis." Textile Research Journal 71, 855-861.

Marmarali A. B. (2003). "Dimensional and physical properties of cotton/spandex single

jersey fabrics." Textile Research Journal 73, 11-14.

Miao M.H. and Chen R. Z. (1993). "Yarn twisting dynamics." Textile Research Journal 63, 150-158.

Mitchell P., Naylor G. R. S. and Phillips D. G. (2006). "Torque in worsted yarns." Textile Research Journal 76, 169-180.

Montgomery D.C. (1996). Introduction to statistical quality control (third edition), John Wiley & Sons Inc.

Morton W. E. (1956). "The arrangement of fibers in singles yarns." Textile Research Journal 26, 325-331.

Morton W. E. and Yen K.C. (1952). "The arrangement of fibers in fibro yarns." Journal of the Textile Institute 43, 60-66.

Munden D. L. (1959). "The geometry and dimensional properties of plain -knit fabrics." Journal of the Textile Institute 50, 448-471.

Myers R.H. and Montgomery D.C. (2002). Response Surface Methodology (second edition), John Wiley & Sons Inc.

Neckar B., Ishtiaque S.M. and Svehlova L. (1988). "Rotor Yarn Structure by Cross-Sectional Microtomy." Textile Research Journal 58, 625-632.

Önder E., A. and Başer G. (1996). "Comprehensive stress and breakages analysis of staple fiber yarns, Part I: Stress analysis of a staple yarn based on a yarn geometer of conical helix fiber paths." Textile Research Journal 66, 562-575.

Palta D. and Kothari V.K. (2002). "Effect of process variables on the properties of air-jet textured yarns using response surface design." Indian Journal of Fiber and Textile Research 27, 224-229.

Pan N. (1992). "Development of a constitutive theory for short fiber yarns: Mechanics of staple yarn without slippage effect." Textile research Journal 62, 749-765.

Pan N. (1993). "Development of a constitutive theory for short fiber yarns, Part II: Mechanics of staple yarn with slippage effect." Textile research Journal 63, 504-514.

Peirce F.T. (1947). "Geometrical principles applicable to the design of functional fabrics." Textile Research Journal 17, 123-147.

Platt M. M. (1950). "Mechanics of elastic performance of textile materials, III: Some aspects of stress analysis of textile structure -- continuous-filament yarns." Textile Research Journal 30, 1-15.

Platt M. M., Klein W. G. and Hamburger W. J. (1958). "Mechanics of elastic performance of textile material, Part XIII: Torque development in yarn systems: singles yarn." Journal of the Textile Institute 49, 1-14.

Postle R. (1968). "Dimensional stability of plain-knitted fabrics." Journal of the Textile Institute 59, 65-77.

Postle R., Burton P. and Chaikin M. (1964). "The torque in twisted singles yarns." Journal of the Textile Institute 55, 448-461.

Postle R., Carnaby G. A. and Jong S.D. (1988). The mechanics of wool structures. Ellis Horwood Ltd.

Postle R. and Munden D. L. (1967). "Analysis of the dry relaxed knitted loop configuration." Journal of the Textile Institute 58, 329-365.

Price J. B. (1983). "Open-end spinning research-Influence of winding tension on yarn properties." Textile Topics 6(6).

Primentas A. (2003). "Spirality of weft-knitted fabrics: Part I-Descriptive approach to

the effect." Indian Journal of Fiber and Textile Research 28, 55-59.

Punj S. K., Mukhopadhyay A. and Chatterjee P. (2000). "Plain knitted properties." Textile Asia (1): 33-38.

Quaynor L., Nakajima M. and Takahashi M. (1999). "Dimensional changes in knitted silk and cotton fabrics with laundering." Textile Research Journal 69, 285-291.

Riding G. (1959). "An experimental study of the geometrical structure of single yarns." Journal of the Textile Institute 50, 425-442.

Riding G. (1964). "Filament migration in singles yarns." Journal of the Textile Institute 55, 9-17.

Schwarz E. R. (1951). "Certain aspects of yarn structure." Textile Research Journal 31, 125-136.

Shanahan W. J. and Postle R. (1970). "A theoretical analysis of the plain-knitted structure." Textile research journal 40, 656-665.

Shanahan W. J. and Postle R. (1974). "A theoretical analysis of the tensile properties of plain-knitted fabrics, Part II: The initial load-extension behavior for fabric extension parallel to the wales." Journal of textile Institute 65, 254-260.

Shinn W.E. (1955). "An energy approach to jersey fabric construction." Textile Research Journal 25, 270-277.

Shinohara T., Takayama J.A., Ohyama S. and Kobayashi A. (2003). "Analysis of textile fabric structure with the CT images." SICE annual conference in Fukui, August 4-6, Fukui University, Japan: 428-432.

Spencer D. J. (2001). Knitting technology (third edition). Woodhead Publishing Ltd.

Stalder H. (2000). "Rieter: Comforspin spinning process." Textile World (4): 32-35.

Stevens J. C. (1986). "The starfish project: an integrated approach to shrinkage control

in cotton knits, Part II: The influence of knitting and finishing variables on the relaxed (reference state) dimensions." knitting International (5): 80-83.

Subramaniam V. and Peer-Mohamed A. (1993). "Compressional behaviour of double-rove yarns." Journal of the Textile Institute 84, 214-220.

Sullivan R.R. (1942). "A theoretical approach to the problem of yarn strength." Journal of Applied Physics 13, 157.

Tandon S. K., Carnaby G. A., Kim S. J. and Choi F. K. F. (1995). "The torsional behavior of singles yarns, Part I: Theory." Journal of the Textile Institute 86, 185-199.

Tao J., Dhingra R. C., Chan C. K. and Abbas M. S. (1997). "Effects of yarn and fabric construction on spirality of cotton single jersey fabrics." Textile Research Journal 67, 57-68.

Tao X.M. (1996). "Mechanical properties of a migrating fiber." Textile Research Journal 66, 754-762.

Tao X.M. (2003). "Torque free singles yarns spun by ring, rotor and other unconventional systems." Seminar of Textile Institute, Hong Kong branch.

Tao X. M., Lo W. K. and Lau Y. M. (1997). "Torque-balanced singles knitting yarns spun by unconventional systems, Part I: Cotton rotor spun yarn." **Te**xtile Research Journal 67, 739-746.

Tao X. M. and Xu B. G. (2002). "Manufacturing method and apparatus for torque-free singles ring spun yarns." Chinese patent: CN02118588.3. 24/4.

Tao X. M., Xu B. G. and Wong S. K. (2004). "Method and apparatus for manufacturing a singles ring yarn." US patent application No.10/858,400 2/6.

Treloar L.R.G. (1965). "The stress-strain properties of multi-ply cords, Part I: Theory."

Journal of the Textile Institute 56, 477-488.

Treloar L.R.G. and Riding G. (1963). "Theory of the stress-strain properties of continuous-filament yarns." Journal of the Textile Institute 54,156-170.

Wada T., Hirai S., Hirano T. and Kawamura S.(1977). "Modeling of plain knitted fabrics for their deformation control." Proceeding of the 1977 IEEE international conference on Robotics and automation, Albuquerque,New Mexico 4,1960-1965.

Wang L. (2001). Intelligent optimization algorithms with applications, Tsinghua University Publication & Springer-Verlag.

Wang X.G., Miao M.H. and How Y.L.(1997)."Studies of JetRing Spinning, Part I: Reducing Yarn Hairiness with the JetRing." Textile Research Journal 67, 253-258.

Wang X. G. and Miao M. H. (1997). "Reducing Yarn Hairiness with an Air-Jet Attachment During Winding." Textile Research Journal 67, 481-485.

Wang Y. J., Shao X. and Qiu Y. P. (2004). "Mechanical analysis of the tensile behavior of low-twist staple fiber assembles." Proceedings of the textile institute 83rd world conference, Shanghai, China.

Wynne A. (1997). Textiles, Macmillian Education Ltd.

Xu B. G., Tao X. M., Wong S. K., Cheng K. P. S., Yip Y. K., Choi K. F., Wong K. K., Leung C. L., Hua T., Yang K. and Murrells C. M. (2004). "Nu-torque singles ring yarn and its production technology." Proceedings of the textile institute 83rd world conference, Shanghai, China.

APPENDICES

Appendix 1. Properties of the Yarns from the Preliminary Spinning Trial

Table of yarn mean tenacity and elongation

Yarn code	Mean Tenacity (cN/tex) [CV%]	Mean Elongation (%) [CV%]	Yarn code	Mean Tenacity (cN/tex) [CV%]	Mean Elongation (%) [CV%]
-	-	-	Modified, TF=2.13	15.00 [6.4]	5.01 [6.7]
-	-	-	Modified, TF=2.34	16.09 [6.3]	5.19 [6.9]
Conventional, TF=2.5	11.89 [10.7]	4.18 [12.3]	Modified, TF=2.53	16.24 [7.4]	5.33 [8.0]
-	-	-	Modified, TF=2.70	16.87 [7.5]	5.50 [8.0]
Conventional, TF=3.0	14.98 [6.6]	4.49 [8.8]	Modified, TF=2.95	17.24 [10.4]	5.62 [9.4]
Conventional, TF=3.6	18.16 [7.1]	5.01 [10.2]	Modified, TF=3.43	16.49 [10.2]	6.01 [10.0]

Table of mean yarn snarling turns

Yarn code	Mean no. of turns [CV%]	Yarn code	Mean no. of turns [CV%]
-	-	Modified, TF=2.13	24 [8.7]
-	-	Modified, TF=2.34	25 [8.1]
Conventional, TF=2.5	36 [9.2]	Modified, TF=2.53	28 [8.3]
-	-	Modified, TF=2.70	30 [6.9]
Conventional, TF=3.0	45 [6.1]	Modified, TF=2.95	32 [8.2]
Conventional, TF=3.6	49 [5.9]	Modified, TF=3.43	34 [8.3]

Appendix 2. Comparison of Diameter and S3 Values between 20Ne Yarns

Table of yarn diameter and hairiness S3 value

Yarn	TBS yarn	Conventional, TF=2.5	Conventional, TF=3.6
Yarn diameter (mm) [CV%]	0.269 [10.1]	0.270 [6.1]	0.267 [5.9]
Hairiness S3 Value [CV%]	408 [20.8]	-	623 [14.5]

Appendix 3. Listing of the Yarn Model Program

```
C ***********************************************************************
C            PROGRAM OF CALCULATION OF YARN TORQUE
C ***********************************************************************
C      Notations:
C
C      Key parameters:
C
C      Rf, R0_I              -  Fiber and yarn radii
C      A                     -  Cross-sectional areas of the initial yarn
C      A0, B, C              -  Coefficients of the migration magnitude, frequency and
C                               phase angle of a fiber
C      s0, s1                -  Arc length of a fiber with angle θ in the initial and
C                               deformed yarns
C      k0, k1                -  Curvature of the fiber in the initial and deformed yarns
C      tor0, tor1            -  Torsion of a fiber in the initial and deformed yarns
C      L                     -  Yarn rotation in radian per cm
C      J                     -  No. of annular zone
C      UE, UB, UT            -  Tensile, bending and torsional energy of a fiber
```

```
C     UE_N, UB_N, UT_N  -  Total tensile, bending and torsional energy of fibers in a
C                          ring of the yarn radius
C     UE_A, UB_A, UT_A  -  Total tensile, bending and torsional energy of  the yarn
C     L_ALL             -  Total  torque of the yarn
C     LE, LB, LT        -  Components of yarn torque due to fiber tension, bending
C                          and torsion
C     L0, L1            -  Fiber length in one turn of twist in the initial and
C                          deformed yarns
C     EPS_f, EPS_y      -  Fiber and yarn tensile strain
C     T0, T1            -  No. of twist per unit of length of the initial and deformed
C                          yarns
C     E, I_b            -  Tensile modulus and moment inertia of the fiber with
C                          respect to the principle axis of its cross section
C     D3, D2, D1, D0    -  Coefficients of yarn radial packing density function
C
C
C     Other variables:
C
C     pi, p, D, R0, R0_A, DELTA_R, u, STEP_u, DELTA_u, DELTA_t, KK, N, N_f,
C     ******************************************************************
      PROGRAM MAIN
      DIMENSION UE(0:1),UB(0:1),UT(0:1),UE_N(0:1),UB_N(0:1),UT_N(0:1),
     &UE_A(0:1),UB_A(0:1),UT_A(0:1),L0(0:1),L1(0:1),EPS_f(0:1), EPS_y
      DOUBLE PRECISION x0,x01,x02,x03,y0,y01,y02,y03,z0,z01,z02,z03,u,t,
```

```
     &x1,x11,x12,x13,y1,y11,y12,y13,z1,z11,z12,z13,s0,s1,uu,
     &k0,k1,tor0,tor1,Mf01,Mf012,Mf11,Mf112,UE_i,UB_i,UT_i,LE,LB,LT,
     &L_ALL,UE,UB,UT,UE_N,UB_N,UT_N,UE_A,UB_A,UT_A,
     &L0,L1,EPS_f,Ms01,Ms11,L0_i,L1_i,Ms01_m,k0_m,k1_m
      DOUBLE PRECISION  STEP_u,DELTA_u,A0_s,A0_c,A0_cc1,A0_cs1,A0_sc2,
     &A0_ss2,A0_cc3,A0_cs3,A1_s,A1_c,A1_cc1,A1_cs1,A1_sc2,A1_ss2,
     &A1_cc3,A1_cs3,P,R1,A,DELTA_t,DELTA_t1,tt1,Ms1,Ms2,Ms3,s0_m,s1_m,
     &s0_1,s0_2,s0_3,s0_a,ss,Up,L00(0:1),L11(0:1), D3, D2, D1, D0, Rf
      INTEGER L,k,KK,I,N1
      REAL PI,E,I_b,R0,A0,B,C,D,T0,T1,U0,PP,N
      DO K=0,15
        WRITE(*,*)' '
      ENDDO
      WRITE(*,*)'************************************************'
      WRITE(*,*)'*    THIS IS A PROGRAM TO SIMULATE THE         *'
      WRITE(*,*)'*    ENERGY OF TENSILE ,BENDING AND TORSION    *'
      WRITE(*,*)'*    OF FIBER AND YARN                         *'
      WRITE(*,*)'************************************************'
      DO K=0,5
        WRITE(*,*)' '
      ENDDO
C     ********************************************************
C     *    To create the output data files          *
C     ********************************************************
```

```
      OPEN (unit=1, FILE='FIBER-YARN.DAT',STATUS='UNKNOWN')
      OPEN (unit=10, FILE='EPS-F.DAT',STATUS='UNKNOWN')
      OPEN (unit=20, FILE='K-TOR.DAT',STATUS='UNKNOWN')
C     ************************************************************
C          *          Input the  parameters value          *
C     ************************************************************
C     WRITE(*,*)'ALL RELEVANT UNITS ARE cm,g,cal,s.'
      READ (*,*)   pi, E, I_b, A, B, C, T0, Ey, R0_I, R0_A, DELTA_R,
      READ (*,*)  A0, D3, D2, D1, D0, STEP_u, DELTA_u, DELTA_t
     A=pi*Rf**2
     T1=T0/(1+EPS_y)
     p=SQRT(T1/T0)
     D=1/(2*pi*T1)
     STEP_u=0.25*pi
     DELTA_u=2.*pi/1000
     DELTA_t=2.*pi/100
     L0(0)=0
     L0(1)=0
     L1(0)=0
     L1(1)=0
     UE(0)=0
     UE(1)=0
     UB(0)=0
     UB(1)=0
```

```
      UT(0)=0
      UT(1)=0
      UE_N(0)=0
      UE_N(1)=0
      UB_N(0)=0
      UB_N(1)=0
      UT_N(0)=0
      UT_N(1)=0
      KK=0
      U0=0
C     ************************************************************
C     *        Main calculating part                             *
C     ************************************************************
      DO L=0,8                  !      (2PI)
        DO KK=0,1
          IF (KK==1) THEN
            u=u0+L*STEP_u+DELTA_u
          ENDIF
          IF (KK==0) THEN
           u=u0+L*STEP_u
          ENDIF
          IF (KK==0) THEN
            UU=u
          ENDIF
```

```
      DELTA_t1=(2.*PI+u/T1)/100
      DO J=0,9
      R0=R0_A+J*DELTA_R
      A0=0
C     A0=R0/10
      R1=p*R0
      PP=(R0_A+J*DELTA_R)/R0_I
      N = D3*PP**3 +D2*PP**2 + D1*PP + D0
      N_f=(INT(N))
      L0(0)=0
      L0(1)=0
      L1(0)=0
      L1(1)=0
      DO I=1,100
      t=DELTA_t*I
C     tt1=DELTA_t1*I
      IF (KK==1) THEN
        u=u0+L*STEP_u+DELTA_u
      ENDIF
      IF (KK==0) THEN
         u=u0+L*STEP_u
      ENDIF
C ************************************************************
     s0 =(1./2.)*SQRT(4*(A0*cos(B*t+C)*B*cos(t)
```

```
     & -(R0+A0*sin(B*t+C))*sin(t))**2+4*(A0*cos(B*t+C)*B*sin(t)
     & +(R0+A0*sin(B*t+C))*cos(t))**2+1/(pi**2*T0**2))
C ************************************************************
      s1 =(1./2.)*SQRT(4*(p*A0*cos(t1*(B+u*D)+C)*(B+u*D)
     & *cos(t1*(1+u*D))
     & -(p*R0+p*A0*sin(t1*(B+u*D)+C))*sin(t1*(1+u*D))*(1+u*D))**2
     & +4*(p*A0*cos(t1*(B+u*D)+C)*(B+u*D)*sin(t1*(1+u*D))
     & +(p*R0+p*A0*sin(t1*(B+u*D)+C))*cos(t1*(1+u*D))*(1+u*D))**2
     & +1/(pi**2*T1**2))
C ************************************************************
      k0=4*(1/(pi**2*T0**2)*(-A0*sin(B*t+C)*B**2*sin(t)
     & +2*A0*cos(B*t+C)
     & *B*cos(t)-(R0+A0*sin(B*t+C))*sin(t))**2+1/(pi**2*T0**2)
     & *(-A0*sin(B*t+C)*B**2*cos(t)-2*A0*cos(B*t+C)*B*sin(t)
     & -(R0+A0*sin(B*t+C))*cos(t))**2+4*((A0*cos(B*t+C)*B*cos(t)
     & -(R0+A0*sin(B*t+C))*sin(t))*(-A0*sin(B*t+C)*B**2*sin(t)
     & +2*A0*cos(B*t+C)*B*cos(t)-(R0+A0*sin(B*t+C))*sin(t))
     & -(A0*cos(B*t+C)*B*sin(t)+(R0+A0*sin(B*t+C))*cos(t))
     & *(-A0*sin(B*t+C)*B**2*cos(t)-2*A0*cos(B*t+C)*B*sin(t)
     & -(R0+A0*sin(B*t+C))*cos(t)))**2)**(1/2)
     & /(4*(A0*cos(B*t+C)*B*cos(t)-(R0+A0*sin(B*t+C))*sin(t))**2
     & +4*(A0*cos(B*t+C)*B*sin(t)+(R0+A0*sin(B*t+C))
     & *cos(t))**2+1/(pi**2*T0**2))**(3/2)
C ************************************************************
```

```
      k1=4*(1/(pi**2*T1**2)*(-p*A0*sin(t*(B+u*D)+C)*(B+u*D)**2
     & *sin(t*(1+u*D))+2*p*A0*cos(t*(B+u*D)+C)*(B+u*D)
     & *cos(t*(1+u*D))*(1+u*D)-(p*R0+p*A0*sin(t*(B+u*D)+C))
     & *sin(t*(1+u*D))*(1+u*D)**2)**2+1/(pi**2*T1**2)
     & *(-p*A0*sin(t*(B+u*D)+C)*(B+u*D)**2*cos(t*(1+u*D))
     & -2*p*A0*cos(t*(B+u*D)+C)*(B+u*D)*sin(t*(1+u*D))*(1+u*D)
     & -(p*R0+p*A0*sin(t*(B+u*D)+C))*cos(t*(1+u*D))*(1+u*D)**2)**2
     & +4*((p*A0*cos(t*(B+u*D)+C)*(B+u*D)*cos(t*(1+u*D))
     & -(p*R0+p*A0*sin(t*(B+u*D)+C))*sin(t*(1+u*D))*(1+u*D))
     & *(-p*A0*sin(t*(B+u*D)+C)*(B+u*D)**2*sin(t*(1+u*D))
     & +2*p*A0*cos(t*(B+u*D)+C)*(B+u*D)*cos(t*(1+u*D))*(1+u*D)
     & -(p*R0+p*A0*sin(t*(B+u*D)+C))*sin(t*(1+u*D))*(1+u*D)**2)
     & *(-p*A0*sin(t*(B+u*D)+C)*(B+u*D)**2*cos(t*(1+u*D))
     & -2*p*A0*cos(t*(B+u*D)+C)*(B+u*D)*sin(t*(1+u*D))*(1+u*D)
     & -(p*R0+p*A0*sin(t*(B+u*D)+C))*cos(t*(1+u*D))*(1+u*D)**2))**2)
     & **(1/2)/(4*(p*A0*cos(t*(B+u*D)+C)*(B+u*D)*cos(t*(1+u*D))
     & -(p*R0+p*A0*sin(t*(B+u*D)+C))*sin(t*(1+u*D))*(1+u*D))**2
     & +4*(p*A0*cos(t*(B+u*D)+C)*(B+u*D)*sin(t*(1+u*D))
     & +(p*R0+p*A0*sin(t*(B+u*D)+C))*cos(t*(1+u*D))
     & *(1+u*D))**2+1/(pi**2*T1**2))**(3/2)
C ************************************************************
      tor0=(-1/(2*pi*T0)*(-A0_ss2+2*A0_cc1-(R0+A0_s)*sin(t))
     & *(-A0_cc3+3*A0_ss2-3*A0_cc1+(R0+A0_s)*sin(t))
     & +1/(2*pi*T0)*(-A0_sc2-2*A0_cs1-(R0+A0_s)*cos(t))
```

```
     & *(-A0_cs3-3*A0_sc2-3*A0_cs1-(R0+A0_s)*cos(t)))
     & /(1/(4*pi**2*T0**2)*(-A0_ss2+2*A0_cc1-(R0+A0_s)
     & *sin(t))**2+1/(4*pi**2*T0**2)*(-A0_sc2-2*A0_cs1
     & -(R0+A0_s)*cos(t))**2+((A0_cc1-(R0+A0_s)*sin(t))
     & *(-A0_ss2+2*A0_cc1-(R0+A0_s)*sin(t))
     & -(A0_cs1+(R0+A0_s)*cos(t))*(-A0_sc2-2*A0_cs1
     & -(R0+A0_s)*cos(t)))**2)
C ************************************************************
       tor1=(-1/(2*pi*T1)*(-p*A0*sin(t*(B+u*D)+C)*(B+u*D)**2
     & *sin(t*(1+u*D))+2*p*A0*cos(t*(B+u*D)+C)*(B+u*D)
     & *cos(t*(1+u*D))*(1+u*D)-(p*R0+p*A0*sin(t*(B+u*D)+C))
     & *sin(t*(1+u*D))*(1+u*D)**2)*(-p*A0*cos(t*(B+u*D)+C)
     & *(B+u*D)**3*cos(t*(1+u*D))+3*p*A0*sin(t*(B+u*D)+C)
     & *(B+u*D)**2*sin(t*(1+u*D))*(1+u*D)-3*p*A0*cos(t*(B+u*D)+C)
     & *(B+u*D)*cos(t*(1+u*D))*(1+u*D)**2
     & +(p*R0+p*A0*sin(t*(B+u*D)+C))*sin(t*(1+u*D))*(1+u*D)**3)
     & +1/(2*pi*T1)*(-p*A0*sin(t*(B+u*D)+C)*(B+u*D)**2*cos(t*(1+u*D))
     & -2*p*A0*cos(t*(B+u*D)+C)*(B+u*D)*sin(t*(1+u*D))*(1+u*D)
     & -(p*R0+p*A0*sin(t*(B+u*D)+C))*cos(t*(1+u*D))*(1+u*D)**2)
     & *(-p*A0*cos(t*(B+u*D)+C)*(B+u*D)**3*sin(t*(1+u*D))
     & -3*p*A0*sin(t*(B+u*D)+C)*(B+u*D)**2*cos(t*(1+u*D))*(1+u*D)
     & -3*p*A0*cos(t*(B+u*D)+C)*(B+u*D)*sin(t*(1+u*D))*(1+u*D)**2
     & -(p*R0+p*A0*sin(t*(B+u*D)+C))*cos(t*(1+u*D))
     & *(1+u*D)**3))/(1/(4*pi**2*T1**2)*(-p*A0*sin(t*(B+u*D)+C)
```

```
     & *(B+u*D)**2*sin(t*(1+u*D))+2*p*A0*cos(t*(B+u*D)+C)
     & *(B+u*D)*cos(t*(1+u*D))*(1+u*D)
     & -(p*R0+p*A0*sin(t*(B+u*D)+C))*sin(t*(1+u*D))
     & *(1+u*D)**2)**2+1/(4*pi**2*T1**2)*(-p*A0*sin(t*(B+u*D)+C)
     & *(B+u*D)**2*cos(t*(1+u*D))-2*p*A0*cos(t*(B+u*D)+C)
     & *(B+u*D)*sin(t*(1+u*D))*(1+u*D)-(p*R0+p*A0*sin(t*(B+u*D)+C))
     & *cos(t*(1+u*D))*(1+u*D)**2)**2+((p*A0*cos(t*(B+u*D)+C)
     & *(B+u*D)*cos(t*(1+u*D))-(p*R0+p*A0*sin(t*(B+u*D)+C))
     & *sin(t*(1+u*D))*(1+u*D))*(-p*A0*sin(t*(B+u*D)+C)
     & *(B+u*D)**2*sin(t*(1+u*D))+2*p*A0*cos(t*(B+u*D)+C)
     & *(B+u*D)*cos(t*(1+u*D))*(1+u*D)
     & -(p*R0+p*A0*sin(t*(B+u*D)+C))*sin(t*(1+u*D))*(1+u*D)**2)
     & -(p*A0*cos(t*(B+u*D)+C)*(B+u*D)*sin(t*(1+u*D))
     & +(p*R0+p*A0*sin(t*(B+u*D)+C))*cos(t*(1+u*D))*(1+u*D))
     & *(-p*A0*sin(t*(B+u*D)+C)*(B+u*D)**2*cos(t*(1+u*D))
     & -2*p*A0*cos(t*(B+u*D)+C)*(B+u*D)*sin(t*(1+u*D))*(1+u*D)
     & -(p*R0+p*A0*sin(t*(B+u*D)+C))*cos(t*(1+u*D))*(1+u*D)**2))**2)
C ************************************************************
           L0_i=s0*DELTA_t
           L0(KK)=L0(KK)+L0_i
           L1_i=s1*DELTA_t
           L1(KK)=L1(KK)+L1_i
           UB_i=(1./2.)*(E*I_b*(k1-k0)**2*s0*DELTA_t)
           UB(KK)=UB(KK)+UB_i
```

```
          UT_i=(1./3.)*(E*I_b*(tor1-tor0)**2*s0*DELTA_t)
          UT(KK)=UT(KK)+UT_i
        ENDDO
          EPS_f(KK)=(L1(KK)-L0(KK))/L0(KK)
          UE(KK)=(0.5)*(L0(KK)*E*A*(EPS_f(KK))**2)
          UE_N(KK)=UE_N(KK)+N_f*UE(KK)
          UB_N(KK)=UB_N(KK)+N_f*UB(KK)
          UT_N(KK)=UT_N(KK)+N_f*UT(KK)
       ENDDO
         UE_A(KK)=T1*UE_N(KK)
         UB_A(KK)=T1*UB_N(KK)
         UT_A(KK)=T1*UT_N(KK)
     ENDDO
       LE=ABS(UE_A(1)-UE_A(0))/DELTA_u
       LB=ABS(UB_A(1)-UB_A(0))/DELTA_u
       LT=ABS(UT_A(1)-UT_A(0))/DELTA_u
       L_ALL=LE+LB+LT
      WRITE(*,*) "torque",U,LE,LB,LT,L_ALL
C       READ*, CHAR
100     FOTMAT(1X,5F11.4)
      WRITE (1,100) (UU,LE, LB, LT, L_ALL)
    ENDDO
C ************************************************************
    WRITE(*,*)' '
```

```
WRITE(*,*)'              **************************'
WRITE(*,*)'              *          THANK YOU!          *'
WRITE(*,*)'              **************************'

END
```